

Electronic Thesis and Dissertation Repository

June 2019

Biochemical and Functional Analyses of PANX1 Variants

Daniel Nouri Nejad, *The University of Western Ontario*

Supervisor: Penuela, Silvia, *The University of Western Ontario*

A thesis submitted in partial fulfillment of the requirements for the Master of Science degree in
Anatomy and Cell Biology

© Daniel Nouri Nejad 2019

Follow this and additional works at: <https://ir.lib.uwo.ca/etd>



Part of the [Molecular Biology Commons](#)

Recommended Citation

Nouri Nejad, Daniel, "Biochemical and Functional Analyses of PANX1 Variants" (2019). *Electronic Thesis and Dissertation Repository*. 6230.

<https://ir.lib.uwo.ca/etd/6230>

This Dissertation/Thesis is brought to you for free and open access by Scholarship@Western. It has been accepted for inclusion in Electronic Thesis and Dissertation Repository by an authorized administrator of Scholarship@Western. For more information, please contact wlsadmin@uwo.ca.

Abstract

Pannexin 1 (PANX1) is a glycoprotein capable of forming large-pore single-membrane channels permeable to signaling molecules such as ATP. In this study, we interrogated different domains by introducing naturally occurring variants reported in melanoma and assessed their impact on the channel function of PANX1 at the cell surface. From this, we discovered a novel tyrosine phosphorylation site at Tyr150, that when disrupted via a missense mutation resulted in hypo-glycosylation and a greater capacity to traffic to the cell-surface and enhanced dye uptake. We have also uncovered a highly conserved ancestral allele, Gln5His, that has a greater allele frequency than the derived allele Gln5 in global and cancer cohorts but was not associated with cancer aggressiveness. Furthermore, Gln5His also did not impact glycosylation, cell-surface localization and channel-function in cancer cells. Our findings demonstrate the utility of studying naturally occurring variants in understanding diverse mechanisms that regulate PANX1 channel function.

Keywords

Pannexin 1 (PANX1), pannexin, tyrosine-phosphorylation, glycosylation, trafficking, polymorphism

Co-Authorship Statement

Daniel Nouri Nejad designed the project, performed experiments and data analysis as well as wrote the manuscript. Chetan Patil performed whole-cell patch clamp electrophysiology recordings. Gregory Gloor designed and executed programming to analyze allele frequencies in cancer cohorts. Rafael Sanchez-Pupo assisted in preparing samples for mass spectrometry. Brooke O'Donnell assisted in generating Fig. 2.1C. Danielle Johnston generated Hs578T(KO) cells and Samar Sayedahosseini generated A375P(KO) cells. Kristina Jurcic performed electrospray-ionization mass spectrometry and assisted in data analysis of mass spectrometry results. Silvia Penuela designed the project, supervised the experiments, and edited the manuscript.

Acknowledgments

Little did I know that when I started working in the Penuela Lab, that I would be working with one of the kindest, smartest, and most hard-working groups that ignited great catalysts to my growth during my undergraduate and graduate years. I will always cherish the memories and friendships from the Penuela Lab. I would like to thank the following people for their immense support over the years, for without them, I would not be the person I am today.

To my family for spending twenty-four years and counting dealing with this rascal and for their undying love and support that has sprouted me to be who I am today. To Parnian Etedali-Zadeh for her constant positivity and dedicated mission to help others.

To Silvia Penuela with her great dedication to help us become great collaborative and passionate scientists and for creating a positive and productive learning environment. It has been truly a great honor to work with one of the kindest and most awesome scientist and teacher during these five years. Thank you for believing in me and mentoring me these years, I will always carry the values you have instilled in me throughout my career.

To Rafael Sánchez-Pupo, who was always there to help no matter how big his mountain of work was and for his endless supply of Mycoplasma jokes. To Danielle Johnston for her devotion to help us growing-scientists and always making sure we were calmly and efficiently working. To Samar Sayedyahosseini for her mentorship and great support, as well as teaching me to notice and appreciate small details. To Brooke O'Donnell for tirelessly helping others and willingness to do weekly lab clean-ups. To Brent Wakefield for his support and inspiration, and his never-ending appetite for helping others. To Kenneth Huang for his great support as well as just simply doing a Good Job overall. To Taylor Freeman for her immense support and teaching, in addition to introducing me to great varieties of music. To Luke Harland for mentoring me and for inspiring me to pursue research during my undergraduate. To Vanessa Lee for her dedication to teaching and helping others. To Carolina Herrera for her dedication towards creating a safe and fun lab environment. To Jenny Ma for her enduring enthusiasm for research.

To Dale Laird, Alison Allan, and Lina Dagnino for their guidance and support.

To all other current and previous Penuela students, thank you for your kind support and friendship.

To the entire Department of Anatomy and Cell Biology Department for creating a warm and friendly environment and for their assistance in many aspects of my undergraduate and graduate career.

To the Canadian Institutes of Health Research, the Cancer Research Technology Transfer, and the Natural Sciences and Engineering Research Agencies for funding this project.

Table of Contents

Abstract	i
Co-Authorship Statement.....	ii
Acknowledgments.....	iii
Table of Contents	v
List of Figures	vii
Chapter 1	1
1 Introduction	1
1.1 General Overview of the Pannexin Family.....	1
1.2 Topological and Conformational Structure of PANX1	3
1.3 Trafficking of PANX1	5
1.4 Diverse Functions of PANX1	6
1.5 Post-Translational Modifications of PANX1.....	7
1.5.1 N-linked Glycosylation.....	8
1.5.2 Phosphorylation	11
1.5.3 Nitrosylation	12
1.5.4 C-terminus Caspase-cleavage.....	13
1.5.5 Oxidation.....	13
1.6 PANX1 in Disease	14
1.7 PANX1 in Cancer	16
1.8 Naturally Occurring <i>PANX1</i> Variants and Mutations.....	18
1.9 Using Cancer-derived <i>PANX1</i> Somatic Mutations as a Source of Naturally Occurring Variants to Study PANX1.....	21
1.10 Rationale and hypothesis	22
1.11 Objectives	23

1.12	References.....	24
2	Manuscript.....	32
2.1	Contributions of Authors	33
2.2	Abstract	34
2.1	Introduction.....	35
2.2	Results.....	38
2.3	Discussion	58
2.4	Experimental Procedures	64
2.5	References.....	78
Chapter 3	83
3	Discussion and Conclusions.....	83
3.1	Overall Study Conclusions	83
3.2	Study Limitations.....	86
3.3	Future Directions	88
3.3.1	The Role of Protonation of PANX1 in Cancer	88
3.3.2	Potential PTMs of PANX1	91
3.4	Summary	92
3.5	References.....	94
Curriculum Vitae	97

List of Figures

Figure 1.1 Topological structure of the pannexin family..	3
Figure 1.2: Anterograde trafficking pathway and glycosylation of PANX1	10
Figure 1.3: Somatic PANX1 mutations reported in tumours of cancer patients in cBioPortal cancer genomics database.	22
Figure 2.1: Y150F alters normal banding patterns of PANX1 in NRK cells.	41
Figure 2.2: Y150F produces a Gly1 species that is partially resistant to EndoH deglycosylation	43
Figure 2.3: Greater amounts of Y150F Gly1 localize at the cell-surface relative to Q5 and Q5H.	45
Figure 2.4: Y150 is a tyrosine phosphorylation site of PANX1	47
Figure 2.5: Y150F enhances basal dye uptake while Q5H does not differ functionally from Q5	49
Figure 2.6: Stable-overexpression of Q5H in Hs578T(KO) cells does not differ in dye-uptake, migration, and cell growth from Q5 controls	51
Figure 2.7: Higher Q5H allele frequency than Q5 in colorectal and skin cutaneous melanoma cancer cohorts.	54
Figure 2.8: Higher Q5H allele frequency than Q5 in global cohorts	57
Supplementary Figure 2.1	75
Supplementary Figure 2.2: Moderate Y150F overexpression allows for cell-surface localization but is prevented upon higher overexpression in NRK cells which also results in lower cell viability.	76
Supplementary Figure 2.3	77

Figure 3.1: Potential spatiotemporal onset and termination pathway of Y150 phosphorylation of PANX184

Chapter 1

1 Introduction

1.1 General Overview of the Pannexin Family

The discovery of the pannexin family, led by Panchin and his colleagues, was first driven to uncover proteins homologous to the invertebrate gap junction family (innexins), in vertebrate taxonomic groups (1). Using degenerate primers, the pannexin pioneers uncovered innexin homologues encoding for PANX1 and PANX2 (1). As a result of their presence in many animal phyla, the novel family was named pannexins, derived from the Latin words Pan- for “all” and nexus for “connection”, as they were initially thought to form gap junctions. Subsequently, the group uncovered and characterized the full human sequences for all three members of the pannexin family, pannexin 1, 2, and 3 (PANX1, PANX2, PANX3 for humans, and Panx1, Panx2, Panx3 for rodents) (2).

The evolutionary rise of the pannexin family is predicted to have occurred during two major genomic duplications early in the divergence of vertebrates (3), of which the former event led to the onset of PANX2 while the latter led to both PANX1 and PANX3 (4). The temporal onset of the trio is also apparent in their human chromosomal locations, with PANX1 and PANX3 located relatively close to each other on chromosome 11 (q21 and q24, respectively), and with PANX2 located on chromosome 22 (2).

Topological similarities persist within the pannexin family, in which all three possess four transmembrane domains with cytosolic N- and C-termini (**Fig. 1.1**), similar to innexins and

connexins. The N-terminus and intracellular loop is found to be highly conserved between the three pannexin members while the C-terminus remains highly variable (5). In addition, there are two cysteine residues preserved in each of the extracellular loops of pannexins (2).

While possessing similar topological and sequence homologies, all three members present different mRNA and protein expression patterns in mammalian tissues (6). The most ubiquitous member is PANX1 with its mRNA and protein detected in most mammalian tissues (6-8). While its expression distribution was initially found to be restricted within the central nervous system specifically neurons and immature astrocytes within the cerebral cortex and cerebellum, there are new reports demonstrating PANX2 to be expressed in kidney tubular cells, seminiferous duct cells of the testis, excretory salivary glands, striated ducts, gastrointestinal tract glandular and epithelial cells, parietal cells, columnar epithelial cells, retina, lung and skin (6-9). Finally, PANX3 expression has been detected in the testis, stomach, spleen, salivary gland, lung, heart, duodenum, adrenal tissue, skeletal structures, skeletal muscle, lactating mammary tissue, sebaceous glands and the small intestine (2,6,7). As a result of its widespread expression pattern within human tissues, PANX1 is the most characterized member and will also be the main focus for the subsequent sections.

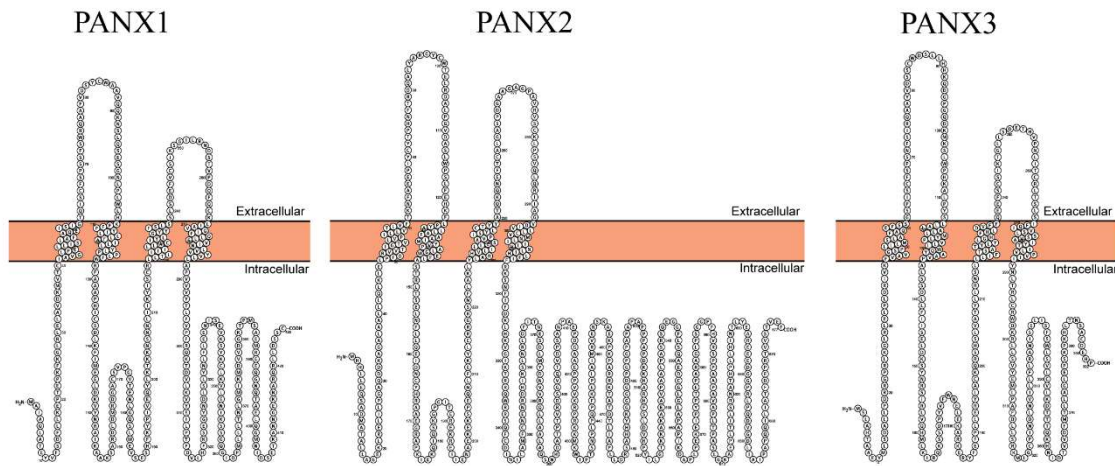


Figure 1.1 Topological structure of the pannexin family. All members possess cytosolic N- and C-termini, four transmembrane domains, two extracellular loops with two conserved cysteine residues in each loop, and one intracellular loop. Images were generated using human PANX1, PANX2, and PANX3 sequences and Protter program.

1.2 Topological and Conformational Structure of PANX1

The topological structure of PANX1 has been established to consist of four transmembrane domains (TM1-4) with two extracellular loops (EL1 and EL2), one intracellular loop (IL), and cytosolic N- and C-termini (NT and CT, respectively) (**Fig. 1.1**), along with two conserved cysteine residues within each EL (10). Six PANX1 monomers oligomerize within the endoplasmic reticulum (ER) to form a functional hexameric channel (11-13).

Using a voltage-activated Panx1 model, substituted cysteine accessibility analyses determined the pore structure of PANX1 channel to consist of the outer and inner portions of TM1 and EL1, respectively (14). Furthermore, they demonstrate that cysteine mutations of several residues near the end of the CT inhibited channel currents after thiol modification, suggesting that the CT plugs the pore. This follows with other studies demonstrating that Panx1 channel activity is regulated by the autoinhibitory CT in a ball-and-chain manner (14-16). However, considering the different possible conformations Panx1 may undertake, a re-analysis demonstrated a loss of carboxy terminal reactivity of cysteines in K⁺-activated states (17). It has been suggested that in the ATP-permeable conformation, Panx1 may adopt a similar structure as ATP-permeable connexin channels do in which the NT lines the pore (18).

The interactions between the different domains have not been fully elucidated but there are extensive reports on interactions of the CT with other domains. A study exploring the diverse functions of the CT demonstrated a short segment (I360-G370) to interact with the membrane as they noticed the α -helical content of a peptide spanning this region (G357-S384) increased in the presence of membrane mimetic lipids (19). Furthermore, complementing the ball-and-chain model, they also demonstrated by using truncated Panx1 constructs and peptides that I372-D379 residues of the CT are involved in pore closure.

1.3 Trafficking of PANX1

Although ectopic expression systems demonstrate predominantly cell-surface localization of Panx1, the localization profile of endogenous Panx1 can vary across different cell types (6,20-22). Endogenously, Panx1 can be detected at the cell surface where its function has been mostly characterized to be an ATP release channel (23-25), and within the ER, where it has been demonstrated to function as a calcium-leak channel (26).

Much of the research conducted on the trafficking pathways of Panx1 have focused on its anterograde pathway. The anterograde journey of Panx1 begins within the ER, where the channel receives high-mannose glycosylation (at N254) and subsequently traffics to the Golgi via anterograde Sar1-dependent COPII vesicles (27). Within the Golgi, Panx1 receives further sugar modifications, forming the complex glycosylated species (27). From there, Panx1 then traffics to the cell-surface. While at the cell-surface, FRAP analyses revealed Panx1-EGFP to be highly dynamic and protein stability is facilitated through interactions between the CT and actin cytoskeleton (27).

An emerging topic in Panx1 trafficking that awaits to be fully elucidated is retrograde trafficking of the channel. The first study conducted in this area demonstrated through inhibitor studies that Panx1 undergoes lysosomal degradation (28). While the same study demonstrated Panx1 was co-distributed with endocytic machinery including clathrin, AP2, dynamin II, caveolin-1, and -2, co-immunoprecipitation results failed to demonstrate direct interactions between Panx1 and the various components (28). Furthermore, Panx1

internalization was shown to be dynamin-II independent (28). Branching from this study, Boyce *et al.* demonstrated that extracellular ATP induces internalization of the channel to endosomes through a cholesterol-dependent process via an ATP-sensitive residue W74 (29). Later work further demonstrated that this ATP-induced cholesterol-dependent internalization process required interactions between PANX1 and P2X7R (30).

1.4 Diverse Functions of PANX1

Despite their limited homology with innexins, pannexins do not form gap-junctions but rather single-membrane channels that function as a conduit for signaling molecules (31). However, there have been a few instances in which Panx1 has demonstrated gap-junctional behavior (26,32-34) but most reports appoint a single-membrane channel function for PANX1 (31), and have suggested that glycosylation of the channel provides a source of steric hindrance for gap-junction formation (28,35,36).

The most well-characterized channel function of PANX1 is ATP release at the cell-surface where it has been demonstrated, that manipulation of channel activity, expression, and chemical modifications of PANX1 can affect overall ATP release (14,37-39). However, other laboratories have conflicting reports that demonstrated PANX1 to be devoid of an ATP release function (40) and is rather a chloride channel with no cation permeability (17,41,42), while one report demonstrated Panx1 to be a Ca²⁺-permeable ion channel (26). To reconcile the divergence of these results, it has been proposed that PANX1 can undertake different conformations dependent on the stimulus applied (17). When PANX1

was stimulated with physiological stimuli such as elevated extracellular potassium levels (23,24) or mechanical stimulation (23,43,44), PANX1 undertakes a conformational shape with a larger pore opening that favors both cation and ATP permeability. In contrast, when PANX1 is activated by positive membrane potentials (14) or caspase-cleavage of the autoinhibitory CT (13,45,46), the channel favors a smaller pore opening with anion permeability (17,41,42). While caspase-cleavage activation is a prevalent theme in cell death, voltage-activation through positive membrane potentials usually occurs during action potentials. Therefore, the latter activation method may only be physiologically relevant to neurons and muscle cells during repolarization. Overall, it is imperative to consider the different activated conformations PANX1 employs to understand interactions between different domains of the channel.

1.5 Post-Translational Modifications of PANX1

PANX1 is a dynamically altered protein that receives a diverse range of post-translational modifications (PTM) throughout its lifespan which has been shown to regulate various aspects of the channel from trafficking, protein stability, and channel activity. The following sub-sections will discuss the various PTMs PANX1 has been experimentally demonstrated to acquire.

1.5.1 N-linked Glycosylation

The most well-characterized and significant PTM is N-linked glycosylation that occurs on N254 of the second extracellular loop (6,11,47). The state of glycosylation of monomeric PANX1 can be deciphered from PANX1's protein banding pattern between approximately 40 and 50 kDa when resolved in SDS-PAGE (**Fig. 1.2**). The banding pattern consists of the fastest-migrating non-glycosylated Gly0, the intermediate-running high-mannose Gly1, and the slowest-migrating complex glycosylated Gly2 species. Glycosylation first begins with the addition of the high-mannose glycosylation that occurs in the ER and is further modified to complex glycosylation in the Golgi (6,36). The extent of glycosylation impacts several properties of Panx1 including the efficiency for cell-surface trafficking, intermixing with other pannexin members, and channel function (6,22,47,48). While complex glycosylation is found predominantly at the cell-surface, this does not indicate that complex glycosylation is required for cell-surface trafficking (11,47). Gly0 and Gly1 still possess the ability to traffic to the cell-surface although to a lesser capacity relative to Gly2. Furthermore, interactions between Panx1 with Panx2 and Panx3 are affected by Panx1's glycosylation state (47). Immunoprecipitation studies conducted by Penuela *et al.* shows that Panx2 interacts with only Panx1's Gly0 and Gly1 as well as the glycosylation-deficient mutant N254Q, but not the Gly2 species. The authors also demonstrated weaker interactions between Panx1 and Panx3 which were enhanced when Panx1 lacked any glycosylation. The extent of glycosylation Panx1 receives is also variable in different tissue types, suggesting that regulation of glycosylation and consequently also channel function is dependent on the cellular context (6,11).

There are several reports of artificial and naturally occurring mutations that do not target N254 but can affect the glycosylation status of PANX1. To uncover possible glycosylation sites in addition to N254, Boassa and colleagues generated glutamine mutations of N204, N254, and N337, and noticed that N337Q banding profile did not result in Gly2 species but produced Gly0 and Gly1 (11). However, N337 site was excluded as an asparagine-glycosylation site since it is found in the cytosolic C-terminus which would not be able to directly encounter the glycosyltransferases within the lumen of the ER and Golgi. In addition, mutations of extracellular cysteine residues (C66S, C84S, C245S, C264S) that have been generated to uncover regulatory mechanisms for channel activity revealed expression of predominantly Gly1 with minimal Gly0 and negligible amounts of Gly2 (49). These mutants also retained the ability to traffic to the cell-surface. Interestingly, when the cysteine mutants were tagged with EGFP at the C-terminus, there was a noticeable increase in Gly2 species, suggesting that attachment of fluorescent protein at the C-terminus may rescue the glycosylation deficiency induced by the cysteine mutations. Furthermore, they demonstrated that mutation of any of the extracellular cysteines resulted in no detectable channel activity. In a separate study also analyzing the role of nitrosylation on PANX1, transmembrane and intracellular cysteine mutants (C40A and C347A, respectively) also resulted in a protein banding pattern consisting primarily of Gly0 and Gly1 species with minimal Gly2 species (37). They also demonstrate that these mutants retain the ability to traffic to the cell-surface and both C40 and C346 experience S-nitrosylation that inhibits channel currents and ATP release. In a separate study that studied the role of patient-derived mutations that induced an oocyte-death phenotype that is later discussed in further details, also reported four mutants (C347S, Q392*, 21_23delTEP, K346E) that resulted in only Gly1 species and localization within the cell-surface (50). In addition to cell-surface

localization, the authors also noted localization of the four mutants within the Golgi and increased calreticulin expression, a chaperone protein for glycoproteins, suggesting the intracellular retention of misfolded PANX1 mutants. Similar to what was observed with the truncated mutant Q392*, expression of the RFP-tagged truncated mutant T307* also resulted in only Gly0 and Gly1 species. Overall, these studies indicate that proper protein folding and possibly nitrosylation of several cysteine residues of the channel may play a key role in PANX1's complex glycosylation process.

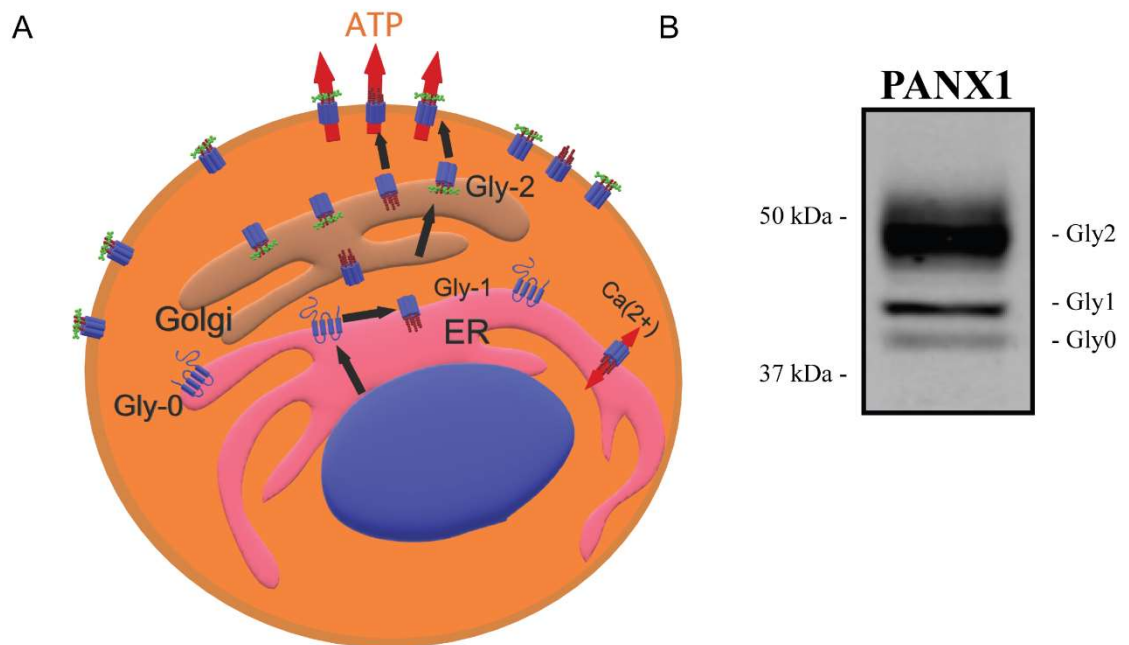


Figure 1.2: Anterograde trafficking pathway and glycosylation of PANX1. **A.** The nascent non-glycosylated PANX1 (Gly0) begins its journey within the ER where it receives high-mannose glycosylation forming the Gly1 species (red). Subsequently PANX1 traffics to the Golgi, where it receives further modifications to its glycosylation, forming the complex glycosylated Gly2 species (green). PANX1 then traffics to the cell-surface where it can mediate the release of signalling molecules such as ATP. **B.** Three distinct glycosylated PANX1 species can be identified via immunoblotting.

1.5.2 Phosphorylation

An emerging PTM that has been shown to greatly regulate PANX1 channel function is phosphorylation. Several reports revealed that the Src family kinases (SFKs) are key modulators of PANX1 phosphorylation (51-55) and their affiliation has been implicated in neuronal excitotoxicity during ischemia amongst other functions (52-56). Interest in the SFK-PANX1 interactome was first generated when Iglesias *et al.* demonstrated that P2X7R-dependent Panx1 activation required Src activation (57). Inhibition of P2X7R-Src interaction via peptides resulted in inhibition of Panx1 channel currents while maintaining P2X7R activity. Subsequent studies explored PANX1 activation in neuronal excitotoxicity with Src-PANX1 at the helm (53,55). Weilinger *et al.* initially uncovered that during neuronal excitotoxicity, N-methyl-D-aspartate receptors (NMDARs) activated Panx1 via stimulating Src Kinase activity (55). Soon after, the mechanistic link leading to Panx1 activation in neuronal excitotoxicity turned out to be phosphorylation of Y308, within the CT that was mediated by SFKs (53). Another group uncovered a tyrosine residue within the intracellular loop, Y198, that is phosphorylated by SFKs and leads to channel activation (52). Y198 phosphorylation has been shown to occur downstream of TNF- α stimulation in primary human venous endothelial cells. Y198 phosphorylation also has been shown to be stimulated by α -1-adrenoreceptors activation in vascular smooth muscle cells, leading to Panx1 activation (58). The same group also demonstrated that Y198 phosphorylation in vascular smooth muscle is constitutive in nature and occurs solely at the cell-surface. Surprisingly, in this context, Y198 phosphorylation is not mediated by α -1-adrenoreceptors activity but rather by SRC kinases (51). Overall, these accumulating studies of the receptor-SRC-Panx1 interactome opens a branch of mechanistic explanations for the effects of

Panx1 in several physiological processes and pathologies such as epilepsy, synaptic plasticity, and astrocyte physiology.

On the other hand, serine and threonine phosphorylation of Panx1 has not been studied as in depth as tyrosine phosphorylation. There are currently two studies that explored the presence and role of Ser/Thr phosphorylation. The first study demonstrated potentiated adult muscle cells via electrical stimulation experienced greater Panx1-mediated ATP release and Ser/Thr phosphorylation of Panx1 (59). Another study demonstrated that a nitric oxide donor, sodium nitroprusside, can inhibit Panx1 channel currents through a cGMP-PKG dependent-pathway that led to greater serine phosphorylation of Panx1 (60). It was suggested that phosphorylation of S206 mediates NO-mediated Panx1 inhibition as mutagenesis of this site abolished the inhibitory effects of sodium nitroprusside (60).

1.5.3 Nitrosylation

Another PTM that influences channel function is S-nitrosylation, the covalent incorporation of nitric oxide (NO) into cysteine thiols. The interest in S-nitrosylation of PANX1 was first generated when a study demonstrated that during oxygen-glucose deprivation in hippocampal neurons, inhibition of neuronal NO synthase resulted in NO- and redox-dependent blocking of PANX1 channel function (61). Subsequently, two studies proposed C282, C40, and C346 as possible sites of PTMs since mutagenesis of these sites resulted in reduced channel function (48,49,62). Extending from these findings, Lohman *et al.* demonstrated S-nitrosylation occurring on C40 and C346 as a regulatory mechanism to inhibit PANX1 currents (37).

1.5.4 C-terminus Caspase-cleavage

The C-termini of the pannexin members is one of the least conserved domains of the channels (16) and it has been suggested that the divergent functional roles of pannexins may be derived from the differences between the C-termini. Regarding Panx1, irreversible caspase cleavage of the CT at D378 constitutively activates the channel by removing the autoinhibitory role of the CT (15,45). Furthermore, Panx1 truncated mutants lacking the CT ($\Delta 307$) resulted in significantly lower cell-surface expression relative to wildtype (28). In addition, a chimeric protein consisting of Panx2 with its CT exchanged with the CT of Panx1 demonstrated altered sub-cellular localization profiles (63). In contrast with wildtype PANX1 and PANX2, which localized primarily at the cell-surface and endolysosomes, respectively, the chimeric PANX2^(PANX1CT) resulted in a diffuse distribution across the cytoplasm (63).

1.5.5 Oxidation

A study that explored the effects of the inflammatory cytokine IFN- γ on Panx1 expression and function in human airway epithelial cells, revealed C426 to be a residue that may form disulfide bonds with other thiols (64). The noted inhibitory effects of H₂O₂ on Panx1 channel function, which leads to the formation of reversible disulfide bonds between thiol groups, was abolished when this residue was mutated to serine (64).

1.6 PANX1 in Disease

Not only is PANX1 expressed in virtually every tissue (1,2,6,32,65), but PANX1 also possesses the ability to release several signaling molecules that contribute to intercellular and autocrine signaling (17,23,26,41). The most well-known signaling molecules released by PANX1 include ATP (23), chloride (41), and calcium (26), all of which participate in countless signaling cascades that, when dysregulated, can induce or accelerate pathophysiological disorders. While the pannexin field has only been discovered in 2000 (1) and the first report associating pannexins to a certain phenotype released in 2006 (54), the realm of diseases associated with pannexins, in particular PANX1, is exponentially expanding (10,66).

Panx1 has been implicated in a large variety of diseases ranging from ischemia to inflammatory diseases and cancer. The contrasting roles of Panx1 in cancer is discussed in further details in the subsequent section. Many of the initial reports on the role of Panx1 in diseases focused on disorders of the nervous system with the first report demonstrating that in ischemic conditions Panx1 induces depolarization of hippocampal neurons leading to neuronal cell death (54). The same group also implicated Panx1 in epilepsy where they demonstrate that Panx1 is expressed in pyramidal neurons of the hippocampus and can augment epileptiform seizure activity after being activated by NMDAR stimulation. From these investigations, subsequent studies followed further establishing Panx1's influence in ischemia and epilepsy (53,55,61,67,68).

Extracellular ATP, which can be derived from PANX1-mediated ATP release, also acts as a chemoattractant for immune cells and thus drive inflammation (69,70). As a result, another area of interest was to determine the function of Panx1 in inflammation. Initial reports of Panx1 promoting immune cell recruitment focused on apoptosis-induced ATP release from Panx1. Cells undergoing apoptosis activate Caspases 3/7 which then cleave the autoinhibitory C-terminus of Panx1 resulting in a constitutively-active Panx1 that leaks a trail of ATP for macrophages to follow for clearing cellular debris (45). A more complex model then followed in which PANX1-mediated ATP release is a crucial component of the NLRP3 inflammasome assembly, a protein complex that leads to the maturation and secretion of proinflammatory cytokines IL1 β and IL18 and can also lead to pyroptosis (71). This pathway has been implicated in various pathophysiological disorders including cancer, osteoarthritis, autoinflammatory diseases, gout, type-2 diabetes, and more (72). However, it has been previously demonstrated by using *Panx1*-null mice that PANX1 is dispensable for NLRP3 inflammasome assembly (73). Furthermore, a group has also previously demonstrated that inhibition of Panx1, P2X7Rs, Asc or caspase activity inhibited inflammation-induced enteric neuron cell death in a mouse colitis model while it was not dependent on NLRP3 expression, suggesting that a separate Panx1-inflammasome complex may be implicated (74). Other pathophysiological disorders that Panx1 has been implicated in include promoting HIV infection (75), infertility (50), obesity (76), multiple sclerosis (77), migraine headaches (78), among others (10,66).

1.7 PANX1 in Cancer

PANX1 appears to have contrasting roles in cancer depending on the tumour type and species being studied (20,34,79-83). There have been numerous studies demonstrating the prevalence of PANX1 upregulation in cancer cell lines and tumours relative to normal tissues (84-86) with a few cases presenting downregulation of PANX1 (80,87). Within cBioPortal, this dichotomy of differential expression levels presents as well, with some tumour types demonstrating amplification copy number variation such as bladder/urinary tract cancer, ovarian epithelial tumours, melanoma, cervical squamous cell carcinoma, prostate adenocarcinoma, and some with deep deletion copy number variation including seminoma, head and neck squamous cell carcinoma, and sarcoma, amongst others (88,89).

In some cases, reducing the levels of PANX1 delays tumour progression. One study illustrated that reduction of PANX1 in the human glioma cell line U87-MG resulted in a significant reduction in proliferation (90). Similarly, another study by our group demonstrated that knocking down mouse *Panx1* expression in the aggressive mouse melanoma B16-BL6 cell line resulted in decreased proliferative and migratory capacities, increased melanin production, and decreased expression of malignant melanoma markers (91). *Panx1* reduction in those cells fundamentally induced a reversion to a more melanocytic-like phenotype and a decreased tumorigenic profile. As of now, only one study demonstrated that elevated levels of *Panx1* induced a tumour suppressive phenotype in which overexpressing *Panx1*-EGFP in mouse C6 glioma cells presented a tumour-suppressive effect (34). However, they later also demonstrate that stable over-expression

of Panx1-EGFP in the same cell line accelerated glioma aggregates, a key feature of glioma progression, by stimulating the P2X7R pathway and in turn modifying the F-actin microfilaments (79).

Expanding from the study uncovering the role of Panx1 in mouse melanoma, we explored the role of PANX1 in human melanoma to determine if similar effects would be observed in human melanoma cells (20). In this report, we have demonstrated that PANX1 mRNA expression was significantly higher from normal skin to primary tumours but did not differ significantly in mRNA and protein expression across different stages of human melanoma tumour progression (20). Similar to what was observed upon knocking down Panx1 expression in mouse melanoma cells, knocking down PANX1 expression in human melanoma cells reduced their cell growth and migratory capacities as well as reduced expression of a malignant melanoma marker, β -catenin. To increase the therapeutic value of the findings of decreasing PANX1 expression in human melanoma, we administered PANX1 channel blockers, carbenoxolone and probenecid, to melanoma cells which similarly reduced malignant properties of the highly-metastatic A375-MA2 human melanoma cell line (20). Furthermore, another group demonstrated that administration of PANX1 channel blockers, 10 Panx1 peptide and carbenoxolone, in mice injected with metastatic human breast cancer cells had reduced metastatic dissemination to the lungs by preventing the tumor-promoting effects of extracellular ATP (83). With the availability of the re-purposed drugs, probenecid and carbenoxolone (FDA-approved for gout and ulcers, respectively), as well as evidence demonstrating the effects that PANX1 inhibition presents in breast and melanoma cancers, PANX1 is becoming increasingly desirable as a viable therapeutic target in cancer.

1.8 Naturally Occurring *PANX1* Variants and Mutations

Most studies on PANX1 have focused on modulating expression levels and inhibiting channel function of PANX1, but few have studied the role of naturally occurring *PANX1* variants in the context of disease. As of now, there have been a total of six reports of *PANX1* variants (50,83,92-96), two of which are genome-wide association studies (GWAS) linking *PANX1* variants with pathologies (95,96).

One of the more commonly-reported *PANX1* variant is the missense Q5H variant which has been shown to be associated with collagen-induced platelet reactivity in healthy subjects and displayed enhanced ATP release when ectopically-expressed (92). The group also later showed that the variant was not associated with platelet reactivity in stable cardiovascular patients in separate cohorts from the prior study (94). In a separate GWAS study identifying common variants associated with autism susceptibility risk, they found *PANX1* to be implicated *in cis* by multiple SNPs that included Q5H (95). Moreover, the variant Q5H was not associated with Schizophrenia in another GWAS study (96).

Subsequent to studies on Q5H, the first report linking a *PANX1* mutation to a disease was released (93). The authors associated a *PANX1* missense variant R217H to a multisystem disorder diagnosed in a female consisting of skeletal defects, sensorineural hearing loss, intellectual disability, kyphoscoliosis, and primary ovarian failure. R217H displayed normal glycosylation and cell-surface trafficking but reduced dye-uptake, channel currents, and ATP release. Furthermore, co-expression of R217H with wildtype PANX1 did not

significantly reduce PANX1 channel currents, suggesting that R217H is not dominant-negative to channel function. Although a causative role for R217H was not established, this was the first report of a germline *PANX1* variant associated with a disease. Interestingly, R217H is also reported in two patient biopsies of prostate adenocarcinoma and glioblastoma multiforme cancers (88,89) and is identified as a single-nucleotide polymorphism (SNP) in dbSNP database that is reported in ExAC's European (non-Finnish) and South Asian populations, and in GnomAD's European population (97,98). Therefore, the impact of R217H may be more widespread than previously thought.

The first report of a *PANX1* mutation associated with tumour aggressiveness has been shown to increase the metastatic efficiency of human breast cancer in areas of microvasculature (83). This somatic mutation produced a truncated form of PANX1, PANX1¹⁻⁸⁹, containing only the amino-terminus, first transmembrane domain, and part of the first extracellular loop. PANX1¹⁻⁸⁹ was found to be significantly enriched in metastatic breast cancer subclones CN-LM1A and MDA-LM2 relative to parental CN34 and MDA breast cancer cell lines. When Q89* was ectopically co-expressed with full-length PANX1, it led to significantly greater ATP release relative to cells ectopically expressing only full-length PANX1. Furthermore, ectopic expression of only Q89* did not significantly alter the amount of PANX1-mediated ATP release relative to vector controls. Overall, this suggests that Q89* and wildtype PANX1 forms a hetero-oligomeric channel that enhances ATP release. The authors later showed that this enhanced ATP release led to the activation of downstream purinergic P2Y signaling to suppress deformation-induced apoptosis of breast cancer cells, a key feature of cancer metastasis. Ultimately, the presence of this mutation in metastatic breast cancer cells enhanced their efficiency to metastasize (83).

The largest study on germline *PANX1* variants explored the role of patient-derived *PANX1* mutations from female patients experiencing familial or sporadic infertility (50). They have uncovered four *PANX1* germline mutations using whole-exome sequencing, each from a different family experiencing oocyte death occurring either before or after *in vitro* fertilization. The four mutants (K346E, C347S, Q392*, and p.21_23delTEP), as aforementioned produced proteins that were hypo-glycosylated consisting of primarily Gly1 species and a lack of Gly2 species. Despite the lack of Gly2 species, the mutants maintained the capacity to traffic to the cell-surface in addition to some intracellular retention of the mutants within the Golgi. In addition, the four mutants enhanced ATP release and *PANX1* channel currents. The authors also demonstrated the ectopic overexpression of Q392* and K346E in oocytes, induced oocyte death from 12 to 20 hours after cRNA injection in a dose-dependent relationship. Ectopic overexpression of C347S and 21_23delTEP in oocytes induced oocyte death 10 hours after *in vitro* fertilization. To discern whether the altered glycosylation profile induces oocyte death, they ectopically expressed N338Q mutant, of which produces solely Gly0 and Gly1 species, in oocytes and observed a similar oocyte death phenotype. Overall, this study demonstrated the important role *PANX1* plays in oocyte development and that certain mutations may induce hypo-glycosylation of *PANX1* and enhance channel activity.

1.9 Using Cancer-derived *PANX1* Somatic Mutations as a Source of Naturally Occurring Variants to Study *PANX1*

A rich source of genetic variants lies within the cancer databases such as cBioPortal.org and the International Cancer Genome Consortium (ICGC) that have accumulated somatic mutations reported in tumour biopsies of cancer patients (88,89,99). As of today, cBioPortal.org has 108 somatic *PANX1* mutations from various cancer types that are dispersed throughout the protein with higher densities of somatic mutations within the

intracellular loop and the C-terminus, two domains that are relevant for channel function (Fig. 1.3).

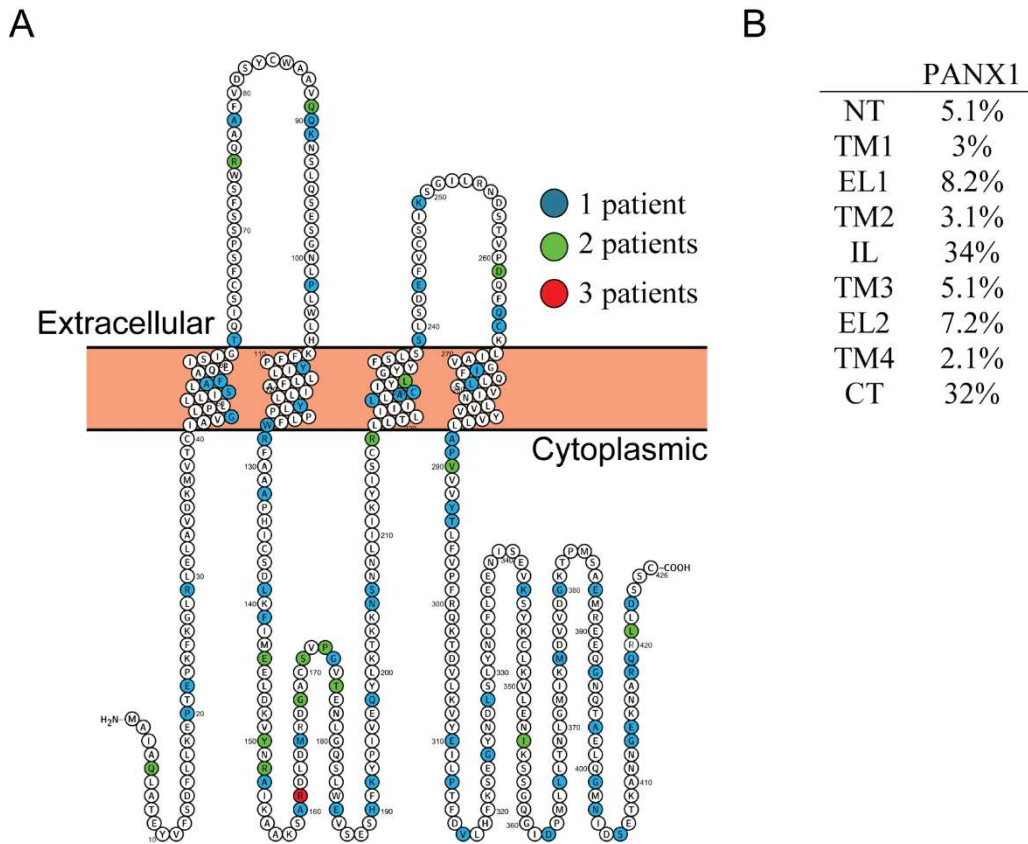


Figure 1.3: Somatic PANX1 mutations reported in tumours of cancer patients in cBioPortal cancer genomics database. A. A schematic of PANX1 denoting location of somatic mutations and indicating how many patients harboured a mutation at that site. **B.** Percentage of somatic mutations reported in each domain.

1.10 Rationale and hypothesis

We have previously demonstrated that inhibition or reduction of PANX1 in melanoma reduced their tumorigenic properties, demonstrating that PANX1 partakes in melanoma tumour progression (20,91). As a result, we analyzed variants derived from tumours of

melanoma patients and from human melanoma cell lines in our laboratory. From this, we uncovered seven *PANX1* variants (Q5H, Y150F, G168E, T176I, H190Y, S239L, and Q264*), whose effects on PANX1 function has not been characterized yet. Therefore, it is unknown if novel naturally occurring *PANX1* variants reported in cancer may affect the biochemical and functional aspects of PANX1. I hypothesized that naturally occurring *PANX1* variants prevent the normal function of PANX1 at the cell surface.

1.11 Objectives

- To analyse the impact of PANX1 variants on glycosylation, trafficking, phosphorylation, and channel activity of PANX1.
- To assess the effect of PANX1 variants on cell growth and migration of cancer cells.

1.12 References

1. Panchin, Y., Kelmanson, I., Matz, M., Lukyanov, K., Usman, N., and Lukyanov, S. (2000) A ubiquitous family of putative gap junction molecules. *Curr Biol* **10**, R473-474
2. Baranova, A., Ivanov, D., Petrash, N., Pestova, A., Skoblov, M., Kelmanson, I., Shagin, D., Nazarenko, S., Geraymovych, E., Litvin, O., Tiunova, A., Born, T. L., Usman, N., Staroverov, D., Lukyanov, S., and Panchin, Y. (2004) The mammalian pannexin family is homologous to the invertebrate innexin gap junction proteins. *Genomics* **83**, 706-716
3. Vandepoele, K., De Vos, W., Taylor, J. S., Meyer, A., and Van de Peer, Y. (2004) Major events in the genome evolution of vertebrates: paranome age and size differ considerably between ray-finned fishes and land vertebrates. *Proc Natl Acad Sci U S A* **101**, 1638-1643
4. Fushiki, D., Hamada, Y., Yoshimura, R., and Endo, Y. (2010) Phylogenetic and bioinformatic analysis of gap junction-related proteins, innexins, pannexins and connexins. *Biomed Res* **31**, 133-142
5. Abascal, F., and Zardoya, R. (2013) Evolutionary analyses of gap junction protein families. *Biochim Biophys Acta* **1828**, 4-14
6. Penuela, S., Bhalla, R., Gong, X. Q., Cowan, K. N., Celetti, S. J., Cowan, B. J., Bai, D., Shao, Q., and Laird, D. W. (2007) Pannexin 1 and pannexin 3 are glycoproteins that exhibit many distinct characteristics from the connexin family of gap junction proteins. *J Cell Sci* **120**, 3772-3783
7. Penuela, S., Gehi, R., and Laird, D. W. (2013) The biochemistry and function of pannexin channels. *Biochim Biophys Acta* **1828**, 15-22
8. Ray, A., Zoidl, G., Weickert, S., Wahle, P., and Dermietzel, R. (2005) Site-specific and developmental expression of pannexin1 in the mouse nervous system. *Eur J Neurosci* **21**, 3277-3290
9. Le Vasseur, M., Lelowski, J., Bechberger, J. F., Sin, W. C., and Naus, C. C. (2014) Pannexin 2 protein expression is not restricted to the CNS. *Front Cell Neurosci* **8**, 392
10. Penuela, S., Harland, L., Simek, J., and Laird, D. W. (2014) Pannexin channels and their links to human disease. *Biochem J* **461**, 371-381
11. Boassa, D., Ambrosi, C., Qiu, F., Dahl, G., Gaietta, G., and Sosinsky, G. (2007) Pannexin1 channels contain a glycosylation site that targets the hexamer to the plasma membrane. *J Biol Chem* **282**, 31733-31743
12. Ambrosi, C., Gassmann, O., Pranskevich, J. N., Boassa, D., Smock, A., Wang, J., Dahl, G., Steinem, C., and Sosinsky, G. E. (2010) Pannexin1 and Pannexin2 channels show quaternary similarities to connexons and different oligomerization numbers from each other. *J Biol Chem* **285**, 24420-24431
13. Chiu, Y. H., Jin, X., Medina, C. B., Leonhardt, S. A., Kiessling, V., Bennett, B. C., Shu, S., Tamm, L. K., Yeager, M., Ravichandran, K. S., and Bayliss, D. A. (2017) A quantized mechanism for activation of pannexin channels. *Nat Commun* **8**, 14324
14. Wang, J., and Dahl, G. (2010) SCAM analysis of Panx1 suggests a peculiar pore structure. *J Gen Physiol* **136**, 515-527

15. Sandilos, J. K., Chiu, Y. H., Chekeni, F. B., Armstrong, A. J., Walk, S. F., Ravichandran, K. S., and Bayliss, D. A. (2012) Pannexin 1, an ATP release channel, is activated by caspase cleavage of its pore-associated C-terminal autoinhibitory region. *J Biol Chem* **287**, 11303-11311
16. Dourado, M., Wong, E., and Hackos, D. H. (2014) Pannexin-1 is blocked by its C-terminus through a delocalized non-specific interaction surface. *PLoS One* **9**, e99596
17. Wang, J., Ambrosi, C., Qiu, F., Jackson, D. G., Sosinsky, G., and Dahl, G. (2014) The membrane protein Pannexin1 forms two open-channel conformations depending on the mode of activation. *Sci Signal* **7**, ra69
18. Dahl, G. (2018) The Pannexin1 membrane channel: distinct conformations and functions. *FEBS Lett* **592**, 3201-3209
19. Spagnol, G., Sorgen, P. L., and Spray, D. C. (2014) Structural order in Pannexin 1 cytoplasmic domains. *Channels (Austin)* **8**, 157-166
20. Freeman, T. J., Sayedyahosseini, S., Johnston, D., Sanchez-Pupo, R. E., O'Donnell, B., Huang, K., Lakhani, Z., Nouri-Nejad, D., Barr, K. J., Harland, L., Latosinsky, S., Grant, A., Dagnino, L., and Penuela, S. (2019) Inhibition of Pannexin 1 Reduces the Tumorigenic Properties of Human Melanoma Cells. *Cancers (Basel)* **11**
21. Langlois, S., Xiang, X., Young, K., Cowan, B. J., Penuela, S., and Cowan, K. N. (2014) Pannexin 1 and pannexin 3 channels regulate skeletal muscle myoblast proliferation and differentiation. *J Biol Chem* **289**, 30717-30731
22. Penuela, S., Celetti, S. J., Bhalla, R., Shao, Q., and Laird, D. W. (2008) Diverse subcellular distribution profiles of pannexin 1 and pannexin 3. *Cell Commun Adhes* **15**, 133-142
23. Bao, L., Locovei, S., and Dahl, G. (2004) Pannexin membrane channels are mechanosensitive conduits for ATP. *FEBS Lett* **572**, 65-68
24. Locovei, S., Bao, L., and Dahl, G. (2006) Pannexin 1 in erythrocytes: function without a gap. *Proc Natl Acad Sci U S A* **103**, 7655-7659
25. Locovei, S., Scemes, E., Qiu, F., Spray, D. C., and Dahl, G. (2007) Pannexin1 is part of the pore forming unit of the P2X(7) receptor death complex. *FEBS Lett* **581**, 483-488
26. Vanden Abeele, F., Bidaux, G., Gordienko, D., Beck, B., Panchin, Y. V., Baranova, A. V., Ivanov, D. V., Skryma, R., and Prevarskaya, N. (2006) Functional implications of calcium permeability of the channel formed by pannexin 1. *J Cell Biol* **174**, 535-546
27. Bhalla-Gehi, R., Penuela, S., Churko, J. M., Shao, Q., and Laird, D. W. (2010) Pannexin1 and pannexin3 delivery, cell surface dynamics, and cytoskeletal interactions. *J Biol Chem* **285**, 9147-9160
28. Gehi, R., Shao, Q., and Laird, D. W. (2011) Pathways regulating the trafficking and turnover of pannexin1 protein and the role of the C-terminal domain. *J Biol Chem* **286**, 27639-27653
29. Boyce, A. K., Kim, M. S., Wicki-Stordeur, L. E., and Swayne, L. A. (2015) ATP stimulates pannexin 1 internalization to endosomal compartments. *Biochem J* **470**, 319-330
30. Boyce, A. K. J., and Swayne, L. A. (2017) P2X7 receptor cross-talk regulates ATP-induced pannexin 1 internalization. *Biochem J* **474**, 2133-2144

31. Sosinsky, G. E., Boassa, D., Dermietzel, R., Duffy, H. S., Laird, D. W., MacVicar, B., Naus, C. C., Penuela, S., Scemes, E., Spray, D. C., Thompson, R. J., Zhao, H. B., and Dahl, G. (2011) Pannexin channels are not gap junction hemichannels. *Channels (Austin)* **5**, 193-197
32. Bruzzone, R., Hormuzdi, S. G., Barbe, M. T., Herb, A., and Monyer, H. (2003) Pannexins, a family of gap junction proteins expressed in brain. *Proc Natl Acad Sci U S A* **100**, 13644-13649
33. Bruzzone, R., Barbe, M. T., Jakob, N. J., and Monyer, H. (2005) Pharmacological properties of homomeric and heteromeric pannexin hemichannels expressed in *Xenopus* oocytes. *J Neurochem* **92**, 1033-1043
34. Lai, C. P., Bechberger, J. F., Thompson, R. J., MacVicar, B. A., Bruzzone, R., and Naus, C. C. (2007) Tumor-suppressive effects of pannexin 1 in C6 glioma cells. *Cancer Res* **67**, 1545-1554
35. Sahu, G., Sukumaran, S., and Bera, A. K. (2014) Pannexins form gap junctions with electrophysiological and pharmacological properties distinct from connexins. *Sci Rep* **4**, 4955
36. Boassa, D., Qiu, F., Dahl, G., and Sosinsky, G. (2008) Trafficking dynamics of glycosylated pannexin 1 proteins. *Cell Commun Adhes* **15**, 119-132
37. Lohman, A. W., Weaver, J. L., Billaud, M., Sandilos, J. K., Griffiths, R., Straub, A. C., Penuela, S., Leitinger, N., Laird, D. W., Bayliss, D. A., and Isakson, B. E. (2012) S-nitrosylation inhibits pannexin 1 channel function. *J Biol Chem* **287**, 39602-39612
38. Penuela, S., Lohman, A. W., Lai, W., Gyenis, L., Litchfield, D. W., Isakson, B. E., and Laird, D. W. (2014) Diverse post-translational modifications of the pannexin family of channel-forming proteins. *Channels (Austin)* **8**, 124-130
39. Locovei, S., Wang, J., and Dahl, G. (2006) Activation of pannexin 1 channels by ATP through P2Y receptors and by cytoplasmic calcium. *FEBS Lett* **580**, 239-244
40. Romanov, R. A., Bystrova, M. F., Rogachevskaya, O. A., Sadovnikov, V. B., Shestopalov, V. I., and Kolesnikov, S. S. (2012) The ATP permeability of pannexin 1 channels in a heterologous system and in mammalian taste cells is dispensable. *J Cell Sci* **125**, 5514-5523
41. Ma, W., Compan, V., Zheng, W., Martin, E., North, R. A., Verkhratsky, A., and Surprenant, A. (2012) Pannexin 1 forms an anion-selective channel. *Pflugers Arch* **463**, 585-592
42. Wang, J., and Dahl, G. (2018) Pannexin1: a multifunction and multiconductance and/or permeability membrane channel. *Am J Physiol Cell Physiol* **315**, C290-C299
43. Ransford, G. A., Fregien, N., Qiu, F., Dahl, G., Conner, G. E., and Salathe, M. (2009) Pannexin 1 contributes to ATP release in airway epithelia. *Am J Respir Cell Mol Biol* **41**, 525-534
44. Forsyth, A. M., Wan, J., Owrutsky, P. D., Abkarian, M., and Stone, H. A. (2011) Multiscale approach to link red blood cell dynamics, shear viscosity, and ATP release. *Proc Natl Acad Sci U S A* **108**, 10986-10991
45. Chekeni, F. B., Elliott, M. R., Sandilos, J. K., Walk, S. F., Kinchen, J. M., Lazarowski, E. R., Armstrong, A. J., Penuela, S., Laird, D. W., Salvesen, G. S., Isakson, B. E., Bayliss, D. A., and Ravichandran, K. S. (2010) Pannexin 1 channels mediate 'find-me' signal release and membrane permeability during apoptosis. *Nature* **467**, 863-867

46. Chiu, Y. H., Schappe, M. S., Desai, B. N., and Bayliss, D. A. (2018) Revisiting multimodal activation and channel properties of Pannexin 1. *J Gen Physiol* **150**, 19-39
47. Penuela, S., Bhalla, R., Nag, K., and Laird, D. W. (2009) Glycosylation regulates pannexin intermixing and cellular localization. *Mol Biol Cell* **20**, 4313-4323
48. Prochnow, N., Hoffmann, S., Vroman, R., Klooster, J., Bunse, S., Kamermans, M., Dermietzel, R., and Zoidl, G. (2009) Pannexin1 in the outer retina of the zebrafish, *Danio rerio*. *Neuroscience* **162**, 1039-1054
49. Bunse, S., Schmidt, M., Hoffmann, S., Engelhardt, K., Zoidl, G., and Dermietzel, R. (2011) Single cysteines in the extracellular and transmembrane regions modulate pannexin 1 channel function. *J Membr Biol* **244**, 21-33
50. Sang, Q., Zhang, Z., Shi, J., Sun, X., Li, B., Yan, Z., Xue, S., Ai, A., Lyu, Q., Li, W., Zhang, J., Wu, L., Mao, X., Chen, B., Mu, J., Li, Q., Du, J., Sun, Q., Jin, L., He, L., Zhu, S., Kuang, Y., and Wang, L. (2019) A pannexin 1 channelopathy causes human oocyte death. *Sci Transl Med* **11**
51. DeLalio, L. J., Billaud, M., Ruddiman, C. A., Johnstone, S. R., Butcher, J. T., Wolpe, A. G., Jin, X., Keller, T. C. S. t., Keller, A. S., Riviere, T., Good, M. E., Best, A. K., Lohman, A. W., Swayne, L. A., Penuela, S., Thompson, R. J., Lampe, P. D., Yeager, M. Y., and Isakson, B. E. (2019) Constitutive SRC-mediated phosphorylation of pannexin 1 at tyrosine 198 occurs at the plasma membrane. *J Biol Chem*
52. Lohman, A. W., Leskov, I. L., Butcher, J. T., Johnstone, S. R., Stokes, T. A., Begandt, D., DeLalio, L. J., Best, A. K., Penuela, S., Leitinger, N., Ravichandran, K. S., Stokes, K. Y., and Isakson, B. E. (2015) Pannexin 1 channels regulate leukocyte emigration through the venous endothelium during acute inflammation. *Nat Commun* **6**, 7965
53. Weilinger, N. L., Lohman, A. W., Rakai, B. D., Ma, E. M., Bialecki, J., Maslieieva, V., Rilea, T., Bandet, M. V., Ikuta, N. T., Scott, L., Colicos, M. A., Teskey, G. C., Winship, I. R., and Thompson, R. J. (2016) Metabotropic NMDA receptor signaling couples Src family kinases to pannexin-1 during excitotoxicity. *Nat Neurosci* **19**, 432-442
54. Thompson, R. J., Zhou, N., and MacVicar, B. A. (2006) Ischemia opens neuronal gap junction hemichannels. *Science* **312**, 924-927
55. Weilinger, N. L., Tang, P. L., and Thompson, R. J. (2012) Anoxia-induced NMDA receptor activation opens pannexin channels via Src family kinases. *J Neurosci* **32**, 12579-12588
56. DeLalio, L. J., Keller, A. S., Chen, J., Boyce, A. K. J., Artamonov, M. V., Askew-Page, H. R., Keller, T. C. S. t., Johnstone, S. R., Weaver, R. B., Good, M. E., Murphy, S. A., Best, A. K., Mintz, E. L., Penuela, S., Greenwood, I. A., Machado, R. F., Somlyo, A. V., Swayne, L. A., Minshall, R. D., and Isakson, B. E. (2018) Interaction Between Pannexin 1 and Caveolin-1 in Smooth Muscle Can Regulate Blood Pressure. *Arterioscler Thromb Vasc Biol* **38**, 2065-2078
57. Iglesias, R., Locovei, S., Roque, A., Alberto, A. P., Dahl, G., Spray, D. C., and Scemes, E. (2008) P2X7 receptor-Pannexin1 complex: pharmacology and signaling. *Am J Physiol Cell Physiol* **295**, C752-760
58. Billaud, M., Chiu, Y. H., Lohman, A. W., Parpaite, T., Butcher, J. T., Mutchler, S. M., DeLalio, L. J., Artamonov, M. V., Sandilos, J. K., Best, A. K., Somlyo, A. V.,

- Thompson, R. J., Le, T. H., Ravichandran, K. S., Bayliss, D. A., and Isakson, B. E. (2015) A molecular signature in the pannexin1 intracellular loop confers channel activation by the alpha1 adrenoreceptor in smooth muscle cells. *Sci Signal* **8**, ra17
59. Riquelme, M. A., Cea, L. A., Vega, J. L., Boric, M. P., Monyer, H., Bennett, M. V., Frank, M., Willecke, K., and Saez, J. C. (2013) The ATP required for potentiation of skeletal muscle contraction is released via pannexin hemichannels. *Neuropharmacology* **75**, 594-603
 60. Poornima, V., Vallabhaneni, S., Mukhopadhyay, M., and Bera, A. K. (2015) Nitric oxide inhibits the pannexin 1 channel through a cGMP-PKG dependent pathway. *Nitric Oxide* **47**, 77-84
 61. Zhang, L., Deng, T., Sun, Y., Liu, K., Yang, Y., and Zheng, X. (2008) Role for nitric oxide in permeability of hippocampal neuronal hemichannels during oxygen glucose deprivation. *J Neurosci Res* **86**, 2281-2291
 62. Bunse, S., Schmidt, M., Prochnow, N., Zoidl, G., and Dermietzel, R. (2010) Intracellular cysteine 346 is essentially involved in regulating Panx1 channel activity. *J Biol Chem* **285**, 38444-38452
 63. Wicki-Stordeur, L. E., Boyce, A. K., and Swayne, L. A. (2013) Analysis of a pannexin 2-pannexin 1 chimeric protein supports divergent roles for pannexin C-termini in cellular localization. *Cell Commun Adhes* **20**, 73-79
 64. Krick, S., Wang, J., St-Pierre, M., Gonzalez, C., Dahl, G., and Salathe, M. (2016) Dual Oxidase 2 (Duox2) Regulates Pannexin 1-mediated ATP Release in Primary Human Airway Epithelial Cells via Changes in Intracellular pH and Not H2O2 Production. *J Biol Chem* **291**, 6423-6432
 65. Dvorianchikova, G., Ivanov, D., Panchin, Y., and Shestopalov, V. I. (2006) Expression of pannexin family of proteins in the retina. *FEBS Lett* **580**, 2178-2182
 66. Jiang, J. X., and Penuela, S. (2016) Connexin and pannexin channels in cancer. *BMC Cell Biol* **17 Suppl 1**, 12
 67. Kim, J. E., and Kang, T. C. (2011) The P2X7 receptor-pannexin-1 complex decreases muscarinic acetylcholine receptor-mediated seizure susceptibility in mice. *J Clin Invest* **121**, 2037-2047
 68. Orellana, J. A., Froger, N., Ezan, P., Jiang, J. X., Bennett, M. V., Naus, C. C., Giaume, C., and Saez, J. C. (2011) ATP and glutamate released via astroglial connexin 43 hemichannels mediate neuronal death through activation of pannexin 1 hemichannels. *J Neurochem* **118**, 826-840
 69. Riteau, N., Baron, L., Villeret, B., Guillou, N., Savigny, F., Ryffel, B., Rassendren, F., Le Bert, M., Gombault, A., and Couillin, I. (2012) ATP release and purinergic signaling: a common pathway for particle-mediated inflammasome activation. *Cell Death Dis* **3**, e403
 70. Dosch, M., Gerber, J., Jebbawi, F., and Beldi, G. (2018) Mechanisms of ATP Release by Inflammatory Cells. *Int J Mol Sci* **19**
 71. Silverman, W. R., de Rivero Vaccari, J. P., Locovei, S., Qiu, F., Carlsson, S. K., Scemes, E., Keane, R. W., and Dahl, G. (2009) The pannexin 1 channel activates the inflammasome in neurons and astrocytes. *J Biol Chem* **284**, 18143-18151
 72. Guo, H., Callaway, J. B., and Ting, J. P. (2015) Inflammasomes: mechanism of action, role in disease, and therapeutics. *Nat Med* **21**, 677-687

73. Qu, Y., Misaghi, S., Newton, K., Gilmour, L. L., Louie, S., Cupp, J. E., Dubyak, G. R., Hackos, D., and Dixit, V. M. (2011) Pannexin-1 is required for ATP release during apoptosis but not for inflammasome activation. *J Immunol* **186**, 6553-6561
74. Gulbransen, B. D., Bashashati, M., Hirota, S. A., Gui, X., Roberts, J. A., MacDonald, J. A., Muruve, D. A., McKay, D. M., Beck, P. L., Mawe, G. M., Thompson, R. J., and Sharkey, K. A. (2012) Activation of neuronal P2X7 receptor-pannexin-1 mediates death of enteric neurons during colitis. *Nat Med* **18**, 600-604
75. Seror, C., Melki, M. T., Subra, F., Raza, S. Q., Bras, M., Saidi, H., Nardacci, R., Voisin, L., Paoletti, A., Law, F., Martins, I., Amendola, A., Abdul-Sater, A. A., Ciccocanti, F., Delelis, O., Niedergang, F., Thierry, S., Said-Sadier, N., Lamaze, C., Metivier, D., Estaquier, J., Fimia, G. M., Falasca, L., Casetti, R., Modjtahedi, N., Kanellopoulos, J., Mouscadet, J. F., Ojcius, D. M., Piacentini, M., Gougeon, M. L., Kroemer, G., and Perfettini, J. L. (2011) Extracellular ATP acts on P2Y2 purinergic receptors to facilitate HIV-1 infection. *J Exp Med* **208**, 1823-1834
76. Lee, V. R., Barr, K. J., Kelly, J. J., Johnston, D., Brown, C. F. C., Robb, K. P., Sayedyahosseini, S., Huang, K., Gros, R., Flynn, L. E., and Penuela, S. (2018) Pannexin 1 regulates adipose stromal cell differentiation and fat accumulation. *Sci Rep* **8**, 16166
77. Negoro, H., Lutz, S. E., Liou, L. S., Kanematsu, A., Ogawa, O., Scemes, E., and Suadican, S. O. (2013) Pannexin 1 involvement in bladder dysfunction in a multiple sclerosis model. *Sci Rep* **3**, 2152
78. Karatas, H., Erdener, S. E., Gursoy-Ozdemir, Y., Lule, S., Eren-Kocak, E., Sen, Z. D., and Dalkara, T. (2013) Spreading depression triggers headache by activating neuronal Panx1 channels. *Science* **339**, 1092-1095
79. Bao, B. A., Lai, C. P., Naus, C. C., and Morgan, J. R. (2012) Pannexin1 drives multicellular aggregate compaction via a signaling cascade that remodels the actin cytoskeleton. *J Biol Chem* **287**, 8407-8416
80. Cowan, K. N., Langlois, S., Penuela, S., Cowan, B. J., and Laird, D. W. (2012) Pannexin1 and Pannexin3 exhibit distinct localization patterns in human skin appendages and are regulated during keratinocyte differentiation and carcinogenesis. *Cell Commun Adhes* **19**, 45-53
81. Sato, T., Neschadim, A., Lavie, A., Yanagisawa, T., and Medin, J. A. (2013) The engineered thymidylate kinase (TMPK)/AZT enzyme-prodrug axis offers efficient bystander cell killing for suicide gene therapy of cancer. *PLoS One* **8**, e78711
82. Derangere, V., Chevriaux, A., Courtaut, F., Bruchard, M., Berger, H., Chalmin, F., Causse, S. Z., Limagne, E., Vegran, F., Ladoire, S., Simon, B., Boireau, W., Hichami, A., Apetoh, L., Mignot, G., Ghiringhelli, F., and Rebe, C. (2014) Liver X receptor beta activation induces pyroptosis of human and murine colon cancer cells. *Cell Death Differ* **21**, 1914-1924
83. Furlow, P. W., Zhang, S., Soong, T. D., Halberg, N., Goodarzi, H., Mangrum, C., Wu, Y. G., Elemento, O., and Tavazoie, S. F. (2015) Mechanosensitive pannexin-1 channels mediate microvascular metastatic cell survival. *Nat Cell Biol* **17**, 943-952
84. Song, B., Tang, J. W., Wang, B., Cui, X. N., Hou, L., Sun, L., Mao, L. M., Zhou, C. H., Du, Y., Wang, L. H., Wang, H. X., Zheng, R. S., and Sun, L. (2005) Identify lymphatic metastasis-associated genes in mouse hepatocarcinoma cell lines using gene chip. *World J Gastroenterol* **11**, 1463-1472

85. Largo, C., Alvarez, S., Saez, B., Blesa, D., Martin-Subero, J. I., Gonzalez-Garcia, I., Brieva, J. A., Dopazo, J., Siebert, R., Calasanz, M. J., and Cigudosa, J. C. (2006) Identification of overexpressed genes in frequently gained/amplified chromosome regions in multiple myeloma. *Haematologica* **91**, 184-191
86. Boyd-Tressler, A., Penuela, S., Laird, D. W., and Dubyak, G. R. (2014) Chemotherapeutic drugs induce ATP release via caspase-gated pannexin-1 channels and a caspase/pannexin-1-independent mechanism. *J Biol Chem* **289**, 27246-27263
87. Schalper, K. A., Carvajal-Hausdorf, D., and Oyarzo, M. P. (2014) Possible role of hemichannels in cancer. *Front Physiol* **5**, 237
88. Cerami, E., Gao, J., Dogrusoz, U., Gross, B. E., Sumer, S. O., Aksoy, B. A., Jacobsen, A., Byrne, C. J., Heuer, M. L., Larsson, E., Antipin, Y., Reva, B., Goldberg, A. P., Sander, C., and Schultz, N. (2012) The cBio cancer genomics portal: an open platform for exploring multidimensional cancer genomics data. *Cancer Discov* **2**, 401-404
89. Gao, J., Aksoy, B. A., Dogrusoz, U., Dresdner, G., Gross, B., Sumer, S. O., Sun, Y., Jacobsen, A., Sinha, R., Larsson, E., Cerami, E., Sander, C., and Schultz, N. (2013) Integrative analysis of complex cancer genomics and clinical profiles using the cBioPortal. *Sci Signal* **6**, p11
90. Wei, L., Yang, X., Shi, X., and Chen, Y. (2015) Pannexin1 silencing inhibits the proliferation of U87MG cells. *Mol Med Rep* **11**, 3487-3492
91. Penuela, S., Gyenis, L., Ablack, A., Churko, J. M., Berger, A. C., Litchfield, D. W., Lewis, J. D., and Laird, D. W. (2012) Loss of pannexin 1 attenuates melanoma progression by reversion to a melanocytic phenotype. *J Biol Chem* **287**, 29184-29193
92. Molica, F., Morel, S., Meens, M. J., Denis, J. F., Bradfield, P. F., Penuela, S., Zufferey, A., Monyer, H., Imhof, B. A., Chanson, M., Laird, D. W., Fontana, P., and Kwak, B. R. (2015) Functional role of a polymorphism in the Pannexin1 gene in collagen-induced platelet aggregation. *Thromb Haemost* **114**, 325-336
93. Shao, Q., Lindstrom, K., Shi, R., Kelly, J., Schroeder, A., Juusola, J., Levine, K. L., Esseltine, J. L., Penuela, S., Jackson, M. F., and Laird, D. W. (2016) A Germline Variant in the PANX1 Gene Has Reduced Channel Function and Is Associated with Multisystem Dysfunction. *J Biol Chem* **291**, 12432-12443
94. Stierlin, F. B., Molica, F., Reny, J. L., Kwak, B. R., and Fontana, P. (2017) Pannexin1 Single Nucleotide Polymorphism and Platelet Reactivity in a Cohort of Cardiovascular Patients. *Cell Commun Adhes* **23**, 11-15
95. Davis, L. K., Gamazon, E. R., Kistner-Griffin, E., Badner, J. A., Liu, C., Cook, E. H., Sutcliffe, J. S., and Cox, N. J. (2012) Loci nominally associated with autism from genome-wide analysis show enrichment of brain expression quantitative trait loci but not lymphoblastoid cell line expression quantitative trait loci. *Mol Autism* **3**, 3
96. Gawlik, M., Wagner, M., Pfuhlmann, B., and Stober, G. (2016) The role of Pannexin gene variants in schizophrenia: systematic analysis of phenotypes. *Eur Arch Psychiatry Clin Neurosci* **266**, 433-437
97. Lek, M., Karczewski, K. J., Minikel, E. V., Samocha, K. E., Banks, E., Fennell, T., O'Donnell-Luria, A. H., Ware, J. S., Hill, A. J., Cummings, B. B., Tukiainen, T., Birnbaum, D. P., Kosmicki, J. A., Duncan, L. E., Estrada, K., Zhao, F., Zou, J.,

- Pierce-Hoffman, E., Berghout, J., Cooper, D. N., Deflaux, N., DePristo, M., Do, R., Flannick, J., Fromer, M., Gauthier, L., Goldstein, J., Gupta, N., Howrigan, D., Kiezun, A., Kurki, M. I., Moonshine, A. L., Natarajan, P., Orozco, L., Peloso, G. M., Poplin, R., Rivas, M. A., Ruano-Rubio, V., Rose, S. A., Ruderfer, D. M., Shakir, K., Stenson, P. D., Stevens, C., Thomas, B. P., Tiao, G., Tusie-Luna, M. T., Weisburd, B., Won, H. H., Yu, D., Altshuler, D. M., Ardissino, D., Boehnke, M., Danesh, J., Donnelly, S., Elosua, R., Florez, J. C., Gabriel, S. B., Getz, G., Glatt, S. J., Hultman, C. M., Kathiresan, S., Laakso, M., McCarroll, S., McCarthy, M. I., McGovern, D., McPherson, R., Neale, B. M., Palotie, A., Purcell, S. M., Saleheen, D., Scharf, J. M., Sklar, P., Sullivan, P. F., Tuomilehto, J., Tsuang, M. T., Watkins, H. C., Wilson, J. G., Daly, M. J., MacArthur, D. G., and Exome Aggregation, C. (2016) Analysis of protein-coding genetic variation in 60,706 humans. *Nature* **536**, 285-291
98. Zlotogora, J., Patrinos, G. P., and Meiner, V. (2018) Ashkenazi Jewish genomic variants: integrating data from the Israeli National Genetic Database and gnomAD. *Genet Med* **20**, 867-871
99. Zhang, J., Baran, J., Cros, A., Guberman, J. M., Haider, S., Hsu, J., Liang, Y., Rivkin, E., Wang, J., Whitty, B., Wong-Erasmus, M., Yao, L., and Kasprzyk, A. (2011) International Cancer Genome Consortium Data Portal--a one-stop shop for cancer genomics data. *Database (Oxford)* **2011**, bar026

Chapter 2

2 Manuscript

<p style="text-align: center;">Diverse outcomes of PANX1 genetic variants on post-translational modifications and channel function</p>
<p>Daniel Nouri-Nejad¹, Brooke O'Donnell¹, Chetan Patil², Danielle Johnston¹, Rafael Sanchez-Pupo¹, Samar Sayedyahosseini¹, Kristina Jurcic³, David Litchfield^{3,4}, Gregory Gloor³, Michael Jackson², Silvia Penuela^{1,4*}</p>
<p>¹Department of Anatomy and Cell Biology, Western University, London, Ontario N6A 5C1, Canada, ²Department of Department of Pharmacology & Therapeutics, University of Manitoba, Winnipeg, Manitoba R3E 0T6, Canada, ³Department of Biochemistry, Western University, London, Ontario N6A 5C1, Canada, and ⁴Department of Oncology, Division of Experimental Oncology, Western University, London, Ontario N6A 5C1, Canada.</p>
<p>*To whom correspondence should be addressed: Dept. of Anatomy and Cell Biology, Western University, London, Ontario N6A 5C1, Canada. Tel.: 519-661-2111, ex. 84735; E-mail: spenuela@uwo.ca.</p>
<p>Keywords: Pannexin 1, PANX1, pannexin, phosphorylation, glycosylation, trafficking, polymorphism.</p>
<p>Running Title: Analyses of <i>PANX1</i> variants</p>

2.1 Contributions of Authors

Daniel Nouri Nejad designed the project, performed experiments and data analysis as well as wrote the manuscript. Brooke O'Donnell assisted with generating Figure 2.1C. Chetan Patil performed whole-cell patch-clamp electrophysiology experiments and performed data analysis demonstrated in Figure 2.5B-C. Danielle Johnston generated Hs578T(KO) cells. Rafael Sanchez-Pupo assisted in preparing samples for mass-spectrometry. Samar Sayedyahosseini generated A375P(KO) cells. Kristina Jurcic performed electrospray-ionization mass-spectrometry and assisted with analyzing mass-spectrometry data. David Litchfield supervised and facilitated proteomic analysis. Gregory Gloor wrote and executed programming to assess allele frequencies of pannexin 1 variants in cancer cohorts. Silvia Penuela designed the project, supervised the experiments, and edited the manuscript.

2.2 Abstract

Pannexin 1 (PANX1) is a glycoprotein capable of forming large pore channels permeable to important signaling molecules such as ATP. In this study, we interrogated different domains of PANX1 by introducing naturally occurring variants reported in cancer and cell lines and assessed their impact on channel function. We discovered a novel tyrosine phosphorylation site at Y150, that when disrupted via a missense mutation resulted in hypo-glycosylation of PANX1, increased cell-surface localization, and dye uptake. We also discovered that the Q5H variant has a greater allele frequency than the wildtype Q5 in both global and cancer cohorts but was not associated with cancer aggressiveness. Furthermore, although Q5 and Q5H did not differ in N-glycosylation, localization or function in cancer cells, we uncovered that 90% of humans carry at least one Q5H allele, which is in fact the conserved ancestral allele of PANX1. Overall, this study demonstrated that other post-translational modifications have the capacity to affect cell-surface PANX1 localization, and we identified a highly prevalent *PANX1* variant in human populations.

2.3 Introduction

Since its discovery in 2000 (1), Pannexin 1 (PANX1 in human, Panx1 in rodents), a channel-forming glycoprotein that mediates the release of signaling molecules below 1 kDa in size, has been emerging as a key player in various physiological and pathological contexts ranging from blood pressure regulation (2,3), skin cell differentiation (4,5), facilitating neuronal cell death in ischemic conditions (7,8), apoptosis and inflammation (9-11), to regulating tumorigenic properties of cancers like melanoma (12,13). Depending on the cellular context and localization of the channel, PANX1 presents different functions. Most studies report PANX1 to be localized at the cell surface and is best-characterized to function as an ATP release channel (14) while others report PANX1 to be found intracellularly within the endoplasmic reticulum (ER) acting as an ER calcium-leak channel (15).

PANX1 is characterized as a tetra-spanning protein with intracellular N- and C-termini and conserved cysteine residues within both extracellular loops (16), and several domains that regulate PANX1 trafficking and channel function have been identified. The intracellular loop and C-terminus have been demonstrated to undergo both tyrosine and serine phosphorylation which has been linked to overall channel function. Disruption of the tyrosine phosphorylation sites, Y198 or Y308, either by mutagenesis or peptide inhibition interferes with Panx1 interactions with N-methyl-D-aspartate receptors (NMDARs) and α 1-adrenergic receptors, and affects channel function (17-19). The first extracellular loop regulates ATP-induced cholesterol-dependent internalization of the channel through its ATP-sensitive W74 residue (20) whereas the second extracellular loop undergoes N-linked

glycosylation on N254 which regulates cell-surface trafficking and intermixing with other Pannexin members (21). Due to the differential N-glycosylation that PANX1 undergoes, the protein is present as three distinct species: the non-glycosylated Gly0 species, the high-mannose ER-resident Gly1 species, and the complex glycosylated Gly2 species which forms in the Golgi (22,23). While all three different species are capable of trafficking to the surface, Gly2 species are more prevalent at the cell membrane (21). PANX1 also undergoes S-nitrosylation at C40 of the N-terminus and C346 of the C-terminus of which inhibits channel function (24). Finally, the channel has been demonstrated to be regulated by the C-terminus in a “ball-and-chain” manner and proteolytic caspase cleavage of the C-terminus results in a constitutively-active channel (10,25).

Only a few recent studies have analyzed the effects of common and rare naturally occurring *PANX1* variants. The first report associating a PANX1 mutation to a physiological disorder was a germline loss-of-function mutant, R217H, that was reported in a young female with intellectual disability, short stature, sensorineural hearing loss, primary ovarian failure, and kyphosis (26). In another report, a somatic nonsense mutation, Q89*, was found to be enriched in two metastatic breast cancer cell lines. The truncated protein Q89* was found to enhance PANX1-mediated ATP release only when co-expressed with full-length PANX1, and was shown to enhance the metastatic efficiency of breast cancer cells by reducing deformation-induced P2Y-mediated apoptosis in areas of microvasculature (27). A recent report revealed *PANX1* germline mutations that caused familial or sporadic female infertility by inducing oocyte cell death. They uncovered four germline mutations (K346E, C347S, Q392*, and p.21_23delITEP) that produced gain-of-function, hypo-glycosylated

mutants consisting of predominantly Gly0 and Gly1 species (28). Finally, one variant that has been commonly reported is a missense variant, Q5H, which has been shown to be associated with collagen-induced platelet reactivity in healthy subjects and displayed enhanced ATP release when ectopically expressed (29). The same group later showed that the variant was not associated with platelet reactivity in stable cardiovascular patients in separate cohorts from the prior study (30). In a separate genome-wide association study (GWAS) identifying common variants associated with autism susceptibility risk, they found *PANX1* to be implicated *in cis* using multiple single-nucleotide polymorphisms (SNPs) that included Q5H (31). Another GWAS study investigating associations of common pannexin variants with Schizophrenia found no associations between Q5H and Schizophrenia (32).

Analyses of these and other naturally occurring variants may provide further information about the domains they reside in and how they might affect functional and biochemical properties of PANX1. In this study, we interrogated three motifs of the PANX1 polypeptide using single amino acid changes and evaluated their role in cell-surface PANX1 function. We introduced seven *PANX1* naturally occurring variants reported in tumours of melanoma patients and human melanoma cell lines. These variants included Q5H, Y150F, G168E, T176I, H190Y, S239L, and Q264* that are in the N-terminus, intracellular loop, and second extracellular loop of the PANX1 polypeptide.

By probing these important motifs, we have uncovered Y150 as a novel tyrosine phosphorylation site that can alter N-glycosylation, trafficking and channel function. In

addition, Q5H is equal to Q5 in channel function, glycosylation, and cell-surface localization in human breast cancer cells. We also discovered Q5H to have a higher allele frequency than Q5 in cancer cohorts but was not associated with cancer aggressiveness. The higher allele prevalence of Q5H than Q5 was also demonstrated in global cohorts and has emerged to be the ancestral allele at this locus.

2.4 Results

Y150F alters normal PANX1 protein banding pattern indicative of glycosylation states

Seven *PANX1* variants identified in tumors of melanoma patients and several established cancer cell lines (**Fig. 2.1A**; **Suppl. Fig. 2.1**) in addition to wildtype (denoted as Q5 from here forth) were assessed initially for their effects on PANX1 glycosylation and localization to investigate any changes that may result in altered PANX1 function. Differential N-glycosylation of PANX1 can occur and be preliminarily inferred by observing the protein banding pattern of PANX1 consisting of Gly0, Gly1, and Gly2 species (22).

Due to their relatively low Panx1 endogenous expression (33) and large cytoplasm for identification of PANX1 localization, normal rat kidney (NRK) cells were used to transiently over-express the various *PANX1* variants. Most of the variants, except for Y150F and Q264*, produced PANX1 banding patterns like Q5 consisting of Gly0, Gly1, and Gly2 (**Fig. 2.1B**). Y150F instead produced predominantly Gly1 species with notably reduced Gly2 and Gly0 species. The Q264* variant, which produces a truncated mutant

lacking the carboxyl-terminus and thus required detection with an antibody targeting the amino-terminus, was not detected at the protein level (**Fig. 2.1C**), despite the presence of mRNA transcripts encoding the mutant (data not shown). Moreover, immunofluorescence analyses revealed that all PANX1 variants localized at the cell surface in NRK cells (**Fig. 2.1D**). As a result of Y150F altering the normal PANX1 banding pattern and Q5H being previously reported to enhance PANX1-mediated ATP release (29), we chose these two variants for further investigation.

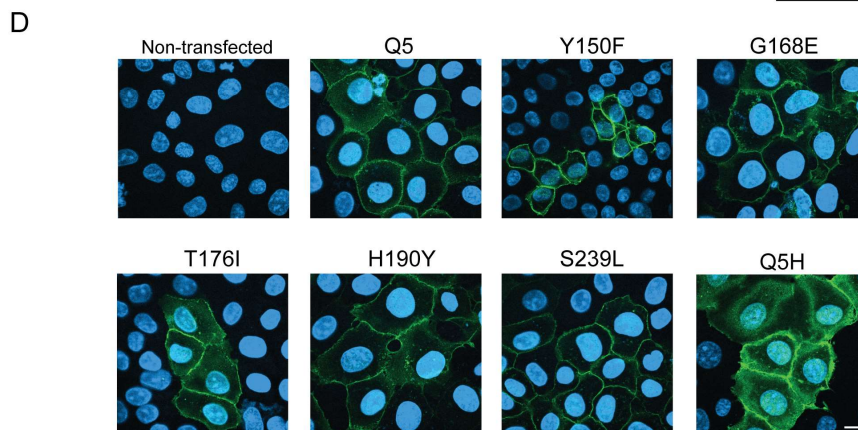
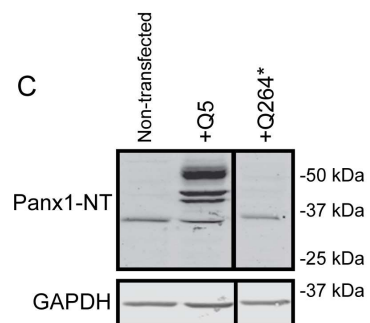
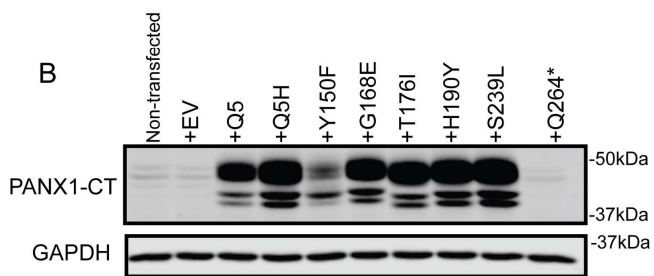
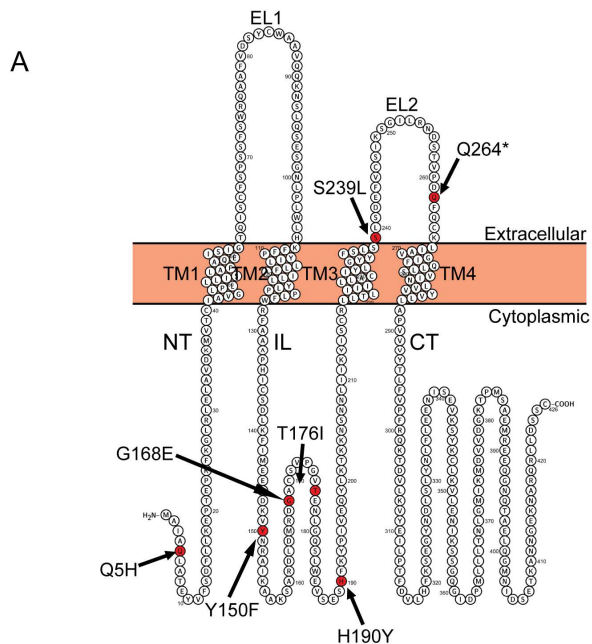


Figure 2.1: Y150F alters normal banding patterns of PANX1 in NRK cells. **A.** Schematic of PANX1 polypeptide demonstrating location of *PANX1* variants Q5H, Y150F, G168E, T176I, H190Y, S239L, and Q264*. Schematic was generated using Protter (6). EV: empty-vector, NT: amino-terminus, TM: transmembrane, EL: extracellular loop, CT: carboxyl-terminus, IL: intracellular loop. **B.** NRK cells were transfected to transiently overexpress selected *PANX1* variants and PANX1 banding pattern was assessed 72 hours post-transfection. Immunoblotting revealed Y150F to disrupt normal banding pattern of PANX1, resulting in primarily Gly1 with minimal Gly0 and Gly2 species. **C.** PANX1 protein was not detected in NRK cells with Q264* using two different antibodies against the CT or the NT. The molecular weight of Q264* is expected to be approximately around 29 kDa. GAPDH was used as a loading control. Protein sizes in kDa. **D.** Immunofluorescence analyses revealed all variants appeared to localize to the cell-surface upon ectopic expression in NRK cells. Bar: 10 μ m.

To eliminate all endogenous wildtype PANX1 that may facilitate the trafficking and glycosylation of the mutants, we generated two cancer cell lines engineered using CRISPR/Cas9 to delete the *PANX1* gene and eliminate PANX1 expression (KO): the human triple-negative breast cancer cell, Hs578T(KO), and human melanoma cell line A375P(KO). Transient overexpression of Q5H and Y150F reproduced a similarly altered PANX1 banding pattern of Y150F consisting of predominantly Gly1 with minimal Gly2 species (**Fig 2.2A**) and cell-surface localization as observed in NRK cells even in the absence of endogenous PANX1 (**Fig. 2.3A**).

The differential banding pattern of Y150F species in NRK, Hs578T(KO), and A375P(KO) cells indicated that Y150F may be experiencing a differential glycosylation process or other post-translational modifications. To confirm N-linked glycosylation is present

throughout the various bands of Q5H and Y150F, we incubated protein samples from Hs578T(KO) overexpressing empty vector (EV), Q5, Q5H, and Y150F with PNGase F, which recognizes and cleaves all N-linked glycosylation that is manifested in Gly1 species and maintained in Gly2 species of wildtype PANX1. This resulted in the downwards shift of all bands to Gly0, indicating the presence of N-linked glycosylation in all bands above Gly0 (**Fig. 2.2B**). Furthermore, we applied EndoH, a de-glycosylation enzyme that cleaves only high-mannose glycosylation as encountered in Gly1 species. Application of EndoH to EV, Q5, Q5H, and Y150F protein lysates resulted in complete digestion and downwards shift of Gly1 band to Gly0 for Q5 and Q5H samples but only a partial digestion of Gly1 species in Y150F lysates (**Fig. 2.2B**), indicating Y150F receives a different editing of the high-mannose species subsequent to its addition.

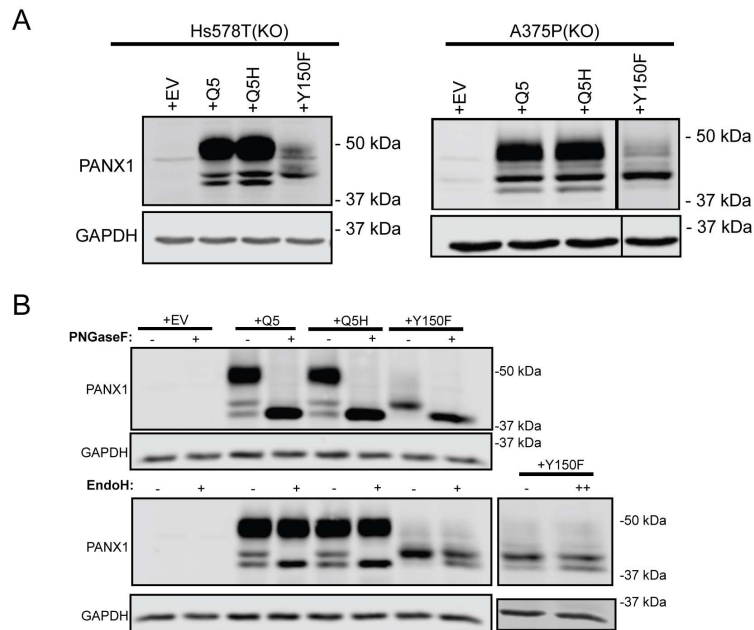


Figure 2.2: Y150F produces a Gly1 species that is partially resistant to EndoH de-glycosylation. **A.** Hs578T(KO) cells and A375P(KO) cells devoid of PANX1 were used to transiently over-express empty-vector (EV), Q5, Q5H, and Y150F and assessed for changes in PANX1 banding pattern via immunoblotting. Western blot analyses revealed that Y150F disrupted the normal banding pattern in both cell lines, resulting in primarily Gly1 species. **B.** PNGaseF digestion of protein lysates from Hs578T(KO) transiently overexpressing PANX1 variants and controls (N=3). EndoH digestion of protein lysates from Hs578T(KO) transiently overexpressing PANX1 variants and controls, resulted in the downwards shift of Gly1 species of Q5 and Q5H to Gly0 band. In contrast, Y150F was partially resistant to EndoH digestion, even when the amount of Endo H was doubled (++). GAPDH was used as a loading control. Representative blots of N=3.

Greater amounts of Y150F Gly1 species detected at the cell-surface

Regulation of PANX1 function is dependent on various factors including the amount of PANX1 localized at the cell surface. Immunofluorescence analyses revealed the capacity of all variants to traffic to the cell surface in NRK (**Fig. 2.1D**), Hs578T(KO), and A375P(KO) cells (**Fig. 2.3A**). To quantify the amount of PANX1 variants at the cell-surface, cell-surface protein biotinylation was performed on Hs578T(KO) transiently expressing EV, Q5, Q5H, and Y150F. Quantification of cell-surface PANX1 protein biotinylation revealed Y150F to be more abundant at the cell surface relative to Q5 and Q5H (**Fig 2.3B-C**). While Q5 and Q5H presented significantly greater Gly2 species than Gly0 and Gly1, Y150F demonstrated similar amounts of Gly2 and Gly1, albeit both at significantly greater quantities than Gly0 (**Fig. 2.3D**). Furthermore, in contrast with Q5 and Q5H in which greater Gly2 species were detected at the cell surface, greater Gly1 and less Gly2 species were detected in pull-down of cell-surface proteins of Y150F (**Fig. 2.3E**).

Contrasting with the previous finding, when higher amounts of Y150F plasmid DNA were used in the transfection (5x increase), we noted that the greater over-expression of Y150F in NRK cells resulted in predominantly intracellular localization of the protein which differs from the cell-surface localization profile of Q5 even at higher DNA concentrations (Suppl. Fig. 2.2A). However, the altered banding pattern of Y150F remained the same as described above (Suppl. Fig. 2.2B). Furthermore, greater Y150F expression also significantly reduced cell viability relative to EV- and Q5-transfected NRK cells while lower expression of the mutant did not affect viability (Suppl. Fig. 2.2C).

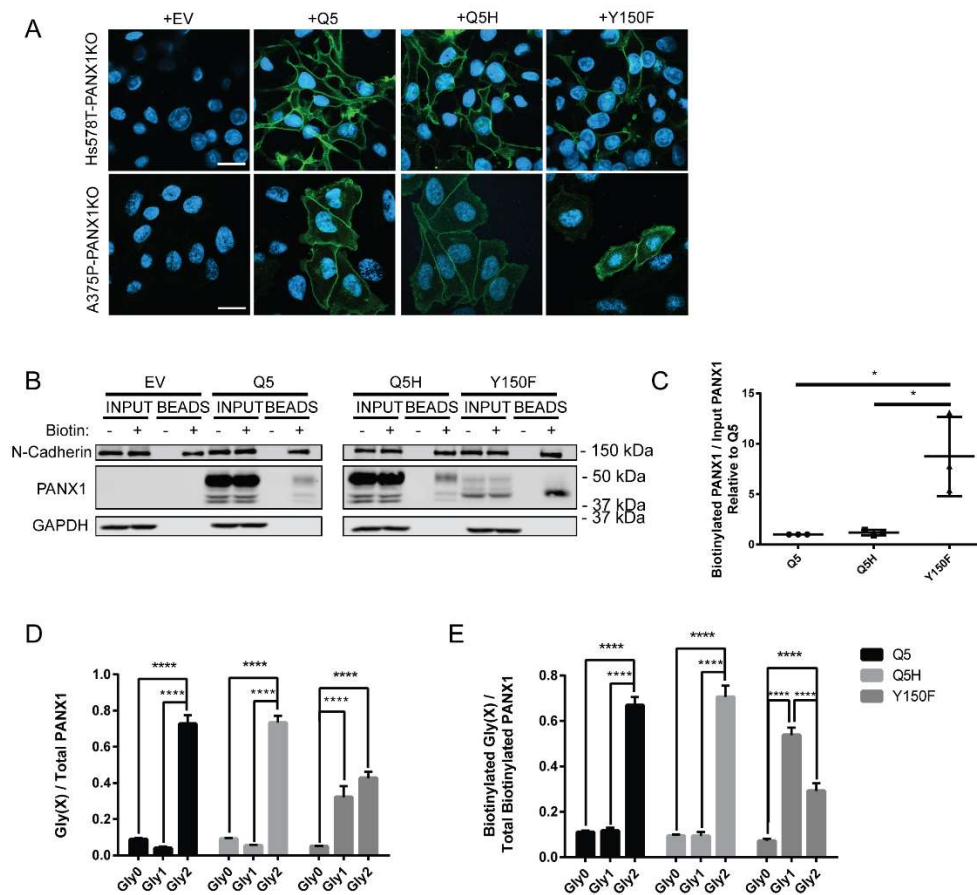


Figure 2.3: Greater amounts of Y150F Gly1 localize at the cell-surface relative to Q5 and Q5H. **A.** Hs578T(KO) and A375P(KO) transiently overexpressing EV, Q5, Q5H, and Y150F were assessed for PANX1 localization via immunofluorescence. (N=3), Bars: 20 μ m. **B.** Cell-surface protein biotinylation was performed on Hs578T(KO) cells transiently over-expressing PANX1 variants (One-way ANOVA; * $p < 0.05$; N=3). N-Cadherin was used as positive cell-surface control and GAPDH as a negative control. **C.** Quantification of cell-surface biotinylation assay of Hs578T(KO) transiently overexpressing PANX1 variants (N=3). **D.** Quantification of individual bands of biotinylated PANX1 relative to total biotinylated PANX1 protein in input lysates (One-way ANOVA; N=3; **** $P < 0.0001$). **E.** Quantification of individual PANX1 bands (Gly0, 1, 2) relative to total biotinylated PANX1 (One-way ANOVA; N=3; **** $p < 0.0001$)

Y150 is a tyrosine phosphorylation site of PANX1

The Y150 site (146-LDKVYNRAI-154) has been predicted to be phosphorylated by epidermal growth factor receptor (EGFR), insulin receptor (INSR) and sarcoma (SRC) kinase, as determined by the phosphorylation prediction software NetPhos 3. (34). Phosphorylation of Y150 (Y150-P) of PANX1 was also previously identified in a high-throughput screening study for tyrosine-phosphorylated proteins in a human leukemic cell line identified by mass spectrometry (35).

To determine whether Y150 is phosphorylated in Hs578T(KO) cells ectopically expressing PANX1, we immunoprecipitated PANX1 species from Hs578T(KO) cells overexpressing EV, Q5, Q5H, or Y150F and sent individual band samples from the different glycosylated species (Gly-0, Gly-1, and Gly-2) for Electrospray Ionization (ESI) mass spectrometry to

identify peptides containing phosphorylated Y150, non-phosphorylated Y150, and peptides containing Y150F (**Fig. 2.4A; Suppl. Fig. 2.3**).

ESI analyses revealed the presence of the phosphorylated Y150-P peptide within Gly-2 species along with the non-phosphorylated Y150 peptide in Gly-0, Gly-1 and Gly-2 in Q5 and Q5H samples. Y150F was detected only in Gly-0, Gly-1, and Gly-2 bands of Y150F, and no Y150-P peptide was detected in any of the Y150F bands (**Fig. 2.4B**).

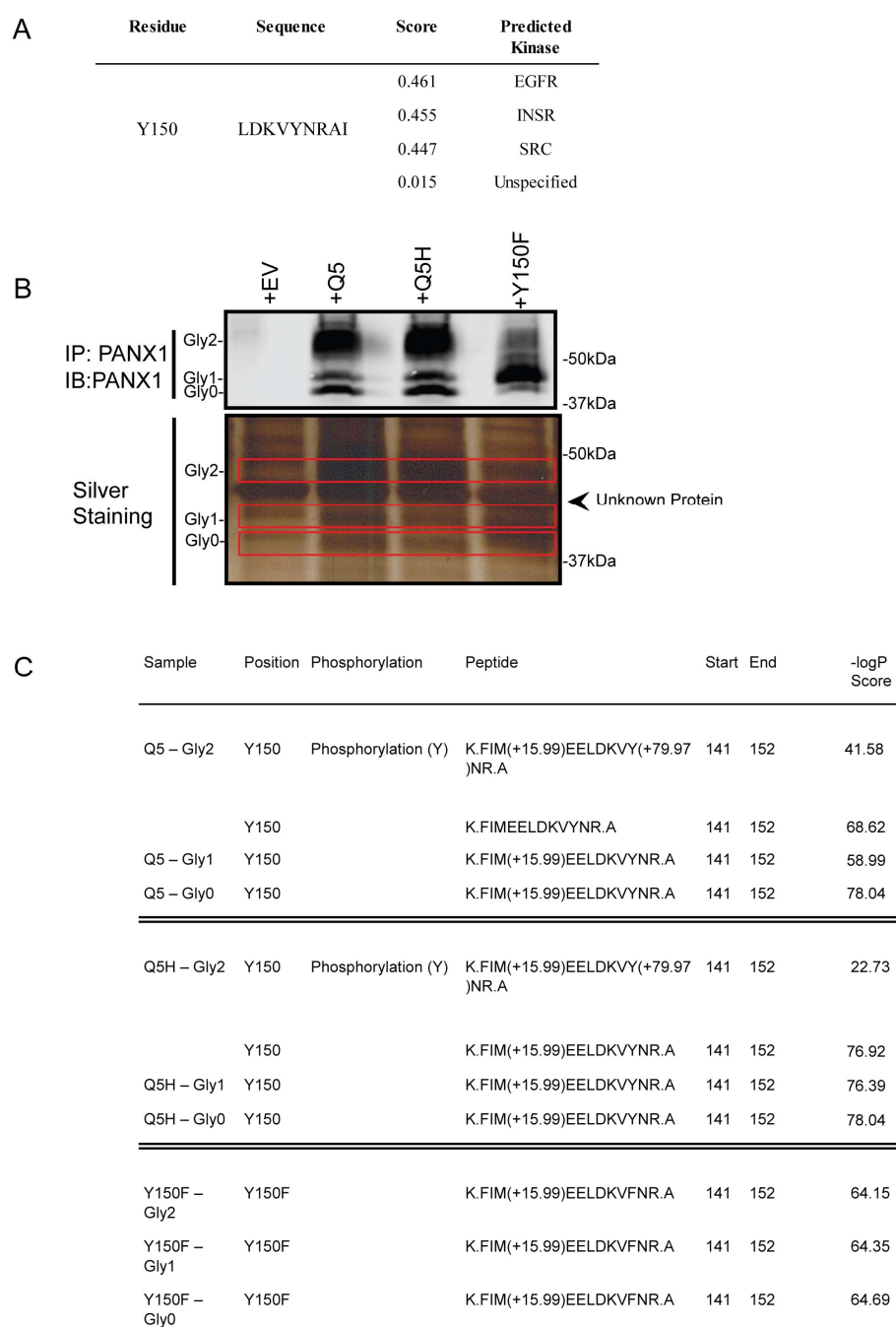


Figure 2.4: Y150 is a tyrosine phosphorylation site of PANX1. A. Y150 is predicted to be a tyrosine-phosphorylation site by NetPhos3.1 Server. Predicted kinases of the Y150 site include Epidermal Growth Factor Receptor (EGFR), Insulin Receptor (INSR), and SRC kinases. **B.** PANX1 was immunoprecipitated (IP) from Hs578T(KO) transiently over-

expressing EV, Q5, Q5H, or Y150F and bands from SDS-PAGE gel representing Gly-0, Gly-1, and Gly-2 of PANX1 were sent for ESI-MS processing and analysis. (N=1) C. Analyses of ESI demonstrating identification of Y150-containing PANX1 peptides.

Y150F enhances basal dye-uptake while Q5H does not differ functionally from Q5

We also sought out to determine if Q5H and Y150F influences PANX1 channel activity as determined by basal (non-stimulated) uptake of the cyanide monomeric dye YO-PRO1 and whole-cell patch clamp electrophysiology recording. Comparing the functional outcome from transient transfections of EV, Q5, Q5H, and Y150F in Hs578T(KO) we observed significantly greater dye uptake in Y150F-transfected cells, and no significant difference in unstimulated dye uptake from EV, Q5, and Q5H expressing cells (**Fig. 2.5A**). Whole-cell patch clamp recordings on HEK293T cells transiently transfected with Q5 and Q5H revealed no significant differences in channel activity, and both peak currents were reduced with the channel blocker carbenoxolone (CBX) (**Fig. 2.5B-C**). HEK293T cells transfected with Y150F experienced significant cell death in those cells, and as a result were not included in electrophysiology recordings.

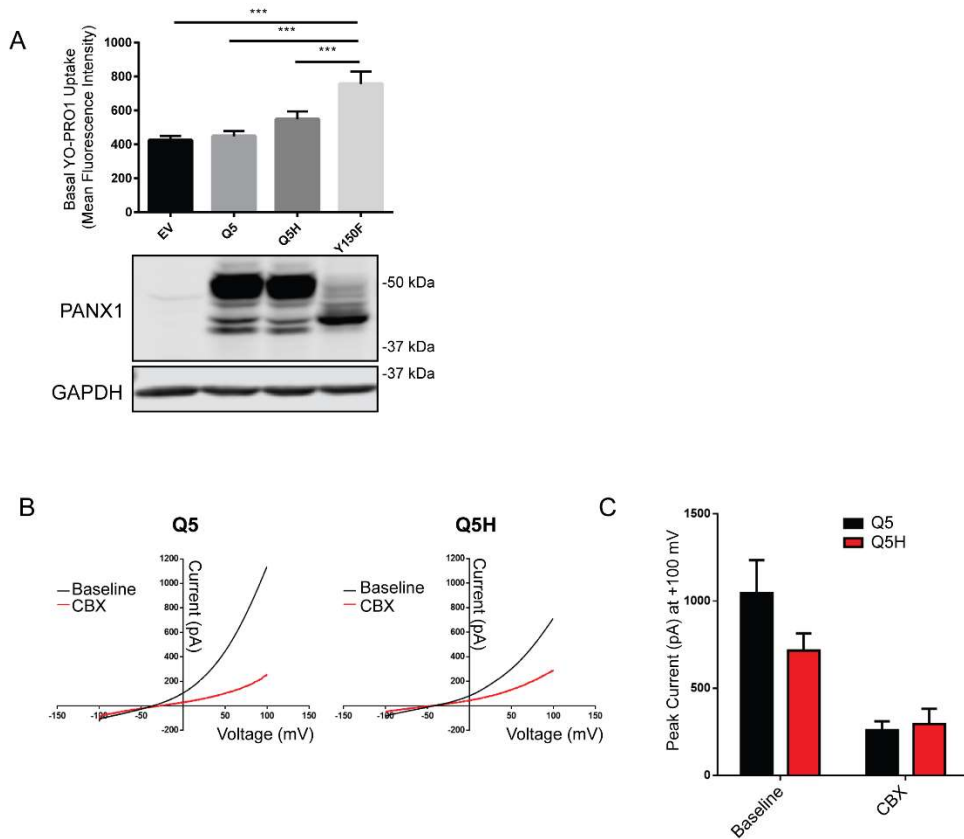


Figure 2.5: Y150F enhances basal dye uptake while Q5H does not differ functionally from Q5. **A.** Basal (unstimulated) dye-uptake of YO-PRO1 was performed on Hs578T(KO) cells transiently over-expressing EV, Q5, Q5H, and Y150F. Flow cytometry analyses revealed a significantly greater amount of dye-uptake in Y150F transfected cells (N=3, n=9, ***P < 0.001). A representative western blot demonstrating protein expression levels of Hs578T(KO) cells transiently overexpressing PANX1 variants (EV: empty vector) (N=3). **B.** Representative current-voltage relationships recorded in the presence or absence of carbenoxolone (CBX, red) in HEK 293T cells expressing Q5 or Q5H. **C.** Summary of ramp currents recorded at +100 mV from Q5- and Q5H-expressing HEK293T cells (Unpaired two-tailed T-test; N=6).

Stable overexpression of Q5H does not affect cellular localization, dye-uptake, cell growth, and migration relative to Q5 controls

To assess if Q5H differs from Q5 regarding channel activity, and if it affects cancer cell properties when expressed, we generated stable clones of Hs578T(KO) overexpressing Q5 or Q5H at similar protein expression levels (**Fig. 2.6A**). Immunofluorescence analyses demonstrate that Q5 and Q5H localize at the cell surface when stably expressed (**Fig. 2.6B**). Channel activity, assessed with basal dye uptake of YO-PRO1, did not differ significantly between Hs578T(KO) stably expressing Q5 or Q5H but both were significantly higher than non-transfected control (**Fig. 2.6C**).

Furthermore, we characterized if the expression of Q5H affects migration and cell growth of cancer cells and found that they did not differ significantly between Hs578T(KO) stably overexpressing Q5 or Q5H but migration was significantly lower in both stable clones compared to controls that had not undergone transfection and selection (**Fig. 2.6D-E**).

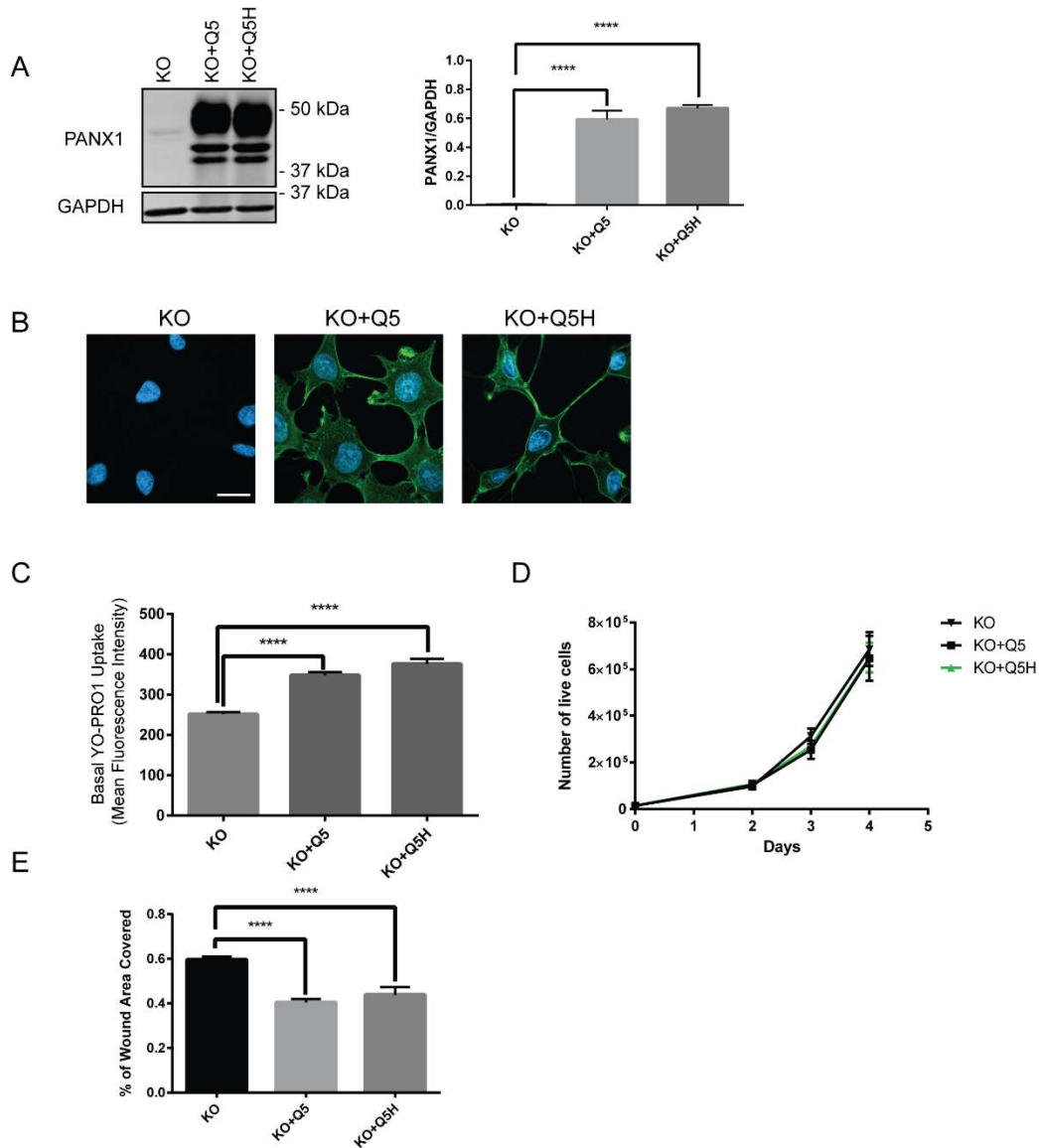


Figure 2.6: Stable-overexpression of Q5H in Hs578T(KO) cells does not differ in dye-uptake, migration, and cell growth from Q5 controls. **A.** Stable clones of Hs578T(KO) overexpressing Q5 or Q5H at similar protein levels were generated. GAPDH used as loading control. **B.** Immunofluorescence analyses (PANX1, green) demonstrate that Q5 and Q5H both localize at the cell surface in stable clones. Bar: 20 μ m. **C.** Q5H did not differ significantly from Q5 in basal uptake of YO-PRO1 dye but both were significantly higher than non-transfected controls (KO). **D.** Cell growth assay was performed by assessing number of viable cells that excluded Trypan blue dye. Cell counts did not differ significantly between Hs578T(KO) stably over-expressing Q5 and Q5H and non-

transfected controls. **E.** Cells were grown to confluence on a petri dish and a scratch was made, upon which the area cells migrated into after 15 hours was recorded. Migration did not differ significantly between Hs578T(KO) stably over-expressing Q5 and Q5H but both were significantly lower than non-transfected/non-selected controls. N=3, **** P < 0.0001.

Q5H has a greater allele and homozygosity frequencies than Q5 in cancer cohorts

Finally, we sought to determine if there may be meaningful correlations between the Y150F and Q5H variants and patients with cancer since these variants were reported in cancer databases. Analyses of cancer cohorts deposited in cBioPortal.org and the International Cancer Genome Consortium databases (36-38) revealed Y150F to be a rare variant detected in only one melanoma biopsy from The Cancer Genome Atlas (TCGA) skin cutaneous melanoma (SKCM) cohort. There is only one other reported missense variant at Y150 across 40,317 sequenced cancer patients in cBioPortal: a Y150C somatic mutation in a bladder urothelial carcinoma biopsy from TCGA's Bladder Urothelial Carcinoma dataset (36,37) (**Suppl. Fig. 2.1B**).

In contrast, the Q5H variant was detected in ten patients with different tumour types within cBioPortal and the International Cancer Genome Consortium databases with the majority of patients from a colorectal cancer dataset with Chinese origin (36-38). Since cancer genomics databases only report somatic mutations, and not genetic polymorphisms such as Q5H, we delved deeper into the whole exome sequencing of patients within a colorectal cancer dataset with Korean descent as a comparable dataset with similar race. Interestingly, the allele frequency of Q5H was significantly higher than Q5 in both normal and colorectal

tumour samples, but there remained no significant differences of Q5H allele frequency between normal and tumour samples (**Fig. 2.7A**). We also assessed TCGA's SKCM cohort that consists of 470 patients with matched normal blood or solid tissue, primary solid tumour, and metastatic samples. The allele frequency of Q5 and Q5H was assessed and the genotype of each individual was inferred by the presence and/or absence of the Q5 and Q5H alleles. Similar to what was seen in the colorectal cancer dataset, the allele frequency of Q5H was significantly greater than Q5 in both normal and tumour samples (**Fig 2.7B**). Despite the greater allele frequency of Q5H, there was no significant differences in overall and disease/progression-free survival between individuals who presented Q5|Q5, Q5|Q5H, and Q5H|Q5H genotypes (**Fig. 2.7F-G**). In correspondence with the previous finding, there were also no significant differences in Q5H allele frequency between tumours of different tumour, lymph node, and neoplasm stages (**Fig. 2.7C-E**) except for a significant reduction in Q5H allele frequency in tumours with N1 neoplasm disease stage relative to N0 (**Fig. 2.7E**).

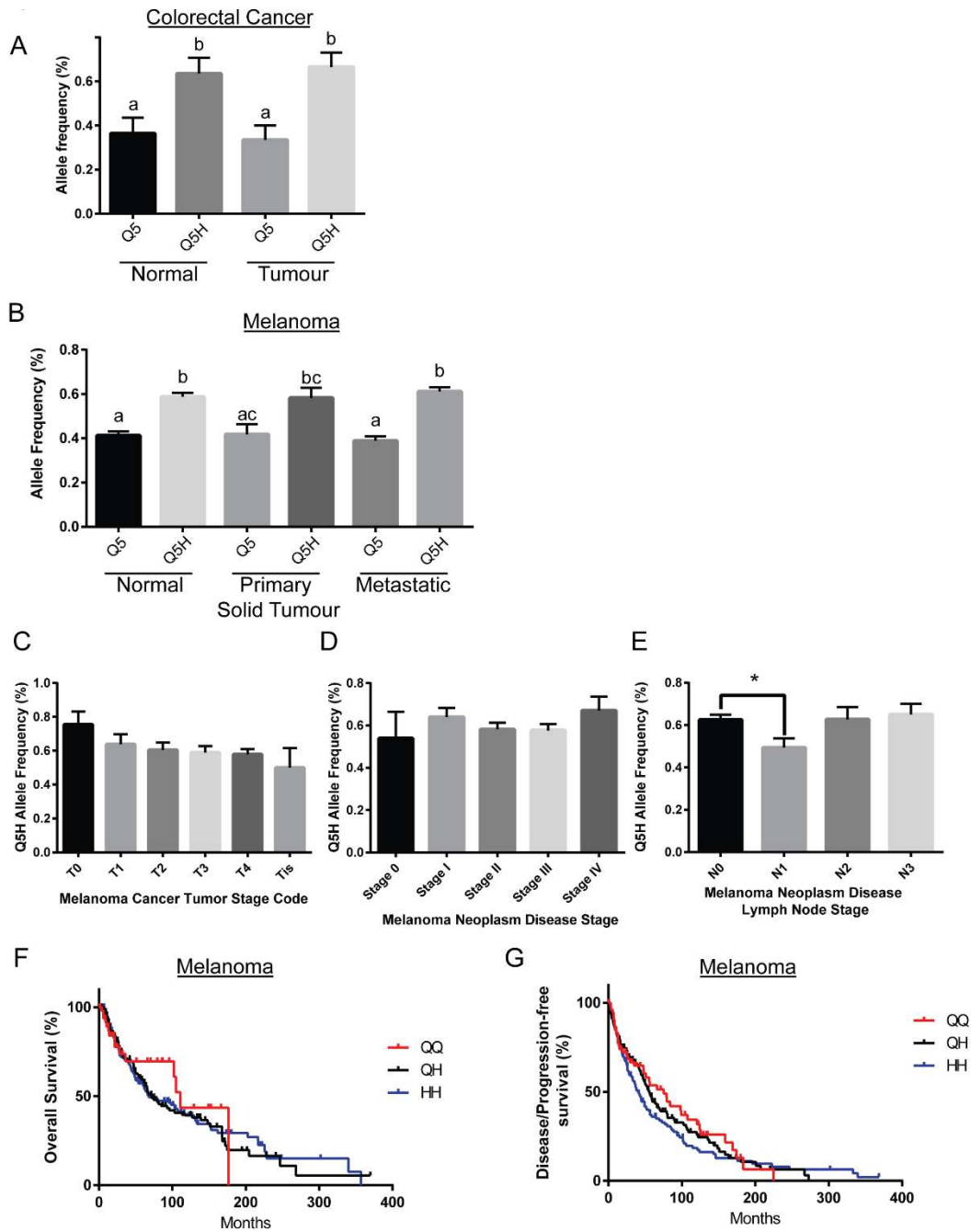


Figure 2.7: Higher Q5H allele frequency than Q5 in colorectal and skin cutaneous melanoma cancer cohorts. A. Significantly higher Q5H allele frequency than Q5 was found in matched colorectal samples from microarray study PRJNA246431. **B.** The allele frequency of Q5 and Q5H was assessed in normal, primary solid tumour, metastatic tumours of melanoma patients from TCGA’s SKCM cohort. Q5H allele frequency was

found to be significantly higher than Q5 allele frequency in normal tissues and metastatic tumours but not in primary solid tumours. (Letters denote significant differences; One-way ANOVA). **C-E.** Q5H allele frequency was assessed across different stages of neoplasm disease, neoplasm lymph node disease, and tumour stages of skin melanoma patients. (One-way ANOVA; N=470; * P< 0.05) **F-G.** Overall and disease-free progression survival did not significantly differ between QQ, QH, and HH skin melanoma patients.

Q5H has a greater allele and homozygosity frequencies than Q5 in global cohorts

To assess the allele frequencies of Q5H and Y150F in global cohorts, we obtained data from the ExAC Browser Exome Aggregation Consortium (39), an assembly of data from a variety of genome-sequencing endeavors that includes 60,706 unrelated individuals sequenced for disease-specific and population-genetic studies. Within ExAC database, the Y150F variant was not detected however a Y150H missense variant was, albeit at a very low allele frequency of 8.24e-06 (39). Like what was seen in cancer cohorts, Q5H also presents a higher allele frequency than Q5 in global cohorts with the highest allele frequency of 83.83% in Latino populations followed by African populations with an average of 82.92% (**Fig. 2.8A-B**). Genotype frequencies of 1000genomes (phase 3) populations, a genome-sequencing endeavor that assembled the genomes of 2,504 individuals across 26 different populations across the world, were also assessed and revealed that approximately 84% of individuals possessed at least one copy of the Q5H allele, demonstrating its high prevalence in human populations (**Fig. 2.8C-D**).

Q5H is highly conserved amongst vertebrate species and is the ancestral allele

The prevalence of the Q5H allele globally and within cancer cohorts indicated that Q5 could be a derived allele, one that arose through evolution as a result of a mutation, and points to Q5H as the ancestral allele. To determine if Q5H is the ancestral allele, we compared it to the allelic state of our last common ancestor, the chimpanzees, as an approximation (40). Comparing the nucleotide codon encoding the fifth amino acid of PANX1 across 31 eutherian mammal species including the chimpanzees and other species used to study PANX1, we uncovered that the RefSeq of all assessed species, excluding humans, possessed nucleotide codons that only encoded for Histidine (**Fig. 2.8E**). Furthermore, some studies have noted that the highest frequency for ancestral alleles are within African populations (41) and African populations have the second highest Q5H allele frequency and highest percentage of Q5H homozygous individuals in the 1000genomes project (**Fig. 2.8B,D**). These findings reveal that Q5H is not only the most representative variant of PANX1 within human populations but also the ancestral allele at this locus for PANX1.

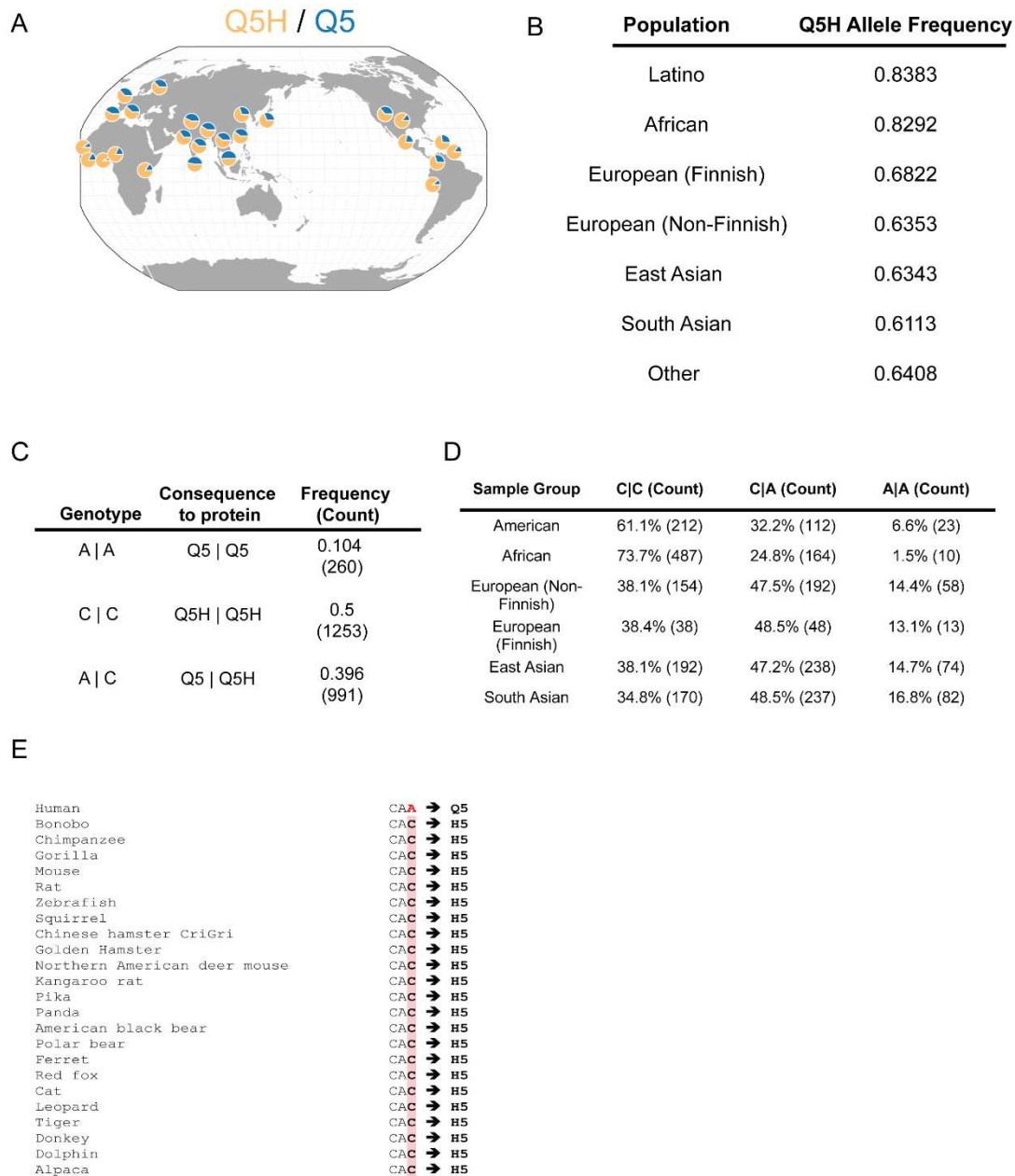


Figure 2.8: Higher Q5H allele frequency than Q5 in global cohorts. **A.** A map representing the distribution of Q5 and Q5H alleles in various populations from the 1000 Genomes Project. Polymorphism rs1138800 (Q5H) was assessed and map was generated by the Geography of Genetic Variants Browser (v0.4 beta). **B.** Allele frequency of Q5H found in diverse populations. Data was extracted from the ExAC Browser Beta. **C-D.** The genotype frequency of individuals sequenced in the 1000 Genomes Project demonstrate

that most individuals (~89%) possess at least one allele copy of Q5H. E. Ensembl phylogenetic context alignment revealed Q5H is a highly conserved site amongst vertebrate species with humans being the only species with Q5.

2.5 Discussion

Given its widespread expression within the human body along with the wide range of signaling molecules it is permeable to, it is not surprising that PANX1 has been implicated in various pathological disorders such as ischemia, HIV infections, melanoma, and others (7,12,13,42). While most studies explored the effects of altering expression or inhibition of PANX1, only six investigations have explored the effects of coding variations on channel function in the context of disease (26,28-32). This report studied the influence of two naturally occurring *PANX1* variants, Q5H and Y150F, on the trafficking and function of PANX1. Overall, we uncovered a novel tyrosine phosphorylation site that influences normal glycosylation and trafficking, and a highly prevalent ancestral *PANX1* variant that contrary to current knowledge is the most common PANX1 found in humans.

The role of Y150 phosphorylation

Mutagenesis of the Y150 residue resulted in disruption of Y150 phosphorylation and alterations to normal N-glycosylation and trafficking of the protein. Although the phosphorylated and non-phosphorylated Y150 peptides were detected only in the Gly2 states of Q5 and Q5H, the spatiotemporal pattern of Y150 phosphorylation remains uncertain. The resistance to EndoH de-glycosylation acquired by Y150F and the reduction in Gly2 species production, suggests that Y150 phosphorylation may establish a

glycosylation pathway leading to complex glycosylation of the protein by either interacting with N-glycosyltransferases or altering protein folding and/or stability. Disrupting its phosphorylation by mutating the residue to phenylalanine led to the formation of a hypo-glycosylated species and enhanced the ability of PANX1 to localize at the cell surface in greater amounts than both Q5 and Q5H. It remains unknown if the greater amounts of Gly1 at the cell-surface are the EndoH-resistant or EndoH-sensitive Gly1 species of Y150F. Nonetheless, this enhanced cell-surface localization of Gly1 and relatively low amounts of cell-surface localization of Gly2 is contrary to previous reports demonstrating that Gly2 has a greater capacity to localize at the cell-surface than Gly1 and Gly0 species (21). Therefore, this suggests that the Gly2 species expressed in Y150F may not be complex glycosylated but rather experiences another type of glycosylation modification such as a 'hybrid glycosylation' (43) that may accelerate trafficking to the cell-surface or further stabilize the channel at the cell-surface. Furthermore, Sang *et al.* (28) has previously unveiled four hypo-glycosylated PANX1 mutants that induced increased expression of calreticulin, a chaperone protein that facilitates glycoprotein folding. This suggests that proper protein folding facilitates editing to complex glycosylation and that, in the case of Y150F, the lack of phosphorylation or merely the mutation, may alter protein folding/stability and favor an alternate glycosylation-editing pathway.

Previous evidence of PANX1 tyrosine phosphorylation, specifically on Y198 and Y308 of mouse and rat Panx1, respectively, demonstrated phosphorylation required interactions with the Src Family Kinases (SFKs) (18,24,44,45). Administration of interfering peptides against SFK consensus phosphorylation sites of Y198 and Y308 sites abolished Panx1

activation mediated by SFKs (17,18). Furthermore, the same group also demonstrated that Y198 phosphorylation occurs at the cell-surface and was dependent on SFK activity (46) and that tyrosine phosphorylation of either Y198 or Y308 activated channel activity, demonstrating that phosphorylation modulates channel activity (17,18). While Y150 is predicted to be phosphorylated by SFKs (among other kinases), it may produce an opposite effect than Y198 and Y308 phosphorylation as mutagenesis of Y150 further enhanced dye uptake. However, it is difficult to attribute this characteristic merely to enhanced channel activity as there were significantly more Y150F channels at the cell-surface to mediate dye-uptake than Q5 or Q5H channels. This is further complicated by the differential glycosylation Y150F receives thus demonstrating that glycosylation may also play a key role in channel function. Differential glycosylation of PANX1 via other naturally-occurring variants has been previously demonstrated to enhance channel activity in mouse germinal vesicle oocytes (28). Thus, this suggests that phosphorylation is not the only indicator of cell-surface channel activity. Finally, since ectopic over-expression Y150F reduces cell viability in NRK cells, it is possible that the enhanced uptake of the YO-PRO1 dye, of which is also commonly used a marker for apoptosis (47), may be due to Y150F potentially driving cell death pathways.

Possessing a Y150F variation in the context of cancer can have different effects depending on the expression level of the mutant. Lower expression levels of Y150F can result in greater overall cell-surface channel function thus potentially promoting tumorigenic properties, depending on tumor type, while higher expression levels can lead to greater intracellular localization of the channel and reduced cell viability. Therefore, not only does

the presence of the variation needs to be considered but also the amount of the mutated protein. As aforementioned, only two cancer patients harbor mutations that disrupt the Y150 site, that includes Y150F and Y150C mutations (36,37). In both cases, the allele frequency for the mutations are less than 0.5, suggesting heterozygosity with wildtype PANX1 which may produce effects different than was observed in this study. Further investigation is required to determine the effects of co-expressing wild-type PANX1 with Y150F on cell-surface trafficking, channel function, and cell viability. Since only two patients possess a mutation at the Y150 site along with many other mutations in other genes, it is difficult to determine the effects of these mutations on the disease status of these patients.

Q5H in cancer

What initiated our interest in Q5H was a previous report demonstrating that the Q5H variant was enriched in healthy Caucasian males with platelets that were hyper-reactive to collagen (29). Interestingly, this study demonstrated that ectopic expression of Q5H in Chinese Hamster Ovary cells resulted in a greater basal and K⁺-activated ATP release than Q5 and controls (29). With the emergence of numerous reports demonstrating the tumor-promoting effects of PANX1 (12,13,27,48,49), along with the finding that Q5H promoted ATP-release in a normal cell line and finally that Q5H was present in cancer patients (36-38) and cancer cell lines, we then developed the premise that Q5H may play a role in promoting tumorigenic properties. Contrary to our hypothesis, Q5H did not impact channel activity when expressed in cancer and HEK293T cells. However, it is important to note

that Molica *et al.* (29) used basal and K⁺-activated ATP release to assess for PANX1 channel activity whereas we employed basal dye uptake and voltage-activation whole-cell patch-clamp electrophysiology. The different stimuli used, voltage activation and elevated extracellular K⁺ conditions, have been previously shown to promote different conformational shapes (50,51); the former involves the C-terminus lining the pore whereas the latter does not. It has been suggested that elevated extracellular K⁺ conditions which favors ATP-permeability may induce a conformation similar to ATP-permeable Connexin channels in which the N-terminus lines the pore of the channel (14,52). Therefore, the divergence in channel activity between these two studies may be attributed to the different techniques used to measure channel function, and we cannot rule out potential differences between Q5 and Q5H in other cell contexts, with other functional assays and stimulation.

Although Q5H allele frequency was significantly greater than Q5 in cancer cohorts, this was also observed in global cohorts. In order to compare the allele frequencies between cohorts, we need to take into consideration the racial distribution as the allele frequency of Q5H can vary greatly across different racial groups of global cohorts with the highest of 83.83% in Latino populations and lowest of 61.13% in South Asian populations. We chose a melanoma cohort because we have previously demonstrated that inhibition or reduction of PANX1 in human melanoma cells reduced their tumorigenic profile, thus implicating PANX1 to play an influential role in human melanoma tumour progression (12). In TCGA's SKCM cohort 447 of 470 samples belonged to white individuals along with 12 Asian, 1 African American individual in addition to 10 non-reported samples. As a result, a suitable comparison would be the Non-Finnish European population in ExAC dataset.

Even though the mean Q5H allele frequency of normal samples from TCGA SKCM is slightly lower than that of ExAC's (58.72% vs 63.53%), it is important to note that the small difference may arise from the different methodologies used to assess allele frequencies. Further corroborating this, ectopic expression of Q5H in cancer cells did not enhance PANX1 channel function, cell growth and migratory capacities of breast cancer cells. Therefore, while Q5H may increase channel function and play a role in platelet aggregation (29), our findings suggest that it may not have the same gain-of-function effect in this breast cancer cell line.

Our discovery that Q5H is a highly conserved and more prevalent ancestral allele than Q5, which is annotated in various genomic and protein sequencing databases to be the best and most representative allele, highlights the necessity to thoroughly analyze and confirm genomic sequences that are representative of the overall population. Ironically, when human PANX1 was fully sequenced in RefSeq in 2003 by Baranova *et al.* (16) (Accession No. AF398509.1), the PANX1 mRNA sequence contained the codon encoding for histidine in the fifth amino residue. However, currently the PANX1 mRNA sequence (Accession No. NM_015368.4) in RefSeq contains the codon that encodes for glutamine at the fifth residue. This has led to numerous studies over the years utilizing the derived allele that is less prevalent than the ancestral Q5H allele. As a result, future studies on human PANX1 need to take into consideration the two prevalent and divergent variants Q5 and Q5H, (or rather, Q5 and H5), since it remains unknown how they may differ in other cellular contexts.

In conclusion, by exploring various naturally occurring *PANX1* variants, we have uncovered two that revealed unknown characteristics of the widely expressed protein. The rare variant Y150F revealed a phosphorylation site that affects glycosylation, trafficking, and function of PANX1, while the common variant Q5H had similar function to Q5 and turned out to be the ancestral allele of PANX1. Q5H is also the more representative allele at this locus within human populations and should be included in future studies of PANX1.

2.6 Experimental Procedures

Cell culture

Normal Rat Kidney (NRK) cells (ATCC® CRL-6509™), human triple-negative breast cancer Hs578T (ATCC® HTB-126™) and human melanoma A375P (ATCC® CRL-3224™), A375-MA2 (ATCC® CRL-3223™), human melanoma 131/4-5B1(53) and human glioblastoma U87MG (ATCC® HTB-14™) cells were cultured in Dulbecco's Modified Eagle Medium 1X (DMEM 1X; ThermoFisher) containing 4.5 g/L D-glucose, L-glutamine, 110 mg/L sodium pyruvate, 10,000 units of penicillin, 10 mg/mL streptomycin, and 10% FBS (Wisent Institute). All cells were incubated at 37°C and 5% CO₂. Cellular dissociation from culture plates was done using trypsin (0.25%, 1mM EDTA 1X; Thermofisher).

Generation of CRISPR/Cas9 Knockout cells

PANX1 knockout cells were generated by CRISPR/Cas9 D10A as described in (54). Briefly, cells were transfected with 1 ug each of pSpCas9n(BB)-2A-Puro (PX462) V2.0 and pSpCas9n(BB)-2A-GFP (PX461) (addgene.org) containing guide RNA sequences for human PANX1 in a 6-well plate. PANX1 gRNAs were designed with <http://tools.genome-engineering.org> (sequences GTTCTCGGATTTCTTGCTGA and CTCCGTGGCCAGTTGAGCGA). 24 hours post transfection, cells were selected with 1 ug/ml Puromycin for 72 hours. Following selection, cells underwent single colony selection via serial dilutions and screened for PANX1 levels by Western blot. Plasmids were a gift from Feng Zhang (Addgene plasmid #48140 and #62987).

Plasmids and transfection

An expression vector encoding for wild-type PANX1 (Q5), pUNO1-hPANX1 was purchased from InvivoGen (San Diego, California, United States). PANX1 variant-encoding expression vectors (Q5H, Y150F, G168E, T176I, H190Y, S239L, and Q264*) were generated by Norclone Biotech Industries (London, Ontario, Canada). For all experiments (except those noted as 5 µg), cells were transfected with 1µg of expression vectors encoding for Q5, Q5H, Y150F, G168E, T176I, H190Y, S239L, and Q264* using Lipofectamine 3000 (ThermoFisher) according to manufacturer's instructions. Cells were analyzed for expression and functional analyses 72- and 96-hours post-transfection. Hs578T(KO) clones stably overexpressing Q5 or Q5H were generated by blasticidin

selection at 15 µg/mL for one week and underwent single-cell colony selection by serial dilution.

Protein Extraction and Immunoblotting

Protein lysates from cells were extracted using IP buffer (50 mM Tris-HCl pH 8.0, 150 mM NaCl, 1% NP-40 (Igepal) (Honeywell Fluka, Seelze, Germany), 0.5% sodium deoxycholate, 1 mM sodium fluoride, 4 mM sodium orthovanadate and one tablet of complete-mini EDTA-free protease inhibitor (Roche, Mannheim, Germany). Protein concentration was quantified using the Pierce bicinchoninic acid (BCA) assay (Thermo Fisher Scientific). 30 µg of protein lysates were subjected to 10% SDS-PAGE, blocked with 3% bovine serum albumin with 0.05% Tween-20 in 1XPBS or 1XTBS and immunoblotted with anti-human PANX1 antibody as previously described in (12) (1:1000; PANX1 CT-412; 0.35 µg/µL(26)), anti-glyceraldehyde 3-phosphodehydrogenase (GAPDH) antibody (1:1000; Millipore Cat# MAB374, RRID: AB_2107445), anti-N-cadherin antibody (Cat. No. 6101; BD Biosciences). For detection, goat anti-rabbit IRDye®-800CW and goat anti-mouse IRDye®-680RD (LI-COR Biosciences, Lincoln, NE, USA) were used as secondary antibodies at 1:10,000 dilutions, and imaged using a LI-COR Odyssey infrared imaging system (LI-COR Biosciences). Western blot quantification and analysis was conducted using Image Studio™ Lite (LI-COR Biosciences).

De-glycosylation

Whole cell lysate (10 µg) from Hs578T-KO transiently overexpressing EV, Q5, Q5H, or Y150F were incubated with either 500 units or 1000 units of EndoH (Cat. No. P0702S; New England BioLabs) or 1 unit of PNGase F (Cat. No. P7367; Sigma-Aldrich) at 37°C overnight along with remaining kit components according to manufacturer's protocol.

Cell-surface biotinylation

Forty-eight hours post-transfection, 1×10^6 cells were cultured in 60-mm culture plates for another 48 hours. Cells were rinsed twice with ice-cold DPBS containing calcium and magnesium and subsequently incubated with 1.5 mg/mL EZ-Link™ Sulfo-NHS-SS-Biotin (Thermo Scientific) in DPBS with calcium and magnesium for 30 min on ice upon which cells were washed twice with DPBS and subsequently incubated with 100 mM glycine in DPBS to quench remaining biotin for 30 min on ice. Protein lysates were collected, and biotinylated proteins were pulled down by incubating 250µg total protein for 16h with 50 µL (50% slurry) NeutrAvidin agarose beads (Thermo Scientific) in a final volume of 250 µL in DPBS. Beads were centrifuged ($\times 500g$, 4°C) and washed three times with lysis buffer and resuspended in 2X Laemmli buffer containing 10% β-mercaptoethanol. Beads were boiled for 5 min, centrifuged, and supernatant was collected. 10µg of whole cell lysate was used as input and 40 µL of bead supernatant was used in immunoblots. Protein expression of N-cadherin and GAPDH via immunoblotting was assessed to use as a positive control

for biotinylated cell-surface protein and as a negative control for non-biotinylated intracellular proteins, respectively.

Immunofluorescence

Cells were grown on glass-coverslips and were fixed 72 hours post-transfection using ice-cold 8:2 methanol:acetone for 15 min at 4°C and blocked with 2% BSA-PBS. Coverslips were incubated with anti-human PANX1 antibody (1:500; PANX1 CT-412; 0.35 µg/µL), Hoechst 33342 (1:1000), and Alexa Fluor 488 goat anti-rabbit IgG (2 mg/mL, 1:700), and mounted using Airvol (Mowiol 4-88; Sigma Aldrich) prior to imaging. Immunofluorescence images were obtained using a Zeiss LSM 800 Confocal Microscope with a Plan-Apochromat 63x/1.40 Oil DIC objective (Carl Zeiss, Oberkochen, Germany). The laser lines used include 405 nm (Hoechst 33342) and 488 nm (Alexa488).

Dye-uptake

Forty-eight hours post-transfection, 300,000 cells were plated on each well of a six-well plate. 48-hour post-plating, cells were washed twice with 1XDPBS containing Ca²⁺ and Mg²⁺ and incubated with DMEM serum media containing 1µM YO-PRO-1 (Cat. No. Y3603) for fifteen minutes at room temperature. Subsequently, cells were washed twice with 1XDPBS containing Ca²⁺ and Mg²⁺ and dissociated from cell-culture plate and processed for flow-cytometry analysis using BD FACSCelesta™. Amount of intracellular

YO-PRO1 dye uptake was assessed using the 488-nm laser and data was analyzed using BD FACSDIVA™ software.

Whole-cell patch clamp recordings from HEK 293T cells

Whole-cell voltage-clamp recordings were performed at room temperature (20-22 °C) using an Axon MultiClamp 700A amplifier and Digidata 1322A data acquisition system (Molecular Devices, Sunnyvale, CA, USA). Patch electrodes were pulled using a Narishige two-stage puller (PP-83; Narishige, Greenvale, NY, USA) from thin-walled borosilicate glass (TW150-F3; WPI, Sarasota, FL, USA). Electrodes had a final resistance of 3-5 MΩ when filled with intracellular solution (ICS) containing (in mM): 142 cesium gluconate, 10 HEPES, 2 MgCl₂, 8 NaCl, pH 7.2 (adjusted with 1M Cs-OH) and osmolarity between 290 and 295 mosmol L⁻¹. Standard extracellular solution (ECS) was composed of (in mM): 140 NaCl, 5.4 KCl, 25 HEPES, 33 glucose, 2 CaCl₂, 1 MgCl₂, pH of 7.4 (adjusted with 10N NaOH) and osmolarity between 300 and 305 mosmol L⁻¹. A computer-controlled, multibarrelled perfusion system (SF-77B; Warner Institute, Hamden, CT, USA) was used to exchange bath solutions from standard ECS to 100 μM carbenoxolone in ECS (Panx1 blocker). Transfected cells (identified by presence of mCherry marker) were voltage-clamped at -60 mV and Panx1 currents were recorded by the application of voltage-ramps (±100 mV, 500 ms) to the membrane every 10 seconds. Current-voltage (I-V) relationships were constructed from these recordings. Currents were filtered at 2 kHz and sampled at 10 kHz, digitized, and acquired using pCLAMP 9.2 software (Molecular

Devices). Data was collected from minimum 3 independent experiments and analysed using Clampfit 10.7 software (Molecular Devices).

Cell Growth Assay

Fifteen thousand cells were plated in a well of a 6-well culture plate at day 0. From day 2 – day 4 after cell plating, cells were dissociated with Trypsin (0.25%, 1mM EDTA 1X; Life Technologies), and number of trypan blue-excluded live cells were counted with an automated cell counter Cell Countess II (Thermofisher) as described previously(12).

Migration Assay

Twenty thousand cells were plated in each well coated with 0.01% poly-L-lysine (Millipore Sigma, Burlington, MA, USA) of a 96-well culture plate and grown to confluence. A scratch wound was inflicted with a P200 pipette tip and serum DMEM was replaced with serum-free DMEM. Pictures were taken with a brightfield microscope within an hour of scratch and at fifteen hours after scratch. Area of migration was quantified with ImageJ software.

Immunoprecipitation and Silver Staining

Protein lysates were collected 96 hours post-transfection from Hs578T(KO) cells transfected with EV, Q5, Q5H, or Y150F upon which confluency was reached. 1 mg of

whole cell protein lysate was incubated overnight at 4°C with Protein A/G beads that were cleaned twice with 1XDPBS (ThermoFisher) along with 10 µg of anti-human PANX1 antibody (PANX1 CT-412) crosslinked to Pierce Protein A/G-Agarose beads (Thermo Scientific). Subsequently, bound proteins underwent four washes with 500µL of IP buffer. Beads were collected and resuspended in 2X Laemmli buffer with 10% β-mercaptoethanol, boiled for 5 min, and supernatant were collected after spinning down. Supernatant then was subjected to 10% SDS-PAGE and gel was stained with Pierce™ Silver Stain Kit (ThermoFisher Scientific) according to manufacturer's protocol.

Peptide Identification Using Mass Spectrometry

The peptides were resuspended in 0.1% formic acid/99.9% water and loaded onto an ACQUITY UPLC Symmetry C18 NanoAcquity, 10K, 2G V/M, 180µm x 20mm, 100A, 5µm trapping column (Waters Corporation, Milford, MA) via a Waters NanoAcquity UPLC, at a flow rate of 10 uL/min for 6 minutes using 99% buffer A (0.1% formic acid) and 1% buffer B (Acetonitrile + 0.1% formic acid). After trapping the peptides were eluted onto the analytical column for separation, using a 95 min run time. Flow was established at 300 nL/min for the ACQUITY UPLC Peptide BEH C18 nanoAcquity Column 10K psi, 130Åm 1.7µm x 25mm which was held at 35 deg C. The gradient initial condition was 5% buffer B. Buffer B then increased to 40% over 60 min, then to 95% over 15 min, then to 5% over 2min, and finally held at 5% for 13 min for re-equilibration to the initial condition. The LC system was directly connected to a NanoFlex (Thermo Electron Corp., Waltham, MA) nanospray ionization source with a source voltage of 2.4 KV and was interfaced to

an Orbitrap Elite, VelosPro mass spectrometer. The mass spectrometer was controlled by Xcalibur software (Thermo, v. 2.7.0) and operated in the data-dependent mode using an FT/IT/CID Top 20 scheme. The MS scan recorded the mass-to-charge ratios (m/z) of ions over the range of 400–1450 in FT (resolution of 120000 at m/z 400), positive ion, profile, full MS mode using a lock mass (445.120025 m/z). The 20 most abundant multiply charged ions were automatically selected for subsequent collisional induced dissociation in ion trap mode (IT/CID) with an isolation width of 2.00 Da, rapid scan rate, centroid mode, with charge state filtering allowing only ions of +2, +3, and +4 charged states. Normalized Collision energy was 35, and precursor ions were then excluded from further CID for 30 s.

Bioinformatics

Allele and genotype frequencies in addition to population genetic distribution information for single nucleotide polymorphism rs1138800 encoding for Q5H was extracted from Ensembl and ExAC databases. BAM files for colorectal cancer genome sequencing dataset from SRA Study Accession No. PRJNA246431 and from WGS files for TCGA SKCM cohort were converted to SAM and accessed for A/T/C/G allele counts at chromosome position 11:93862493 (GRCh38.p12) using Perl Script. Clinical attributes for TCGA SKCM cohort was downloaded from cBioPortal database (36,37). The results for TCGA SKCM cohort shown in this investigation are in whole based upon data generated by the TCGA Research Network: <https://www.cancer.gov/tcga>.

Q5 and Q5H genome sequencing of cancer cell lines

Genomic DNA was extracted from cancer cell lines (A375-MA2, U87MG, BeWo, & 131/4-5B1) using PureLink™ Genomic DNA Mini Kit (Cat. No. K182001; ThermoFisher) according to manufacturer's instructions. Genomic DNA was converted to cDNA using High-Capacity cDNA Reverse Transcription Kit (Cat. No. 4368813; ThermoFisher) and primers spanning the N-terminus of PANX1 (Forward: 5'-GGAAGCGCTTTGTTCCGC-3', Reverse: 5'-CCTCCCACAACTTTGCCCTA-3'). cDNA products were sent for DNA sequencing at the Robarts Research Institute DNA Sequencing Facility (London, Ontario, Canada).

Statistical analyses

Statistical analyses were performed using GraphPad Prism software (version 8.0; San Diego, CA). Data error bars indicate mean \pm standard error mean.

Conflict of Interest:

The authors declare no conflicts of interest of any kind.

Acknowledgements:

We thank Victoria Clarke and Dr. Laszlo Gyenis for processing samples for ESI, and helpful discussions on the study. We would also like to thank Dr. Jessica Esseltine for generating gRNA used for CRISPR/Cas9 editing of PANX1.

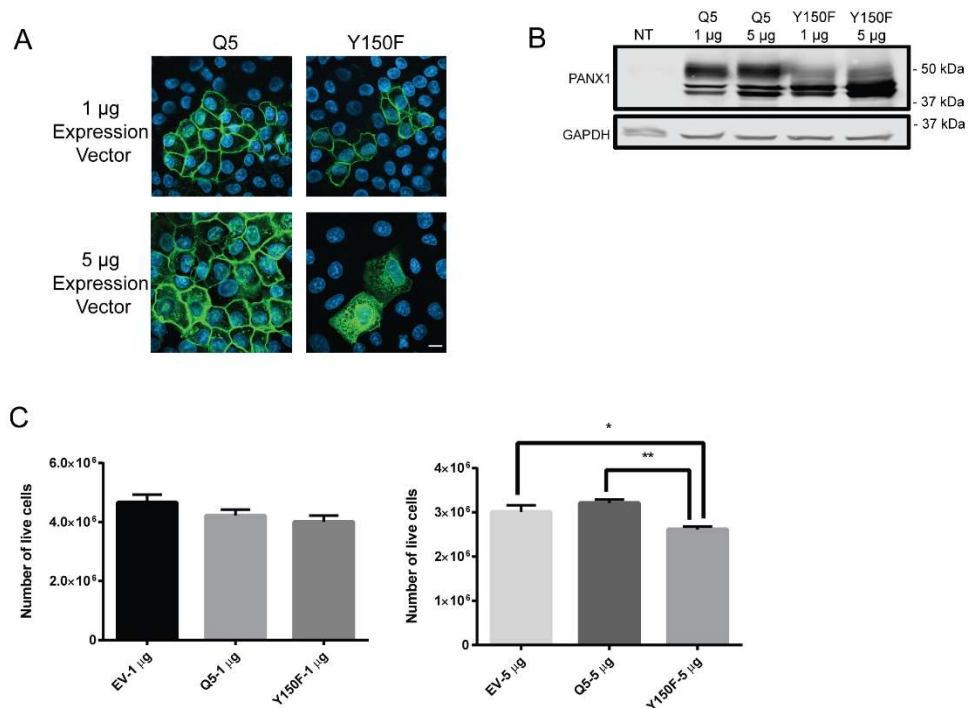
A

Cell line	Cell Type	<i>PANXI</i> Sequence
BeWo	Human placenta choriocarcinoma	Q5H
Hs578T	Human Breast Carcinosarcoma	Q5H
U87MG	Human glioblastoma	Q5
A375-MA2	Metastatic human melanoma	Q5H
131/4-5B1	Metastatic human melanoma	Q5/Q5H

B

Somatic Mutation	Other Mutations at Position	Summary of Pathology Report	Predicted Functional Impact
Y150F	Y150C missense mutation reported in Bladder Urothelial Carcinoma (TCGA, US)	<ul style="list-style-type: none"> Involvement of regional lymph nodes No distant metastases found Invasion into reticular dermis 	Medium
G168E	G168E reported in uterine corpus endometrial carcinoma (GDC Data Portal)	<ul style="list-style-type: none"> Invasion into the subcutaneous fat Diagnosed with basal and squamous cell carcinoma Involvement of regional lymph nodes No distant metastases found 	Medium
T176I	T176S missense mutations reported in Colorectal Adenocarcinoma and lung carcinoma (DFCI, Cell Reports 2016 ; GDC Data Portal)	NA	Low
H190Y	NA	<ul style="list-style-type: none"> No distant metastases found Invasion into reticular dermis No involvement of regional lymph nodes 5% of tissue sample comprised of lymphocytic infiltrates 	Low
S239L	NA	<ul style="list-style-type: none"> No distant metastases found Involvement of regional lymph nodes 	Medium
Q264*	NA	NA	N/A

Supplementary Figure 2.1: **A.** Genome sequencing for Q5 and Q5H of various cancer cell lines. **B.** Brief clinical summaries of *PANXI* somatic mutations derived from melanoma patients obtained from cBioPortal database.



Supplementary Figure 2.2: Moderate Y150F overexpression allows for cell-surface localization but is prevented upon higher overexpression in NRK cells which also results in lower cell viability. **A.** Y150F preserves the ability to traffic to the cell-surface upon moderate ectopic expression (1µg of DNA) but is retained intracellularly upon overexpression (5µg of DNA) in NRK cells. Green = PANX1, blue = nuclei. Bar = 10 µm. **B.** Both moderate and overexpression of Y150F in NRK result in predominantly Gly-0 and Gly-1 species with minimal Gly-2 species relative to wildtype. **C.** Greater overexpression of Y150F significantly reduced number of live cell counts in NRK relative to EV- and Q5-transfected cells (One-way ANOVA; N=3, n=3; * p < 0.05, ** p < 0.01).

Sample	Position	Post-translational modification	Peptide	Start	End	Predicted Kinases
Q5 – Gly0	S159	Phosphorylation (STY)	R.AIKAAKS(+79.97)AR.D	153	161	GSK3, CaM-II, RSK, cdc2, CKI, DNAPK, CKII, PKG, p38MAPK, PKC, ATM, cdk5, PKA, PKB
Q5 – Gly2	Y309	Phosphorylation (STY)	K.VY(+79.97)EILPTFDVLHFK.S	308	321	EGFR, INSR, SRC
	A2	Acetylation (Protein N-term)	M.A(+42.01)IAHLATEYVFSDFLLKEPTEPK.F	2	24	
	Y150	Oxidation (M); Phosphorylation (STY)	K.FIM(+15.99)EELDKVY(+79.97)NR.A	141	152	EGFR, INSR, SRC
	T382	Phosphorylation (STY); Oxidation (M)	K.T(+79.97)PM(+15.99)SAEM(+15.99)REEQGNQTAELQGM(+15.99)NIDSETK.A	382	409	P38MAPK, cdk5, GSK3, CaM-II, CKI, CKII, cdc2, DNAPK, ATM, RSK, PKG, PKB, PKA, PKC
	T368	Oxidation (M); Phosphorylation (STY)	K.SSGQGIDPM(+15.99)LLLT(+79.97)NLGM(+15.99)IK.M	356	374	Cdc2, CaM-II, GSK3, CKI, p38MAPK, PKG, DNAPK, CKII, ATM, RSK, cdk5, PKC, PKA, PKB
	S357	Phosphorylation (STY); Oxidation (M)	K.SS(+79.97)GQGIDPM(+15.99)LLLTNLGM(+15.99)IK.M	356	374	PKA, cdc2, CaM-II, GSK3, CKI, CKII, DNAPK, ATM, PKG, RSK, p38MAPK, PKC, cdk5, PKB
	T368	Deamidation (NQ); Phosphorylation (STY)	K.SSGQ(+98)GIDPMLLLT(+79.97)N(+98)LG.M	356	371	Cdc2, CaM-II, GSK3, CKI, p38MAPK, PKG, DNAPK, CKII, ATM, RSK, cdk5, PKC, PKA, PKB
Q5H – Gly1	S344	Phosphorylation (STY)	L.EENISEVKS(+79.97)YK.C	336	346	PKC, GSK3, CaM-II, cdc2, RSK, CKI, DNAPK, CKII, p38MAPK, ATM, PKG, cdk5, PKA, PKB
	Y150	Oxidation (M); Phosphorylation (STY)	K.FIM(+15.99)EELDKVY(+79.97)NR.A	141	152	EGFR, INSR, SRC
Q5H – Gly2	A2	Acetylation (Protein N-term)	M.A(+42.01)IAHLATEYVFSDFLLKEPTEPK.F	2	24	
	Y150F – Gly1	Acetylation (Protein N-term)	M.A(+42.01)IAHLATEYVFSDFLLKEPTEPK.F	2	24	
Y150F – Gly2	S159	Phosphorylation (STY)	R.AIKAAKS(+79.97)AR.D	153	161	GSK3, CaM-II, RSK, cdc2, CKI, DNAPK, CKII, PKG, p38MAPK, PKC, ATM, cdk5, PKA, PKB
	C136 & S137	S-nitrosylation & Phosphorylation				GSK3, CaM-II, cdc2, CKII, CKI, PKG, DNAPK, PKC, p38MAPK, ATM, RSK, PKA, cdk5, PKB

Supplementary Figure 2.3: Post-translational modifications of PANX1 detected via electrospray-ionization mass-spectrometry in Hs578T(KO) cells transiently overexpressing Q5, Q5H, or Y150F.

2.7 References

1. Panchin, Y., Kelmanson, I., Matz, M., Lukyanov, K., Usman, N., and Lukyanov, S. (2000) A ubiquitous family of putative gap junction molecules. *Curr Biol* **10**, R473-474
2. Locovei, S., Bao, L., and Dahl, G. (2006) Pannexin 1 in erythrocytes: function without a gap. *Proc Natl Acad Sci U S A* **103**, 7655-7659
3. Billaud, M., Chiu, Y. H., Lohman, A. W., Parpaite, T., Butcher, J. T., Mutchler, S. M., DeLalio, L. J., Artamonov, M. V., Sandilos, J. K., Best, A. K., Somlyo, A. V., Thompson, R. J., Le, T. H., Ravichandran, K. S., Bayliss, D. A., and Isakson, B. E. (2015) A molecular signature in the pannexin1 intracellular loop confers channel activation by the $\alpha 1$ adrenoreceptor in smooth muscle cells. *Sci Signal* **8**, ra17
4. Celetti, S. J., Cowan, K. N., Penuela, S., Shao, Q., Churko, J., and Laird, D. W. (2010) Implications of pannexin 1 and pannexin 3 for keratinocyte differentiation. *J Cell Sci* **123**, 1363-1372
5. Penuela, S., Kelly, J. J., Churko, J. M., Barr, K. J., Berger, A. C., and Laird, D. W. (2014) Panx1 regulates cellular properties of keratinocytes and dermal fibroblasts in skin development and wound healing. *J Invest Dermatol* **134**, 2026-2035
6. Omasits, U., Ahrens, C. H., Muller, S., and Wollscheid, B. (2014) Protter: interactive protein feature visualization and integration with experimental proteomic data. *Bioinformatics* **30**, 884-886
7. Thompson, R. J., Zhou, N., and MacVicar, B. A. (2006) Ischemia opens neuronal gap junction hemichannels. *Science* **312**, 924-927
8. Bargiotas, P., Krenz, A., Monyer, H., and Schwaninger, M. (2012) Functional outcome of pannexin-deficient mice after cerebral ischemia. *Channels (Austin)* **6**, 453-456
9. Pelegrin, P., and Surprenant, A. (2009) The P2X(7) receptor-pannexin connection to dye uptake and IL-1 β release. *Purinergic Signal* **5**, 129-137
10. Chekeni, F. B., Elliott, M. R., Sandilos, J. K., Walk, S. F., Kinchen, J. M., Lazarowski, E. R., Armstrong, A. J., Penuela, S., Laird, D. W., Salvesen, G. S., Isakson, B. E., Bayliss, D. A., and Ravichandran, K. S. (2010) Pannexin 1 channels mediate 'find-me' signal release and membrane permeability during apoptosis. *Nature* **467**, 863-867
11. Qu, Y., Misaghi, S., Newton, K., Gilmour, L. L., Louie, S., Cupp, J. E., Dubyak, G. R., Hackos, D., and Dixit, V. M. (2011) Pannexin-1 is required for ATP release during apoptosis but not for inflammasome activation. *J Immunol* **186**, 6553-6561
12. Freeman, T. J., Sayedyahosseini, S., Johnston, D., Sanchez-Pupo, R. E., O'Donnell, B., Huang, K., Lakhani, Z., Nouri-Nejad, D., Barr, K. J., Harland, L., Latosinsky, S., Grant, A., Dagnino, L., and Penuela, S. (2019) Inhibition of Pannexin 1 Reduces the Tumorigenic Properties of Human Melanoma Cells. *Cancers (Basel)* **11**
13. Penuela, S., Gyenis, L., Ablack, A., Churko, J. M., Berger, A. C., Litchfield, D. W., Lewis, J. D., and Laird, D. W. (2012) Loss of pannexin 1 attenuates melanoma progression by reversion to a melanocytic phenotype. *J Biol Chem* **287**, 29184-29193
14. Bao, L., Locovei, S., and Dahl, G. (2004) Pannexin membrane channels are mechanosensitive conduits for ATP. *FEBS Lett* **572**, 65-68

15. Vanden Abeele, F., Bidaux, G., Gordienko, D., Beck, B., Panchin, Y. V., Baranova, A. V., Ivanov, D. V., Skryma, R., and Prevarskaya, N. (2006) Functional implications of calcium permeability of the channel formed by pannexin 1. *J Cell Biol* **174**, 535-546
16. Baranova, A., Ivanov, D., Petrash, N., Pestova, A., Skoblov, M., Kelmanson, I., Shagin, D., Nazarenko, S., Geraymovych, E., Litvin, O., Tiunova, A., Born, T. L., Usman, N., Staroverov, D., Lukyanov, S., and Panchin, Y. (2004) The mammalian pannexin family is homologous to the invertebrate innexin gap junction proteins. *Genomics* **83**, 706-716
17. Lohman, A. W., Leskov, I. L., Butcher, J. T., Johnstone, S. R., Stokes, T. A., Begandt, D., DeLalio, L. J., Best, A. K., Penuela, S., Leitinger, N., Ravichandran, K. S., Stokes, K. Y., and Isakson, B. E. (2015) Pannexin 1 channels regulate leukocyte emigration through the venous endothelium during acute inflammation. *Nat Commun* **6**, 7965
18. Weilinger, N. L., Lohman, A. W., Rakai, B. D., Ma, E. M., Bialecki, J., Maslieieva, V., Rilea, T., Bandet, M. V., Ikuta, N. T., Scott, L., Colicos, M. A., Teskey, G. C., Winship, I. R., and Thompson, R. J. (2016) Metabotropic NMDA receptor signaling couples Src family kinases to pannexin-1 during excitotoxicity. *Nat Neurosci* **19**, 432-442
19. Poornima, V., Vallabhaneni, S., Mukhopadhyay, M., and Bera, A. K. (2015) Nitric oxide inhibits the pannexin 1 channel through a cGMP-PKG dependent pathway. *Nitric Oxide* **47**, 77-84
20. Boyce, A. K., Kim, M. S., Wicki-Stordeur, L. E., and Swayne, L. A. (2015) ATP stimulates pannexin 1 internalization to endosomal compartments. *Biochem J* **470**, 319-330
21. Penuela, S., Bhalla, R., Nag, K., and Laird, D. W. (2009) Glycosylation regulates pannexin intermixing and cellular localization. *Mol Biol Cell* **20**, 4313-4323
22. Penuela, S., Bhalla, R., Gong, X. Q., Cowan, K. N., Celetti, S. J., Cowan, B. J., Bai, D., Shao, Q., and Laird, D. W. (2007) Pannexin 1 and pannexin 3 are glycoproteins that exhibit many distinct characteristics from the connexin family of gap junction proteins. *J Cell Sci* **120**, 3772-3783
23. Boassa, D., Ambrosi, C., Qiu, F., Dahl, G., Gaietta, G., and Sosinsky, G. (2007) Pannexin1 channels contain a glycosylation site that targets the hexamer to the plasma membrane. *J Biol Chem* **282**, 31733-31743
24. Lohman, A. W., Weaver, J. L., Billaud, M., Sandilos, J. K., Griffiths, R., Straub, A. C., Penuela, S., Leitinger, N., Laird, D. W., Bayliss, D. A., and Isakson, B. E. (2012) S-nitrosylation inhibits pannexin 1 channel function. *J Biol Chem* **287**, 39602-39612
25. Sandilos, J. K., Chiu, Y. H., Chekeni, F. B., Armstrong, A. J., Walk, S. F., Ravichandran, K. S., and Bayliss, D. A. (2012) Pannexin 1, an ATP release channel, is activated by caspase cleavage of its pore-associated C-terminal autoinhibitory region. *J Biol Chem* **287**, 11303-11311
26. Shao, Q., Lindstrom, K., Shi, R., Kelly, J., Schroeder, A., Juusola, J., Levine, K. L., Esseltine, J. L., Penuela, S., Jackson, M. F., and Laird, D. W. (2016) A Germline Variant in the PANX1 Gene Has Reduced Channel Function and Is Associated with Multisystem Dysfunction. *J Biol Chem* **291**, 12432-12443

27. Furlow, P. W., Zhang, S., Soong, T. D., Halberg, N., Goodarzi, H., Mangrum, C., Wu, Y. G., Elemento, O., and Tavazoie, S. F. (2015) Mechanosensitive pannexin-1 channels mediate microvascular metastatic cell survival. *Nat Cell Biol* **17**, 943-952
28. Sang, Q., Zhang, Z., Shi, J., Sun, X., Li, B., Yan, Z., Xue, S., Ai, A., Lyu, Q., Li, W., Zhang, J., Wu, L., Mao, X., Chen, B., Mu, J., Li, Q., Du, J., Sun, Q., Jin, L., He, L., Zhu, S., Kuang, Y., and Wang, L. (2019) A pannexin 1 channelopathy causes human oocyte death. *Sci Transl Med* **11**
29. Molica, F., Morel, S., Meens, M. J., Denis, J. F., Bradfield, P. F., Penuela, S., Zufferey, A., Monyer, H., Imhof, B. A., Chanson, M., Laird, D. W., Fontana, P., and Kwak, B. R. (2015) Functional role of a polymorphism in the Pannexin1 gene in collagen-induced platelet aggregation. *Thromb Haemost* **114**, 325-336
30. Stierlin, F. B., Molica, F., Reny, J. L., Kwak, B. R., and Fontana, P. (2017) Pannexin1 Single Nucleotide Polymorphism and Platelet Reactivity in a Cohort of Cardiovascular Patients. *Cell Commun Adhes* **23**, 11-15
31. Davis, L. K., Gamazon, E. R., Kistner-Griffin, E., Badner, J. A., Liu, C., Cook, E. H., Sutcliffe, J. S., and Cox, N. J. (2012) Loci nominally associated with autism from genome-wide analysis show enrichment of brain expression quantitative trait loci but not lymphoblastoid cell line expression quantitative trait loci. *Mol Autism* **3**, 3
32. Gawlik, M., Wagner, M., Pfuhlmann, B., and Stober, G. (2016) The role of Pannexin gene variants in schizophrenia: systematic analysis of phenotypes. *Eur Arch Psychiatry Clin Neurosci* **266**, 433-437
33. Sanchez-Pupo, R. E., Johnston, D., and Penuela, S. (2018) N-Glycosylation Regulates Pannexin 2 Localization but Is Not Required for Interacting with Pannexin 1. *Int J Mol Sci* **19**
34. Blom, N., Sicheritz-Ponten, T., Gupta, R., Gammeltoft, S., and Brunak, S. (2004) Prediction of post-translational glycosylation and phosphorylation of proteins from the amino acid sequence. *Proteomics* **4**, 1633-1649
35. Gu, T. L., Goss, V. L., Reeves, C., Popova, L., Nardone, J., Macneill, J., Walters, D. K., Wang, Y., Rush, J., Comb, M. J., Druker, B. J., and Polakiewicz, R. D. (2006) Phosphotyrosine profiling identifies the KG-1 cell line as a model for the study of FGFR1 fusions in acute myeloid leukemia. *Blood* **108**, 4202-4204
36. Cerami, E., Gao, J., Dogrusoz, U., Gross, B. E., Sumer, S. O., Aksoy, B. A., Jacobsen, A., Byrne, C. J., Heuer, M. L., Larsson, E., Antipin, Y., Reva, B., Goldberg, A. P., Sander, C., and Schultz, N. (2012) The cBio cancer genomics portal: an open platform for exploring multidimensional cancer genomics data. *Cancer Discov* **2**, 401-404
37. Gao, J., Aksoy, B. A., Dogrusoz, U., Dresdner, G., Gross, B., Sumer, S. O., Sun, Y., Jacobsen, A., Sinha, R., Larsson, E., Cerami, E., Sander, C., and Schultz, N. (2013) Integrative analysis of complex cancer genomics and clinical profiles using the cBioPortal. *Sci Signal* **6**, p11
38. Zhang, J., Baran, J., Cros, A., Guberman, J. M., Haider, S., Hsu, J., Liang, Y., Rivkin, E., Wang, J., Whitty, B., Wong-Erasmus, M., Yao, L., and Kasprzyk, A. (2011) International Cancer Genome Consortium Data Portal--a one-stop shop for cancer genomics data. *Database (Oxford)* **2011**, bar026

39. Lek, M., Karczewski, K. J., Minikel, E. V., Samocha, K. E., Banks, E., Fennell, T., O'Donnell-Luria, A. H., Ware, J. S., Hill, A. J., Cummings, B. B., Tukiainen, T., Birnbaum, D. P., Kosmicki, J. A., Duncan, L. E., Estrada, K., Zhao, F., Zou, J., Pierce-Hoffman, E., Berghout, J., Cooper, D. N., DeFlaux, N., DePristo, M., Do, R., Flannick, J., Fromer, M., Gauthier, L., Goldstein, J., Gupta, N., Howrigan, D., Kiezun, A., Kurki, M. I., Moonshine, A. L., Natarajan, P., Orozco, L., Peloso, G. M., Poplin, R., Rivas, M. A., Ruano-Rubio, V., Rose, S. A., Ruderfer, D. M., Shakir, K., Stenson, P. D., Stevens, C., Thomas, B. P., Tiao, G., Tusie-Luna, M. T., Weisburd, B., Won, H. H., Yu, D., Altshuler, D. M., Ardissino, D., Boehnke, M., Danesh, J., Donnelly, S., Elosua, R., Florez, J. C., Gabriel, S. B., Getz, G., Glatt, S. J., Hultman, C. M., Kathiresan, S., Laakso, M., McCarroll, S., McCarthy, M. I., McGovern, D., McPherson, R., Neale, B. M., Palotie, A., Purcell, S. M., Saleheen, D., Scharf, J. M., Sklar, P., Sullivan, P. F., Tuomilehto, J., Tsuang, M. T., Watkins, H. C., Wilson, J. G., Daly, M. J., MacArthur, D. G., and Exome Aggregation, C. (2016) Analysis of protein-coding genetic variation in 60,706 humans. *Nature* **536**, 285-291
40. Spencer, C. C., Deloukas, P., Hunt, S., Mullikin, J., Myers, S., Silverman, B., Donnelly, P., Bentley, D., and McVean, G. (2006) The influence of recombination on human genetic diversity. *PLoS Genet* **2**, e148
41. Takahata, N., Lee, S. H., and Satta, Y. (2001) Testing multiregionality of modern human origins. *Mol Biol Evol* **18**, 172-183
42. Seror, C., Melki, M. T., Subra, F., Raza, S. Q., Bras, M., Saidi, H., Nardacci, R., Voisin, L., Paoletti, A., Law, F., Martins, I., Amendola, A., Abdul-Sater, A. A., Ciccocanti, F., Delelis, O., Niedergang, F., Thierry, S., Said-Sadier, N., Lamaze, C., Metivier, D., Estaquier, J., Fimia, G. M., Falasca, L., Casetti, R., Modjtahedi, N., Kanellopoulos, J., Mouscadet, J. F., Ojcius, D. M., Piacentini, M., Gougeon, M. L., Kroemer, G., and Perfettini, J. L. (2011) Extracellular ATP acts on P2Y2 purinergic receptors to facilitate HIV-1 infection. *J Exp Med* **208**, 1823-1834
43. Moremen, K. W., Tiemeyer, M., and Nairn, A. V. (2012) Vertebrate protein glycosylation: diversity, synthesis and function. *Nat Rev Mol Cell Biol* **13**, 448-462
44. Weilinger, N. L., Tang, P. L., and Thompson, R. J. (2012) Anoxia-induced NMDA receptor activation opens pannexin channels via Src family kinases. *J Neurosci* **32**, 12579-12588
45. Iglesias, R., Locovei, S., Roque, A., Alberto, A. P., Dahl, G., Spray, D. C., and Scemes, E. (2008) P2X7 receptor-Pannexin1 complex: pharmacology and signaling. *Am J Physiol Cell Physiol* **295**, C752-760
46. DeLalio, L. J., Billaud, M., Ruddiman, C. A., Johnstone, S. R., Butcher, J. T., Wolpe, A. G., Jin, X., Keller, T. C. S. t., Keller, A. S., Riviere, T., Good, M. E., Best, A. K., Lohman, A. W., Swayne, L. A., Penuela, S., Thompson, R. J., Lampe, P. D., Yeager, M. Y., and Isakson, B. E. (2019) Constitutive SRC-mediated phosphorylation of pannexin 1 at tyrosine 198 occurs at the plasma membrane. *J Biol Chem*
47. Wlodkowic, D., Telford, W., Skommer, J., and Darzynkiewicz, Z. (2011) Apoptosis and beyond: cytometry in studies of programmed cell death. *Methods Cell Biol* **103**, 55-98

48. Bao, B. A., Lai, C. P., Naus, C. C., and Morgan, J. R. (2012) Pannexin1 drives multicellular aggregate compaction via a signaling cascade that remodels the actin cytoskeleton. *J Biol Chem* **287**, 8407-8416
49. Wei, L., Yang, X., Shi, X., and Chen, Y. (2015) Pannexin1 silencing inhibits the proliferation of U87MG cells. *Mol Med Rep* **11**, 3487-3492
50. Wang, J., Ambrosi, C., Qiu, F., Jackson, D. G., Sosinsky, G., and Dahl, G. (2014) The membrane protein Pannexin1 forms two open-channel conformations depending on the mode of activation. *Sci Signal* **7**, ra69
51. Wang, J., and Dahl, G. (2010) SCAM analysis of Panx1 suggests a peculiar pore structure. *J Gen Physiol* **136**, 515-527
52. Dahl, G. (2018) The Pannexin1 membrane channel: distinct conformations and functions. *FEBS Lett* **592**, 3201-3209
53. Cruz-Munoz, W., Man, S., Xu, P., and Kerbel, R. S. (2008) Development of a preclinical model of spontaneous human melanoma central nervous system metastasis. *Cancer Res* **68**, 4500-4505
54. Ran, F. A., Hsu, P. D., Wright, J., Agarwala, V., Scott, D. A., and Zhang, F. (2013) Genome engineering using the CRISPR-Cas9 system. *Nat Protoc* **8**, 2281-2308

Chapter 3

3 Discussion and Conclusions

3.1 Overall Study Conclusions

The overall objective of this study was to provide a further understanding of various domains of the PANX1 polypeptide by introducing naturally occurring *PANXI* variants and evaluating their effects. By exploring seven *PANXI* variants reported in tumours of melanoma patients and in human melanoma cell lines, we interrogated three domains of the protein implicated in glycosylation and channel function. From this study, we uncovered a novel tyrosine phosphorylation site, Y150, that may also regulate complex glycosylation of the channel and consequently its cell-surface trafficking. Disruption of this phosphorylation site by mutagenesis led to a differentially glycosylated protein with a greater capacity to traffic to the cell surface. This finding broadens the novel area of PANX1 phosphorylation in that phosphorylation of the channel does not only impact cell-surface-associated channel activity via interacting proteins but also other aspects that can begin prior to reaching the cell-surface. Y150F is not the first reported amino acid substitution that does not target the glycosylation site N254 but still affect the glycosylation profile of PANX1. Previous studies have demonstrated various PANX1 mutants in separate domains that prevent complete development of Gly2 species, similar to Y150F (1-4), thus demonstrating that different domains contribute to the delivery of complex glycosylation. Lastly, while we were not able to clearly delineate the spatiotemporal onset of Y150 phosphorylation, we deduce that Y150 phosphorylation may occur at the transition between high-mannose and complex glycosylation. This is because of the partial resistance to the high-mannose deglycosylation enzyme EndoH that Y150F acquires and due to the

detection of Y150 phosphorylation in only Gly2 species (**Fig. 3.1**). Furthermore, since phosphorylated and non-phosphorylated Y150 was detected in the Gly2 state, this suggests that Y150 phosphorylation may be lost either at the Golgi or the cell-surface where Gly2 has been previously demonstrated to localize at (2,5-7), however this requires further investigation.

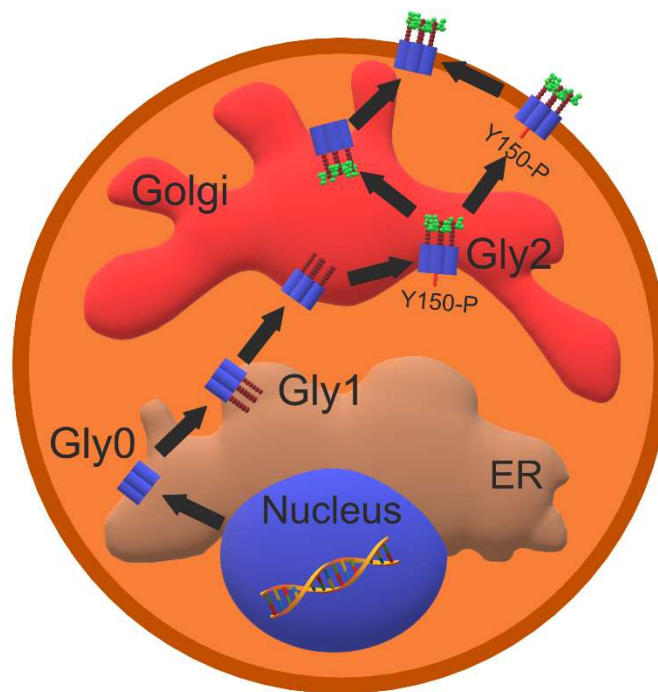


Figure 3.1: Potential spatiotemporal onset and termination pathway of Y150 phosphorylation of PANX1. PANX1 may receive Y150 phosphorylation at the Gly-2 state within the Golgi prior to trafficking to the cell-surface upon which loss of Y150 phosphorylation may occur at the Golgi or at the cell-surface.

Furthermore, we uncovered an ancestral *PANX1* variant, Q5H, mistakenly identified as a single-nucleotide polymorphism in various nucleotide and protein sequencing databases. What led our interest to this variant was its presence in various human melanoma cell lines and other cancer cell lines. It was also classified as a somatic mutation in a minority of

tumours of cancer patients in cBioPortal and ICGC databases. Combined with a previous finding demonstrating that ectopic expression of Q5H in Chinese Hamster Ovary cells led to greater ATP release than Q5, this piqued our interest to develop a proposal in which Q5H may be associated with cancer properties, in particular with cancers where PANX1 has been reported to promote their tumorigenic properties such as breast and melanoma cancers. As a result, we generated stable clones of the triple-negative breast cancer Hs578T(KO) cells expressing Q5 or Q5H and assessed basic readouts of changes to migration and cell growth. In this cellular context, we did not see any changes in channel activity, migration, and cell growth. We also assessed if the allele frequency of Q5H was associated with clinical attributes of colorectal and melanoma patients. As was seen at the cellular level, possessing Q5H did not affect an individual's risk to developing colorectal or melanoma cancers nor did it affect the severity of melanoma cancer. However, we did observe that Q5H has a greater allele frequency than Q5 in melanoma and colorectal cancer cohorts but was not associated with increased cancer risk. We then found out that this variant should be classified as the ancestral allele, and it was also found to be more prevalent than the derived allele, Q5, in both global and cancer cohorts. This has implications in the Pannexin community where countless researchers have used the less common allele, Q5, in their studies as they believed this to be the best and most representative PANX1 sequence. Despite our findings that Q5H does not differ significantly in the assessed properties of PANX1, we should be prudent before dismissing the role of Q5H in other cellular contexts as it has been previously reported to affect channel function in a non-cancer cell line (8). Collectively, this work highlights that

studying rare and common *PANX1* variants can unveil previously unknown properties of the widely expressed protein.

3.2 Study Limitations

The first limitation is that the direct effects of Y150F on channel activity was not fully elucidated. While there was an increase in dye-uptake relative to Q5 and controls, there was also more PANX1 channels at the cell-surface to mediate dye-uptake. To determine the direct effects of Y150F on channel function, we resorted to whole-cell patch-clamp electrophysiology recordings in HEK293T cells, however, the ectopic expression of Y150F in these cells resulted in great amounts of cell death preventing further studies of Y150F in this cell line. The reduced cell viability also presents another pressing matter in which the dye used for dye uptake, YO-PRO1, is also commonly used for assessing apoptosis. To alleviate concerns regarding apoptosis, one can exclude apoptotic cells from flow cytometric analysis by including an apoptosis marker such as annexin-V. Therefore, the enhanced dye uptake in cells expressing Y150F may be a result of greater amounts of PANX1 channels at the cell-surface and/or induction of apoptosis.

Another limitation is the inadequate comparison of Q5H allele frequencies between cancer and global cohorts. While the allele frequencies were found to be comparable, it is important to note that different methodologies were used to assess for Q5H allele frequencies in our study and ExAC's. Therefore, our crude comparison of Q5H allele frequency may be overlooking potential significant differences between global and cancer cohorts. Future work should employ the same method, such as analyzing only SNP microarrays for both cohorts, to assess allele frequencies across different cohorts to make an established comparison.

The patient harboring the Y150F mutation possessed an allele frequency of 0.46 within the tumour sample (9,10), thus demonstrating that the patient was heterozygous for Y150F. The experiments conducted analyzed only expression of Y150F and not the co-expression of Y150F and wildtype PANX1, which would further recapitulate the biological setting within the patient. As a result, future experiments should analyze the effects of expressing Y150F along with wildtype PANX1 on glycosylation, trafficking, and Y150 phosphorylation.

Furthermore, the full breadth of the effects of Q5H on PANX1 channel function was not explored. In this thesis, Y150F was only explored in the basal state while Q5H was studied in both basal and voltage-activated states. As mentioned before, Q5H has been previously reported to affect channel function in K^+ -activated states (8) and it has been suggested that the N-terminus lines the pore in K^+ -activated states for PANX1 (11). Therefore, it is possible that Q5H may impact channel function in cancer cells in K^+ -stimulated states, which should be explored.

The last limitation is the control used for the experiments comparing Hs578T(KO) stable clones expressing Q5 and Q5H. The control was non-transfected and non-selected Hs578T(KO) cells and therefore a comparison between the stable clones and the control is not sufficient as the process of transfection and colony-selection may induce cellular changes that affect dye-uptake, cell growth, and migration. Future experiments should include a control that has undergone transfection and colony selection to avoid this.

3.3 Future Directions

The findings of this study highlight several areas that requires further investigation such as exploring the role of PANX1 protonation in cancer and related PANX1 mutational signatures in cancer, as well as uncovering previously unreported post-translational modifications and their role in modulating cancer properties.

3.3.1 The Role of Protonation of PANX1 in Cancer

There is accumulating evidence demonstrating that PANX1 channel function is regulated by both extracellular and intracellular pH levels. Cytoplasmic acidification by CO₂ attenuated Panx1 currents in oocytes (12) and similarly, intracellular acidification by immersing taste receptor cells and *Xenopus* oocytes in sodium acetate resulted in reduced extracellular ATP and channel currents, respectively. Conversely, cytoplasmic alkalization with ammonium chloride and IFN- γ in airway epithelial cells increased ATP release relative to cells exposed to IFN- γ only (13). In addition, the activity level of Zebrafish PANX1 has been previously shown to be pH-dependent, with greater dye-uptake occurring as extracellular pH increases (14). Vroman *et al.* (15) has also shown that local acidification of the synaptic cleft between photoreceptors, bipolar cells, and horizontal cells as a result of PANX1-mediated ATP release, resulted in reduced PANX1 channel activity. Overall, as shown in different PANX1 species, lower intracellular and extracellular pH levels resulted in a reduction of PANX1 channel activity while it is enhanced with greater intracellular and extracellular pH. The mechanism through which how acidification inhibits PANX1 channel function may be through internalization of the channel, however this requires further investigation. Currently, there is a report demonstrating that

administration of ATP to N2A cells stably-expressing Panx1-EGFP resulted in significantly greater internalization relative to administration of the slowly hydrolysable analogue ATP γ S (16). It is important to note that hydrolysis of ATP not only releases the different subunits of ATP, but also protons which may act upon PANX1. Therefore, it is possible that these effects we see with altering pH may be affecting PANX1 channel activity by inducing internalization of the channel. A developing rationale for PANX1 to acquire pH-sensitivity is a negative-feedback mechanism for PANX1-mediated ATP release. In this model, extracellular ATP that may be derived from PANX1-mediated ATP release undergoes enzymatic degradation to adenosine and consequently releases protons. The released protons can then act upon the side groups of histidine and cysteine residues on the channel to reduce channel activity by inducing PANX1 internalization. This field requires further investigations to elucidate the mechanisms of how protonation affects overall PANX1 channel function.

Protonation of cytoplasmic residues is dependent on intracellular pH (pHi), whose dynamics often act as a signaling mechanism to regulate several cellular processes and is dysregulated in several diseases including cancer where pHi is constitutively increased (17,18) and neurodegenerative disorders where pHi is constitutively lower (19,20). It has been suggested that cancer cells, which possess increased intracellular pH and decreased extracellular pH relative to normal cells, exploit the dysregulated pH system by altering the structure and function of pH-sensitive proteins (21). With PANX1 as a novel pH-sensitive function, it remains unknown how PANX1 channel function differs between cancer and normal cells with differential extracellular and intracellular pH levels.

The field of PANX1 protonation can be further expanded into the roles of PANX1 in cancer. There are notable mutational signatures in the Pannexin family in the context of protonation which can be further explored in cancer. PANX1, in addition to PANX2 and PANX3, possess a noticeable amount of R → H/C/Q somatic mutations, not including other missense and nonsense mutations at arginine residues, representing 10.1%, 19.9%, and 14.9% of all reported somatic mutations for PANX1, PANX2, and PANX3, respectively (9,10). These types of mutations have been found to be dominant in driver mutations relative to passenger mutations (22)(23)(22) and a physiological implication, specifically for R → H mutations, has been shown to enhance pH sensing in mutated proteins (23). The latter study demonstrated epidermal growth factor receptor EGFR and tumor suppressor p53 harbouring an R → H mutation exhibited greater or lower tumorigenic effects when intracellular pH was raised or lowered, respectively, relative to wildtype. The biochemical significance of R → H mutations is the gain of titrable behavior within physiological pH from Histidine as its imidazole ring possesses a pKa of 6.5. This finding demonstrated that certain somatic mutations may provide an advantage for cancer cells that typically have higher intracellular pH. As of now, there has only been one R → H *PANX1* mutation studied, R217H, which resulted in a loss-of-function mutant in HEK293T cells (24). Surprisingly, R217H is also reported in two patients diagnosed with prostate adenocarcinoma and glioblastoma multiforme cancers. As aforementioned, there is increasing evidence that PANX1 channel function is regulated by both intracellular and extracellular pH levels that may be mediated by specific residues that confer pH sensing to the protein. In cancer, somatic mutations such as R → H may provide a gain in pH sensing for PANX1 and possibly providing a fitness advantage for cancer cells harboring such

mutations. Future studies can focus on the role of protonation on PANX1 channel function and the fitness advantages certain R→H/C/Q mutations of PANX1 may confer to cancer cells.

3.3.2 Potential PTMs of PANX1

Our study's mass spectrometry results have unveiled previously unidentified post-translational modifications (**Suppl. Fig. 2.3**) that may play key roles in various aspects of PANX1 as described below.

As of now, only three tyrosine phosphorylation sites of PANX1 (Y150, Y198 and Y308) have been experimentally established, along with a report strongly suggesting that S206 is a serine phosphorylation site. Our results demonstrate that PANX1 in Hs578T(KO) cells also undergo phosphorylation at the following residues between Q5, Q5H, and Y150F as indicated: S159 (Y150F), S137 (Y150F), Y309 (Q5), Y150(Q5 & Q5H), T382 (Q5), T368 (Q5), S357 (Q5), T396 (Q5), S344 (Q5H), and S159 (Q5) (**Suppl. Fig. 2.3**). As discussed in Chapter 1.5.2, phosphorylation has been shown to play key roles in regulating channel function and it remains unknown how phosphorylation at the indicated sites affect channel function. Therefore, it would be of great interest to analyze how mutagenesis of these sites affect glycosylation, trafficking, and channel-function.

3.3.2.1 N-terminal methionine cleavage and acetylation

While rarely occurring in prokaryotes, the co-translational process of initial methionine cleavage and N-terminus acetylation is one of the most common PTMs occurring in eukaryotic cells. N-terminal acetylation is the covalent addition of an acetyl group to the

free α -amino group at the N-terminus. Due to the lack of N-terminal deacetylases discovered, it is believed that N-terminal acetylation is an irreversible process (25). Nonetheless, N-terminal acetylation has been demonstrated to impact the acetylated protein in different ways depending on the substrate and its cellular context. N-terminal acetylation has been shown to influence protein stability by targeting proteins for polyubiquitination and proteasomal degradation (26), protein folding by acting as protein quality control (27-30), formation of protein complexes by altering charge and increasing hydrophobicity (31-33), as well as targeting proteins to the membrane through interacting with protein-protein interactions or through increasing the substrate's affinity for moderately charged vesicles (34-36). As of now, there has only been one report of an ion channel experiencing N-terminal methionine cleavage and acetylation (37).

PANX1 is predicted to undergo these two co-translational processes as analyzed by Terminus (v0.4.1) (38), and mass spectrometry results from our lab demonstrate that PANX1 does experience these two PTMs, but their impact remains unknown on overall PANX1 function.

3.4 Summary

In conclusion, from studying seven naturally occurring *PANX1* variants, we have uncovered two that have deeper implications in our understanding of PANX1 and are significant contributions to the pannexin research field. The variant Y150F produced a hypo-glycosylated channel that lacked phosphorylation of Y150 but possessed a greater capacity to traffic to the cell-surface. We also identified an ancestral variant, Q5H, that is the more representative allele at this locus in global and cancer cohorts but was not

associated with risk to colorectal and melanoma cancers. Q5H also did not differ from Q5 in glycosylation, cell-surface localization, and channel activity in breast cancer cells, although it has been previously demonstrated to confer a gain in channel activity in normal cells. Overall, these findings open up a new area of research in the role of phosphorylation beyond channel activity and the expansion of the study of Q5H into other diseases.

3.5 References

1. Sang, Q., Zhang, Z., Shi, J., Sun, X., Li, B., Yan, Z., Xue, S., Ai, A., Lyu, Q., Li, W., Zhang, J., Wu, L., Mao, X., Chen, B., Mu, J., Li, Q., Du, J., Sun, Q., Jin, L., He, L., Zhu, S., Kuang, Y., and Wang, L. (2019) A pannexin 1 channelopathy causes human oocyte death. *Sci Transl Med* **11**
2. Boassa, D., Ambrosi, C., Qiu, F., Dahl, G., Gaietta, G., and Sosinsky, G. (2007) Pannexin1 channels contain a glycosylation site that targets the hexamer to the plasma membrane. *J Biol Chem* **282**, 31733-31743
3. Lohman, A. W., Weaver, J. L., Billaud, M., Sandilos, J. K., Griffiths, R., Straub, A. C., Penuela, S., Leitinger, N., Laird, D. W., Bayliss, D. A., and Isakson, B. E. (2012) S-nitrosylation inhibits pannexin 1 channel function. *J Biol Chem* **287**, 39602-39612
4. Bunse, S., Schmidt, M., Hoffmann, S., Engelhardt, K., Zoidl, G., and Dermietzel, R. (2011) Single cysteines in the extracellular and transmembrane regions modulate pannexin 1 channel function. *J Membr Biol* **244**, 21-33
5. Bhalla-Gehi, R., Penuela, S., Churko, J. M., Shao, Q., and Laird, D. W. (2010) Pannexin1 and pannexin3 delivery, cell surface dynamics, and cytoskeletal interactions. *J Biol Chem* **285**, 9147-9160
6. Penuela, S., Celetti, S. J., Bhalla, R., Shao, Q., and Laird, D. W. (2008) Diverse subcellular distribution profiles of pannexin 1 and pannexin 3. *Cell Commun Adhes* **15**, 133-142
7. Penuela, S., Bhalla, R., Nag, K., and Laird, D. W. (2009) Glycosylation regulates pannexin intermixing and cellular localization. *Mol Biol Cell* **20**, 4313-4323
8. Molica, F., Morel, S., Meens, M. J., Denis, J. F., Bradfield, P. F., Penuela, S., Zufferey, A., Monyer, H., Imhof, B. A., Chanson, M., Laird, D. W., Fontana, P., and Kwak, B. R. (2015) Functional role of a polymorphism in the Pannexin1 gene in collagen-induced platelet aggregation. *Thromb Haemost* **114**, 325-336
9. Cerami, E., Gao, J., Dogrusoz, U., Gross, B. E., Sumer, S. O., Aksoy, B. A., Jacobsen, A., Byrne, C. J., Heuer, M. L., Larsson, E., Antipin, Y., Reva, B., Goldberg, A. P., Sander, C., and Schultz, N. (2012) The cBio cancer genomics portal: an open platform for exploring multidimensional cancer genomics data. *Cancer Discov* **2**, 401-404
10. Gao, J., Aksoy, B. A., Dogrusoz, U., Dresdner, G., Gross, B., Sumer, S. O., Sun, Y., Jacobsen, A., Sinha, R., Larsson, E., Cerami, E., Sander, C., and Schultz, N. (2013) Integrative analysis of complex cancer genomics and clinical profiles using the cBioPortal. *Sci Signal* **6**, pl1
11. Dahl, G. (2018) The Pannexin1 membrane channel: distinct conformations and functions. *FEBS Lett* **592**, 3201-3209
12. Locovei, S., Wang, J., and Dahl, G. (2006) Activation of pannexin 1 channels by ATP through P2Y receptors and by cytoplasmic calcium. *FEBS Lett* **580**, 239-244
13. Krick, S., Wang, J., St-Pierre, M., Gonzalez, C., Dahl, G., and Salathe, M. (2016) Dual Oxidase 2 (Duox2) Regulates Pannexin 1-mediated ATP Release in Primary Human Airway Epithelial Cells via Changes in Intracellular pH and Not H2O2 Production. *J Biol Chem* **291**, 6423-6432

14. Kurtenbach, S., Prochnow, N., Kurtenbach, S., Klooster, J., Zoidl, C., Dermietzel, R., Kamermans, M., and Zoidl, G. (2013) Pannexin1 channel proteins in the zebrafish retina have shared and unique properties. *PLoS One* **8**, e77722
15. Vroman, R., Klaassen, L. J., Howlett, M. H., Cenedese, V., Klooster, J., Sjoerdsma, T., and Kamermans, M. (2014) Extracellular ATP hydrolysis inhibits synaptic transmission by increasing pH buffering in the synaptic cleft. *PLoS Biol* **12**, e1001864
16. Boyce, A. K., Kim, M. S., Wicki-Stordeur, L. E., and Swayne, L. A. (2015) ATP stimulates pannexin 1 internalization to endosomal compartments. *Biochem J* **470**, 319-330
17. Cardone, R. A., Casavola, V., and Reshkin, S. J. (2005) The role of disturbed pH dynamics and the Na⁺/H⁺ exchanger in metastasis. *Nat Rev Cancer* **5**, 786-795
18. Webb, B. A., Chimenti, M., Jacobson, M. P., and Barber, D. L. (2011) Dysregulated pH: a perfect storm for cancer progression. *Nat Rev Cancer* **11**, 671-677
19. Syntichaki, P., Samara, C., and Tavernarakis, N. (2005) The vacuolar H⁺-ATPase mediates intracellular acidification required for neurodegeneration in *C. elegans*. *Curr Biol* **15**, 1249-1254
20. Harguindey, S., Reshkin, S. J., Orive, G., Arranz, J. L., and Anitua, E. (2007) Growth and trophic factors, pH and the Na⁺/H⁺ exchanger in Alzheimer's disease, other neurodegenerative diseases and cancer: new therapeutic possibilities and potential dangers. *Curr Alzheimer Res* **4**, 53-65
21. White, K. A., Grillo-Hill, B. K., and Barber, D. L. (2017) Cancer cell behaviors mediated by dysregulated pH dynamics at a glance. *J Cell Sci* **130**, 663-669
22. Anoocha, P., Sakthivel, R., and Michael Gromiha, M. (2016) Exploring preferred amino acid mutations in cancer genes: Applications to identify potential drug targets. *Biochim Biophys Acta* **1862**, 155-165
23. White, K. A., Ruiz, D. G., Szpiech, Z. A., Strauli, N. B., Hernandez, R. D., Jacobson, M. P., and Barber, D. L. (2017) Cancer-associated arginine-to-histidine mutations confer a gain in pH sensing to mutant proteins. *Sci Signal* **10**
24. Shao, Q., Lindstrom, K., Shi, R., Kelly, J., Schroeder, A., Juusola, J., Levine, K. L., Esseltine, J. L., Penuela, S., Jackson, M. F., and Laird, D. W. (2016) A Germline Variant in the PANX1 Gene Has Reduced Channel Function and Is Associated with Multisystem Dysfunction. *J Biol Chem* **291**, 12432-12443
25. Ree, R., Varland, S., and Arnesen, T. (2018) Spotlight on protein N-terminal acetylation. *Exp Mol Med* **50**, 90
26. Lee, K. E., Heo, J. E., Kim, J. M., and Hwang, C. S. (2016) N-Terminal Acetylation-Targeted N-End Rule Proteolytic System: The Ac/N-End Rule Pathway. *Mol Cells* **39**, 169-178
27. Trexler, A. J., and Rhoades, E. (2012) N-Terminal acetylation is critical for forming alpha-helical oligomer of alpha-synuclein. *Protein Sci* **21**, 601-605
28. Holmes, W. M., Mannakee, B. K., Gutenkunst, R. N., and Serio, T. R. (2014) Loss of amino-terminal acetylation suppresses a prion phenotype by modulating global protein folding. *Nat Commun* **5**, 4383
29. Oh, J. H., Hyun, J. Y., and Varshavsky, A. (2017) Control of Hsp90 chaperone and its clients by N-terminal acetylation and the N-end rule pathway. *Proc Natl Acad Sci U S A* **114**, E4370-E4379

30. Bartels, T., Kim, N. C., Luth, E. S., and Selkoe, D. J. (2014) N-alpha-acetylation of alpha-synuclein increases its helical folding propensity, GM1 binding specificity and resistance to aggregation. *PLoS One* **9**, e103727
31. Monda, J. K., Scott, D. C., Miller, D. J., Lydeard, J., King, D., Harper, J. W., Bennett, E. J., and Schulman, B. A. (2013) Structural conservation of distinctive N-terminal acetylation-dependent interactions across a family of mammalian NEDD8 ligation enzymes. *Structure* **21**, 42-53
32. Arnaudo, N., Fernandez, I. S., McLaughlin, S. H., Peak-Chew, S. Y., Rhodes, D., and Martino, F. (2013) The N-terminal acetylation of Sir3 stabilizes its binding to the nucleosome core particle. *Nat Struct Mol Biol* **20**, 1119-1121
33. Yang, D., Fang, Q., Wang, M., Ren, R., Wang, H., He, M., Sun, Y., Yang, N., and Xu, R. M. (2013) N-alpha-acetylated Sir3 stabilizes the conformation of a nucleosome-binding loop in the BAH domain. *Nat Struct Mol Biol* **20**, 1116-1118
34. Behnia, R., Panic, B., Whyte, J. R., and Munro, S. (2004) Targeting of the Arf-like GTPase Arl3p to the Golgi requires N-terminal acetylation and the membrane protein Sys1p. *Nat Cell Biol* **6**, 405-413
35. Setty, S. R., Strohlic, T. I., Tong, A. H., Boone, C., and Burd, C. G. (2004) Golgi targeting of ARF-like GTPase Arl3p requires its N-alpha-acetylation and the integral membrane protein Sys1p. *Nat Cell Biol* **6**, 414-419
36. Dikiy, I., and Eliezer, D. (2014) N-terminal acetylation stabilizes N-terminal helicity in lipid- and micelle-bound alpha-synuclein and increases its affinity for physiological membranes. *J Biol Chem* **289**, 3652-3665
37. Beltran-Alvarez, P., Tarradas, A., Chiva, C., Perez-Serra, A., Batlle, M., Perez-Villa, F., Schulte, U., Sabido, E., Brugada, R., and Pagans, S. (2014) Identification of N-terminal protein acetylation and arginine methylation of the voltage-gated sodium channel in end-stage heart failure human heart. *J Mol Cell Cardiol* **76**, 126-129
38. Charpillot, C., Veuthey, A. L., Chopard, B., and Falcone, J. L. (2014) Motifs tree: a new method for predicting post-translational modifications. *Bioinformatics* **30**, 1974-1982

Curriculum Vitae

Name: Daniel Ariel Nouri Nejad

**Post-secondary
Education and
Degrees:** Western University
London, Ontario, Canada
2013-2017 B.M.Sc.

Western University
London, Ontario, Canada
2017-Present M.Sc. (*Expected June 2019*)

**Honours and
Awards:** CIHR Frederick Banting and Charles Best Canada Graduate
Scholarships
2018-2019

Anatomy and Cell Biology Travel Award
2018

OPA College University Powerlifting 1st Place 74KG
2018

Cancer Research and Technology Transfer Trainee Award
2017-2018

Charlie Hanes Student Award
2017

OPA College University Powerlifting 1st Place 74KG
2016

Blanche Box Bursary in Physiology
2016

UWO Bursaries Science MET
2016

NSERC-Undergraduate Summer Research Award
2016

University of Western Ontario Continuing Admissions Scholarship
2013-2017

University of Western Ontario Dean's Honour List
2013-2017

Sunnybrook's St. John's Rehab Hospital Ambassador Award –
National Volunteer Week
2013

Norman Forma Bursary
2013

Related Work Experience Teaching Assistant – Physiology & Pharmacology 3000E
Western University
2018-2019

Teaching Assistant – Anatomy and Cell Biology 3309
Western University
2017-2018

Publication:

- Freeman T, Sayedyahosseini S, Johnston D, Sanchez-Pupo R, O'Donnell B, Huang K, Lakhani Z, **Nouri-Nejad D**, Barr KJ, Harland L, Latosinsky S, Grant A, Dagnino L, Penuela S (2018). Inhibition of Pannexin 1 Reduces the Tumorigenic Properties of Human Melanoma cells. *Cancers* 11, 102.

Oral Presentations:

1. *Biochemical and functional analyses of PANX1 variants Q5H and Y150F*. 13th Annual Nexin Research Forum. Western University, London, ON, March 29, 2019.
2. *Characterization of PANX1 mutations from patient derived melanoma tumours*. 11th Annual Nexin Research Forum. Western University, London, ON, May 26, 2017.

Poster Presentations:

1. **Nouri Nejad D**, O'Donnell B, Patil C, Sanchez-Pupo R, Johnston D, Jurcic K, Litchfield D, Jackson M, Gloor G, Penuela S (2019). "Identification of a prevalent ancestral PANX1 variant and a novel tyrosine phosphorylation site affecting that affects glycosylation and trafficking of PANX1." Oncology Research & Education Day 2019". June 14, 2019. Poster Presentation.
2. Freeman TJ, Sayedyahosseini S, Johnston D, Sanchez-Pupo RE, O'Donnell B, Huang K, Lakhani Z, **Nouri Nejad D**, Barr KJ, Harland L, Latosinsky S, Grant A, Penuela S

- (2019). “Inhibition of Pannexin 1 channels reduces tumorigenic properties of melanoma.” London Health Research Day 2019. April 30, 2019. Poster Presentation.
3. Freeman TJ, Sayedyahosseini S, Johnston D, Sanchez-Pupo RE, O’Donnell B, Huang K, Lakhani Z, **Nouri Nejad D**, Barr KJ, Harland L, Latosinsky S, Grant A, Penuela S (2019). “Inhibition of Pannexin 1 channels reduces tumorigenic properties of melanoma.” Experimental Biology 2019. April 6-9, 2019. Poster Presentation.
 4. **Nouri Nejad D**, O’Donnell B, Johnston D, Sanchez R, Barr K, Penuela S (2018). “Pannexin1 and its mutant isoforms in the crosstalk between melanoma and immune cells.” Oncology Research & Education Day 2018. June 8, 2018. Poster Presentation.
 5. **Nouri Nejad D**, O’Donnell B, Johnston D, Sanchez R, Barr K, Penuela S (2018). “Pannexin1 and its mutant isoforms in the crosstalk between melanoma and immune cells.” Oncology Research & Education Day 2018. June 8, 2018. Poster Presentation.
 6. **Nouri Nejad D**, O’Donnell B, Johnston D, Rafael Sanchez, Kevin Barr, Penuela S (2018). “Pannexin1 and its mutant isoforms in the crosstalk between melanoma and immune cells.” Oncology Research & Education Day 2018. June 8, 2018. Poster Presentation.
 7. **Nouri Nejad D**, O’Donnell B, Johnston D, Rafael Sanchez, Kevin Barr, Penuela S (2018). “Pannexin1 and its mutant isoforms in the crosstalk between melanoma and immune cells.” Oncology Research & Education Day 2018. June 8, 2018. Poster Presentation.
 8. **Nouri Nejad D**, O’Donnell B, Johnston D, Rafael Sanchez, Kevin Barr, Penuela S (2018). “Pannexin1 and its mutant isoforms in the crosstalk between melanoma and immune cells.” London Health Research Day 2018. May 10, 2018. Poster Presentation.
 9. **Nouri Nejad D**, O’Donnell B, Johnston D, Rafael Sanchez, Kevin Barr, Penuela S (2018). “Pannexin1 and its mutant isoforms in the crosstalk between melanoma and immune cells. The 11th Conference on Signalling in Normal and Cancer Cells. Banff, AB. April 15-19th, 2018. Poster Presentation.
 10. **Nouri Nejad D**, Johnston D, O’Donnell B, Penuela S (2017). Characterization of PANX1 mutations from patient derived melanoma tumours. 14th Annual Oncology Research and Education Day. London, ON. June 16th, 2017. Poster 48.
 11. **Nouri Nejad D**, Johnston D, O’Donnell B, Penuela S (2017). Characterization of PANX1 mutations from patient derived melanoma tumours. London Health Research Day. London, ON. March 28th, 2017. Poster 150.